The Effects of YAP Activity on Retinoic Acid Signaling in the Embryonic Epicardium

by

Danika P. Bongfeldt

A thesis submitted in partial fulfillment
of the requirements for the degree of
Masters of Science (M.Sc.) in Biology

The Faculty of Graduate Studies
Laurentian University
Sudbury, Ontario, Canada

THESIS DEFENCE COMMITTEE/COMITÉ DE SOUTENANCE DE THÈSE
Laurentian Université/Université Laurentienne
Faculty of Graduate Studies/Faculté des études supérieures

Title of Thesis Titre de la thèse	The Effects of YAP Activity on Retinoic Acid Signaling in the Embryonic Epicardium
Name of Candidate Nom du candidat	Bongfeldt, Danika
Degree Diplôme	Master of Science
Department/Program Département/Programme	Biology
Date of Defence Date de la soutenance	Decembre 17, 2020

APPROVED/APPROUVÉ

Thesis Examiners/Examinateurs de thèse:

Dr. Alex Moise
(Supervisor/Directeur(trice) de thèse)

Dr. Alain Simard
(Committee member/Membre du comité)

Dr. Jeff Gagnon
(Committee member/Membre du comité)

Dr. Robin Clugston
(External Examiner/Examinateur externe)

Approved for the Faculty of Graduate Studies
Approuvé pour la Faculté des études supérieures
Dr. Lace Marie Brogden
Madame Lace Marie Brogden
Acting Dean, Faculty of Graduate Studies
Doyenne intérimaire, Faculté des études supérieures

ACCESSIBILITY CLAUSE AND PERMISSION TO USE

ABSTRACT

Retinoic acid (RA), a metabolite of vitamin A, is primarily produced by epicardial cells and is required for the proper differentiation of epicardial cells into cardiac fibroblasts and VSMCs during heart development. Recent literature has suggested that both mechanotransduction, which is mechanical stimuli eliciting chemical responses within the cell, and the Hippo signaling pathway could potentially regulate RA-signaling. The transcriptional co-activator YAP is regulated by the Hippo-pathway and mechanotransduction and elicits changes in gene transcription through the TEAD transcription factor. Recently it was found that there were TEAD motifs in the *Dhrs3* gene and YAP showed specific binding to the *Dhrs3* enhancer via chromatin immunoprecipitation combined with qPCR (ChIP-PCR) in the mouse epicardial cell line MEC1. However, beyond its effects on the expression of *Dhrs3* it is not clear if YAP actually affects RA-signaling. We hypothesized that YAP regulates retinoic acid signaling in embryonic epicardial cells. The first aim was to assess if YAP regulates the transcription of enzymes and receptors involved in RA metabolism or signaling in MEC1 cells. Using RT-qPCR we investigated the effect of constitutively active YAP, or conversely suppressed YAP activity on *Dhrs3*, *Raldh2*, *RARβ*, *Cyp26A1*, and *Cyp26B1* expression. To suppress YAP activity, a YAP small interfering RNA (siRNA), or the YAP-TEAD chemical inhibitor, Verteporfin, were utilized but these manipulations did not show significant effects on YAP targets, or retinoid receptors and enzymes in MEC1 cells. To overexpress YAP, a constitutively active form of YAP, YAP25SA, was transfected into MEC1 cells. We were able to confirm a direct relationship between *Cyp26a1* expression and YAP activity as YAP25SA increased *Cyp26a1* mRNA expression by 37.8-fold within 6 hours of transfection. As well, we were able to determine that YAP25SA affected *Cyp26a1* expression through a TEAD mechanism; as co-transfection of YAP25SA with YTIP-GFP, a plasmid expressing a peptide that

interferes with YAP-TEAD interaction significantly diminished the effects of YAP25SA on *Cyp26a1* expression. The second aim investigated if YAP regulates the metabolism of retinol into RA by utilizing the two-hybrid Gal4-RAR;UAS-tk-Gaussia luciferase reporter system that estimate the amount of RA produced by monitoring the activation of the Gal4RAR reporter. Transfection of MEC1 cells with YAP25SA allowed more retinol to be converted to RA and for a longer period of time when compared to the control. Since the activity of YAP influences the expression of *Cyp26a1* and metabolism of retinol, it was concluded that YAP activity plays a role in RA-signaling.

KEYWORDS:
Retinoic acid signaling, embryonic epicardium, YAP signaling, epithelial to mesenchymal transition, mechanical tension, cell proliferation, heart development and heart failure.

ACKNOWLEDGEMENTS:

There are many people I would like to thank who made the completion of this M.Sc. thesis possible. First, I would like to acknowledge my supervisor Dr. Alexander Moise for allowing me the opportunity to become a part of the NOSM research team and for helping me attain my goals. You have provided me with countless hours of support and advice both professionally as well as personally that have made me a better student and scientist. The many thought-provoking meetings have instilled in me the ability to think more critically about research and the questions that need to be answered. I am also grateful for my committee for their time, support and guidance.

Next I would like to acknowledge my fellow lab group members: Amelia, Parisa, Adam, Ben and Phil. Thank you for the assistance with experiments, teaching me how to work collaboratively on research projects and for making experiments and late lab nights fun.

Thank you to all the other laboratory groups at NOSM. Working in the NOSM research labs has been incredible as many of the other groups were able to teach me new techniques, shared equipment and protocols, and provided me with new knowledge from their own research projects. I will cherish the laughs, lunch time chats, experimental struggles and new friendships I have made with the other M.Sc. students at NOSM; specifically: Maryse, Ed, Isabelle, Meghan, Shannon and Danika. I also need to dedicate a special thank you to Natalie Lefort for being the absolute best laboratory manager. Thank you for everything you do for the NOSM laboratory and planning fun events for us students. You were always available to offer assistance and guidance for not only my experiments but also with personal challenges. You truly have a heart of gold and just being around you has made me a better person. As well, thank you to Dr. Robert Lafrenie for all of his guidance.

In addition, I would like to thank all of the funding agencies that have made this work possible: NSERC, OGS, and the NIH.

Finally, I would like to acknowledge my friends and family for all of the love and support throughout my academic journey. Thank you so much Mom, Dad, Ashlee, Bryce, Val, Alex and Lauren. Not only did you guys have to listen about my research constantly, but you willingly sat through countless practice presentations throughout my M.Sc. and for that I am very grateful. On the toughest of days, you have all reassured me that I could finish this thesis. Also, thank you to my guardian angel Christine who I know provided me guidance with this M.Sc. project and for inspiring me to pursue a career in science.

Table of Contents

LIST OF TABLES

LIST OF FIGURES

1. Introduction

1.1 Vitamin A Metabolism and Signaling

1.1.1 Vitamin A Metabolism

Vitamin A is an essential micronutrient that is critical for all stages of life; from embryonic development through adult homeostasis. Vitamin A is essential for a wide array of physiological processes, such as proper bone development, protection of the skin and mucosa, epithelial integrity, immune system defense and even the normal development and function of the reproductive organs, the diaphragm, hair and teeth.[1–9] Cells use vitamin A by converting it to its two main bioactive metabolites: 11-*cis*-retinaldehyde and all-*trans*-retinoic acid (RA).[10–12] Vitamin A is most commonly known for its role in vision; specifically, 11-*cis*-retinaldehyde is the universal light sensing molecule in all animals and it is required in visual phototransduction.[13–15] Meanwhile, RA is a short-range signaling molecule that regulates gene expression throughout life, and with especially important roles during embryonic development.[15–17] RA levels are maintained within a tight physiological range because excess or deficiency can result in birth defects and adult disorders.[2,19,20] This strict regulation is provided by a number of synthesizing and metabolizing enzymes that facilitate the precise spatiotemporal control of vitamin A metabolism and RA synthesis and signaling; as depicted in Figure 1.[21]

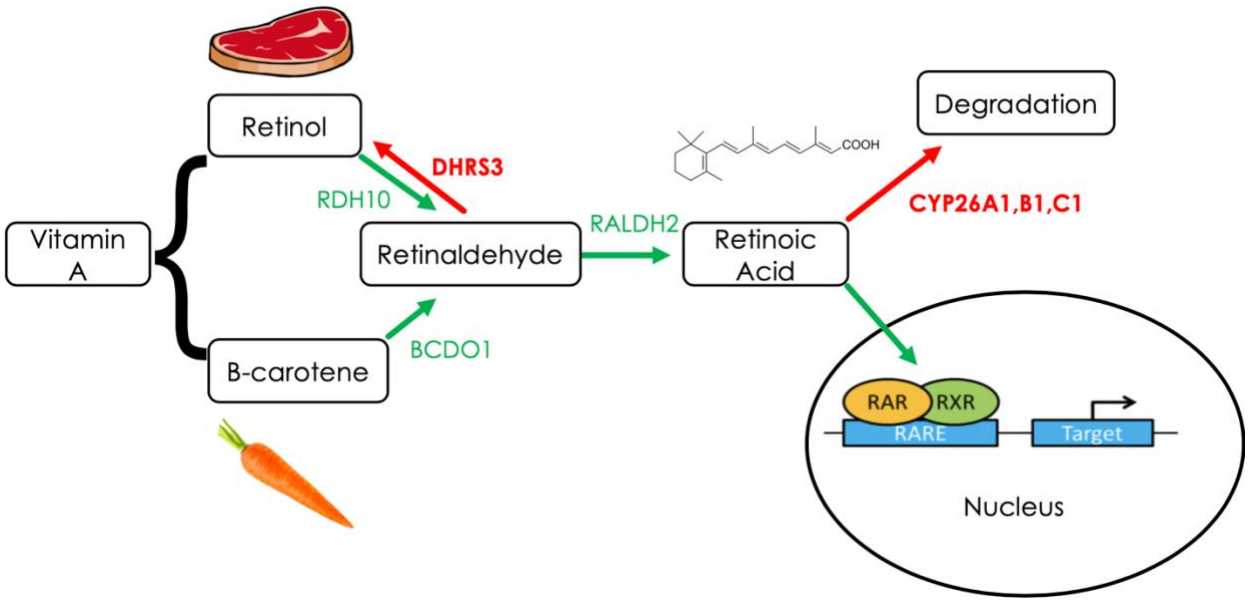

Figure 1: Key summary of the retinoic acid signaling pathway. There are two forms of Vitamin A we supplement in our diet, retinol found in meat and β-carotene found in vegetables. The enzymes β-carotene-15,15-dioxygenase (BCDO1) and retinol dehydrogenases (RDH) convert β-carotene and retinol respectively into retinaldehyde. Retinaldehyde is then irreversibly converted to RA by retinaldehyde dehydrogenases 2 or 3. RA then can enter the nucleus where it acts as a ligand to retinoic acid receptors (RAR) and retinoid x receptors (RXRs) heterodimers and through direct association with retinoic acid response element (RAREs) control the transcription of target genes. The dehydrogenase/reductase 3 (DHRS3) and cytochrome p450 enzymes of the CYP26 family maintain the appropriate levels of RA within cells. If there is too much RA, Dhrs3 will convert RA into retinol and the CYP26 family will degrade RA. Only enzymes with a known role in embryonic development derived from genetic ablation studies are shown here.

Since our bodies cannot manufacture vitamin A, we must include it in our diets. As illustrated in Figure 1, there are two dietary sources of vitamin A: provitamin A carotenoids and preformed vitamin A.[22] Provitamin A carotenoids are derived from plant sources, such as β-carotene found in many vegetables. Alternatively, preformed vitamin A comes largely from animal products, such as retinol and retinyl esters found in liver, milk and eggs.[22] Retinol is a long-chain, unsaturated alcohol containing five conjugated double bonds and a β-ionone ring. Retinol, and its metabolites or synthetic compounds with vitamin A activity, are commonly referred to as retinoids. Retinoids both naturally-occurring and synthetic forms are lipid-soluble compounds.[23] Preformed

vitamin A is hydrolyzed and taken up by enterocytes from the intestinal lumen.[24,25] Enterocytes esterify and package retinol into chylomicrons so that they can be secreted into lymphatic and then systemic circulation for distribution throughout the body.[24,25] Eventually, most of the retinol is stored as retinyl esters within the liver's hepatic stellate cells.[20,24,26,27] When needed, stores of retinyl esters can undergo hydrolysis back to retinol.[28,29] Retinol is transported throughout the vasculature in association with serum retinol binding protein (RBP4).[28,29] Target cells express the stimulated by retinoic acid 6 receptor (STRA6), which binds to RBP4-retinol complexes to coordinate retinol uptake.[26]

Once inside the cell, retinol is bound cellular retinol binding protein (CRBP) 1, 2 and 3 in the cytoplasm.[30,31] CRBP1 is widely distributed throughout the body, whereas CRBP2 is restricted to the small intestine and CRBP3 is restricted to the heart and skeletal muscles.[31] CRBPs serve as chaperone proteins that protect retinol and interact with various retinoid-metabolizing enzymes.[32,33] Retinol undergoes two consecutive oxidation steps to become RA.[34] In the first reversible oxidation step, CRBP- retinol complex is recognized and then oxidized to retinal (or retinaldehyde) by short-chain retinol dehydrogenases (RDH).[35,36] The alternative way to produce retinal is from β-carotene. Similar to retinol, β-carotene is transported by lipoproteins and taken up by target cells. Then β-carotene is converted to retinal by β-carotene-15,15-dioxygenase (BCDO1).[37] The second oxidation step is the irreversible conversion of retinal to RA by retinal dehydrogenases: ALDH1A1, ALDH1A2, AND ALDH1A3 (also known as RALDH1, RALDH2, and RALDH3).[5,38–40]

Due to the tight regulation of RA needed throughout life, there are enzymes that can regulate the amount of RA within target cells. As mentioned earlier, the first oxidation step is reversible. If there is too much RA within the cell, retinal can be reduced back into retinol by

dehydrogenase/reductase 3 (DHRS3).[41] Furthermore, DHRS3 can convert the retinal derived from β-carotene into retinol which can be used to produce RA, transported or stored as retinyl esters if there is excess RA.[32,33(p3)] Another way to maintain the appropriate levels of RA within cells are cytochrome p450 enzymes of the CYP26 family, which oxidize RA to 4-oxo-RA and other more polar metabolites.[6,43]. Interestingly, CYP26A1 forms the primary metabolite of RA, 4-oxo-RA, a compound that is capable of binding to RARs and was proposed to have biological activity, but this activity does not seem to be required to sustain normal embryonic development.[44]

RA is transported from the cytosol to the nucleus by cellular retinoic acid binding protein (CRABP) 1 and 2.[45,46] Both CRABP 1 and 2 are present in mouse embryos at various stages in development and show specific patterns of distribution.[47] CRABP2 is more widely spread throughout embryogenesis and even found in structures not known to be specifically vulnerable to raised RA levels.[47] There is also evidence that CRABPs are also involved in targeting RA for degradation by CYP26 enzymes.[48,49(p1)]

The physiological functions of RA are mediated in the nucleus by a heterodimer composed of retinoic acid receptors (RARs), and retinoid x receptors (RXRs).[50,51] There are three separate RAR genes encoding nuclear receptor: RARα, RARβ and RARγ.[50] As well, there are three separate RXR genes encoding nuclear receptor: RXRα, RXRβ and RXRγ.[51] The RARs are able to bind both *all-trans*-retinoic acid and *9-cis*-retinoic acid, but the RXRs only bind to the *9-cis* isomer as well as other metabolites.[50,51] Each of these nuclear receptors have different spatial patterns of their expression. For example, RARα is expressed in the hindbrain, spinal cord, and eye; RARβ is expressed broadly; and RARγ is expressed most strongly in the skin.[52] In addition, RXRα is mainly expressed in the skin, liver, lung, muscle, kidney, epidermis, and intestine; RXRβ is the ubiquitously expressed; and RXRγ is predominantly found in brain, cardiac and skeletal muscle.[52]

The heterodimer of RAR and RXR regulate gene transcription through binding to RA response elements (RAREs) of target genes. In the absence of RA, RAR-RXRs associate with RAREs and repress gene expression through recruitment of co-repressors that include nuclear receptor corepressor (NCoR), silencing mediator of RA and thyroid hormone receptor (SMRT), histone deacetylases and methyltransferases. In contrast, when RA is present, it binds as a ligand to RARE-associated RAR-RXR and initiates transcription of target genes by disassociating the corepressors and recruiting co-activators that include steroid receptors (SRC-1, SRC-2 and SRC-3).[23] It should be noted that in some specific cases, RA binding may cause increased repression of target genes.[53]

1.1.2 Homeostatic Mechanisms of RA-signaling.

Cells and tissues employ multiple feedback mechanisms to govern the levels of retinol, retinal and RA. The key retinoid enzymes and receptors that were reviewed in the previous section are highly responsive and regulated by RA. In this section we will overview how RARb and RDH10, RALDH2, DHRS3, CYP26 enzymes are not only regulated by RA, but how they also regulate the amount of RA to allow for proper homeostasis.

In order to produce sufficient amounts of RA for proper homeostatic regulation, both RDH and RALDH enzymes are needed. A dysregulation in either RDH10 or RALDH2 leads to a deficiency in the amount of RA in embryos. *Sandell et al*. (2007), demonstrated that RDH10 plays a critical role in the oxidization of retinol to retinal in most embryonic tissues.[54] Using a forward genetic screen, they discovered a midgestational lethal mouse mutant, called trex, that had a mutation in *Rdh10*. Trex lacked the ability to oxidize retinol to retinal and displayed craniofacial, limb, and organ abnormalities, such as the heart.[54] R*hinn et al.* (2011) confirmed *Sandell* et al.

(2007) finding that *Rdh10* loss of function affects embryonic RA-signaling by crossing *Rdh10* mutants with RAR-hsp68-lacZ mice harbouring an RA-responsive transgene.[55] They found that the embryos completely lacked lacZ activity and therefore RA-signaling was severely downregulated in the absence of RDH10 function. As well, they reported that lack of RDH10 function affected endogenous RA target genes.[55]

There is extensive negative feedback regulation by RA on its own metabolism. Exogenous RA administration lead to a downregulation of *Raldh2* expression in some tissues, indicating that this enzyme is heavily regulated by its product.[38] As well, the expression of another RA-responsive gene, *Rarb*, was almost undetectable in *Rdh10*$^{-/-}$ embryos, which supports other observations that *Rarb* is highly regulated by RA-signaling.[55] *Rarb* is also regulated through changes in RALDH2 function. Treatment *of* pregnant *RARE-LacZ* reporter mice with WIN, a chemical inhibitor of RALDH2, not only caused 60% reduction in RA but also reduced RARE reporter activities and decreased expression of *Rarb*.[56] The most interesting finding from *Rhinn et al.* (2011) study was that maternal retinaldehyde supplementation in early fetal stages was able to rescue most phenotypic defects, leading to viable *Rdh10*$^{-/-}$ mice.[55] Further, retinaldehyde was able to rescue more *Rdh10*$^{-/-}$ embryos than RA, which hinted at a model where RDH10 and RALDHs are not only important for RA synthesis but for controlling embryonic RA distribution.[55] This shows the importance of controlling the level of RA during development.

CYP26 and DHRS3 enzymes also function in RA homeostasis by reducing RA levels. *Billings et al.* (2013) found that *Dhrs3*$^{-/-}$ embryos lead to a 40% increase in RA and a 60% to 55% decrease in retinol and retinyl esters, compared to their wild type littermates.[41] Furthermore, accumulation of excess RA from the *Dhrs3*$^{-/-}$ embryos is accompanied by a downregulation in *Rdh10, Raldh1, 2,* and *3,* while *Cyp26a1* was up-regulated.[41] Not only does DHRS3 regulate the

amount of RA, but RA is known to upregulate the expression of *Dhrs3* itself, which limits the amount of RA by increasing the rate of reduction of retinaldehyde to retinol.[42] Therefore, DHRS3 regulates RA biosynthesis through a feedback inhibition mechanism.[42] This feedback inhibition mechanism by DHRS3 is critical because *Dhrs3* deficiency causes late gestation/ perinatal lethality mice.[41] *Wang et al.* (2018) discovered that coronary vessel malformations in *Dhrs3*$^{-/-}$ embryos were solely due to *Dhrs3* ablation causing excessive RA because when Dhrs3$^{+/-}$ dams were fed a vitamin A deficient diet, it led to restoration of the vascular coverage in the Dhrs3$^{-/-}$ embryos and rescued the embryonic lethality of the *Dhrs3*$^{-/-}$ mice.[57] Like Dhrs3, CYP26 enzymes are highly responsive to RA.[43] When endogenous levels of RA are too high, *Cyp26* genes are activated to help degrade excess RA.[36] For example, when HepG2 Cells were treated with 1μM of RA there was an induction of *Cyp26a1* mRNA expression within 5 hours and by 12 hours there was a 100-fold change difference.[43] As well, C*yp26*$^{-/-}$ mutant embryos exhibit elevated RA in the domains in which *Cyp26* is normally expressed. A lack of CYP26 has also been found to impair the distribution of RA in tissues known to harbour RA and result in abnormal patterning that can lead to birth defects during development and embryonic lethality.[58]

In summary if there is too much RA the activity of DHRS3 would prevent more RA from being formed, while the activity of CYP26 enzymes degrade the excess RA. Both *Dhrs3* and *Cyp26* genes are upregulated in response to excess RA[30,34,35], while RDH and ALDH gene expression is reduced in the presence of excess RA.[44,60] Alternatively, if the levels of RA are too low, there would be an upregulation of RDH and ALDH enzymes to increase RA synthesis and maintenance.[36] Therefore, the RA signaling pathway is a very tightly regulated pathway. There are many enzymes that maintain the appropriate levels of RA. This is crucial because RA regulates gene expression that is needed for proper embryonic development and maintaining adult

homeostasis. Furthermore, in excess of 500 genes are thought to be regulated by RA.[9] As well, several of the proteins responsible for transporting retinol and RA are encoded by genes that are controlled by enhancer regions that contain RAREs.[18] This therefore provides additional opportunities for modulating vitamin A metabolism, and RA synthesis and signaling. In the next chapter another signaling pathway: the Hippo pathway, is introduced. Then we will discuss how proper regulation of both RA signaling and the Hippo pathway are crucial for cardiac development and regeneration. So far there is little evidence in literature supporting a relationship between the Hippo pathway and RA signaling, although both pathways are involved in the regulation of organ development.[61] Investigating whether there is a relationship between RA and YAP signaling during heart development will be the scope of this thesis.

1.2 Mechanisms of YAP activity

1.2.1 The Hippo Signaling and YAP

The Hippo signaling pathway is an evolutionarily conserved serine/threonine kinase signaling cascade originally identified in fruit flies.[62] The Hippo signaling pathway is most famously known for its ability to act as a tumour suppressor, and control organ size and development. In mammals, the core Hippo pathway is largely characterized by serine/ threonine kinases: mammalian Sterile 20-related 1 and 2 kinases (MST1 and MST2) and Large tumor suppressor 1 and 2 kinases (LATS1 and LATS2).[63]

As seen in Figure 2, the Hippo pathway begins when MST1 and MST2 form a heterodimer: MST1/2. The carboxyl terminus of both the MST kinases have a distinctive coiled-coil structure called the SARAH domain that mediates homo- and hetero-dimerization.[63] The SARAH domain is named after three genes that contain the homologous structures: Salvador

1(SAV1), Ras Association Domain Family Member 1 (RASSF1-6) and Hippo (MST1/MST2).[63] Mechanistically, there are two ways to activate the MST1/2. The first is by thousand and one amino acid (TAO) kinases (TAOK1/2/3), which phosphorylate the activation loop of MST1/2 (Thr183 for MST1 and Thr180 for MST2) and thereby lead to MST1/2 activation.[64] The second way to activate MST1/2 is by auto-activation through auto-phosphorylation on the activation loop at Thr183 and Thr180. Therefore, it is possible that MST1/2 activation can be initiated by dimerization and does not necessarily require upstream kinases. Active MST1/2 heterodimer phosphorylates and forms a complex with SAV1.[63] As well, MST1/2 activates Mps one binder (MOB) kinase activator 1A and 1B (MOB1A and MOB1B) by phosphorylation at Thr35 and Thr12. SAV1 and MOB1A1/MOB1AB act as scaffold proteins that allow the MST1/2-SAV1 complex to activate LATS1 and LATS2 by phosphorylation at Thr1079 and Thr1041, respectively.[63] As well, phosphorylation of MOB1A/MOB1B promotes its affinity to LATS1 and LATS2 creating a LATS1/2-MOB complex. This interaction leads to the auto-phosphorylation of LATS1/LATS2 at the activation loop (Ser909 at LATS1 and Ser872 at LATS2).[65] Therefore, in order for LATS1/2 to become active both phosphorylation by MST1/MST2 kinases and autophosphorylation of LATS are required.[63] LATS1/2-MOB complex will then phosphorylate the transcription co-activators Yes-associated protein (YAP) and Tafazzin (TAZ).[64] Phosphorylation of YAP and TAZ leads to cytoplasmic sequestration by 14-3-3 proteins or ubiquitin-mediated protein degradation.[63,66] When LATS1/LATS2 kinases are inactive, YAP/TAZ are not phosphorylated and translocate to nucleus and regulate gene expression through the TEAD family of transcription factors; specifically TEAD1-4. TEAD1-4 regulate the expression of genes involved in development, cell growth and proliferation, tissue homeostasis, regeneration, and suppress apoptosis.[63] Loss of any of the core Hippo-pathway components such

as MST1/MST2, Salvador-1, LATS1/2, MOB1A/MOB1B will cause an upregulation of YAP/TAZ-TEAD target gene transcription.[63]

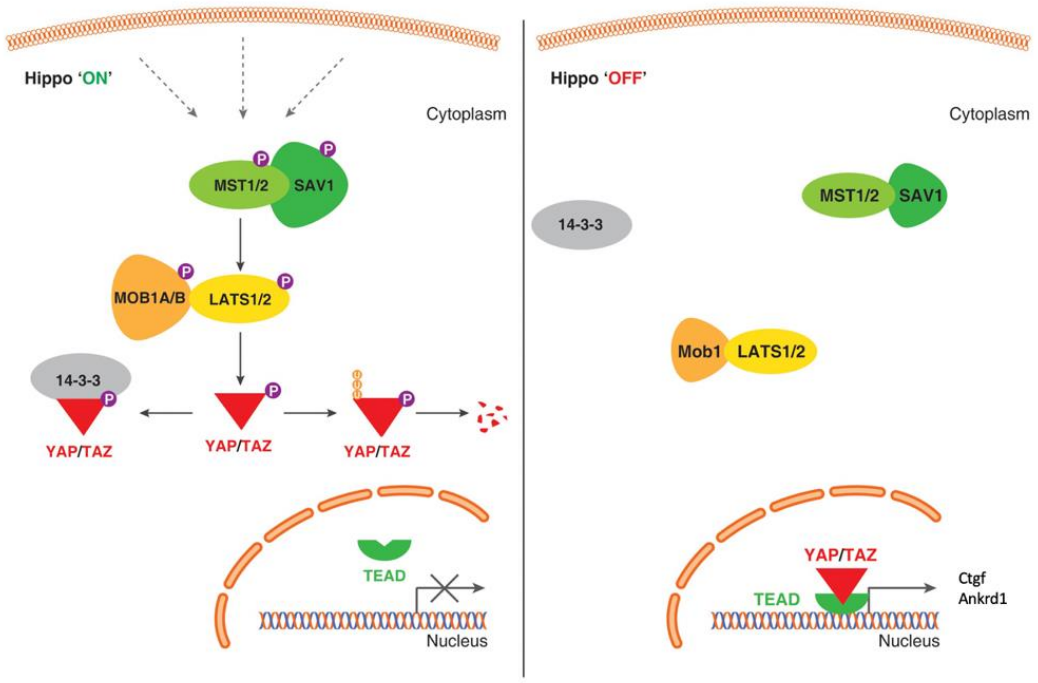

Figure 2: Summary of the Hippo pathway (modified from Boopathy and Hong (2019).[63] When upstream regulators activate the Hippo pathway a phosphorylation cascade occurs. MST1/2 and SAV1 heterodimer phosphorylate the Mob1 and LATS1/2 heterodimer that then subsequently phosphorylate YAP/TAZ co-activators, which causes their deactivation as they are sequestered in the cytoplasm. When the Hippo pathway is deactivated, YAP/TAZ are no longer phosphorylated and can enter the nucleus where they interact with TEAD to regulate gene transcription.

This thesis will focus on YAP activity. Since YAP was first isolated in 1995 by Marius Sudol, it has been discovered that YAP is involved in many regulatory mechanisms.[67] Genome-wide analysis of YAP transcriptional targets both in vivo and invitro have led to the identification of important target genes used to monitor YAP activity such as connective tissue growth factor (CTGF), Cysteine-rich angiogenic inducer 61 (CYR61), Ankyrin Repeat Domain 1 (ANKRD1),

and etc.[68] Not only does YAP regulate many genes, many mechanisms regulate YAP activity, such as epithelial to mesenchymal transition (EMT), mechanotransduction, and cell contact. In the next section these mechanisms that regulate YAP will be discussed.

1.2.2 Epithelial to Mesenchymal Transition and YAP Activity

Epithelial cells commonly rest on a basal lamina, and cell-cell and cell-basal lamina contact stabilize and coordinate the epithelial architecture. As well, cell-cell junctions are important to maintain epithelial cell and tissue polarity and integrity. There are three intercellular junction systems: gap junctions, tight junctions, and anchoring junctions. Gap junctions serve as intercellular channels that permit direct cell-cell transfer of ions and small molecules. Tight junctions act as an epithelial barrier. Anchoring junctions associate with the cortical cytoskeleton to mediate cell and tissue behaviour and include desmosomes and adherens junctions.[69] In contrast to epithelial cells, mesenchymal cells lack tight and adherens junctions to have an amoeboid or stellate morphology that allows their movement as individual cells through the extracellular matrix. Mesenchymal cells are also capable of differentiating into a number of distinct cell types making them developmentally pliable. To undergo EMT, an epithelial cell must disassemble the cell-cell junctions that connect it to neighboring cells, lose epithelial cell polarity and undergo cytoskeletal and gene expression changes to acquire a motile phenotype.[70] For example, the downregulation of the epithelial cell adhesion protein, E-cadherin, is a key event in EMT because E-cadherin forms intercellular junctions and participates in intracellular signaling pathways that promote epithelial identity and repress mesenchymal activity.[69] Finally, expression of extracellular matrix remodelling enzymes facilitate breakdown of the basement membrane, permitting the mesenchymal cell to exit the epithelium and migrate into sub adjacent tissue.

EMT regulates YAP activity via the Hippo-pathway. Epithelial architecture, characterized by cell-cell junctions and apicobasal polarity, is a potent suppressor of YAP activity by activating the Hippo cascade.[71,72] Disruption of tight junctions or adherens junctions by EMT turn on YAP/TAZ nuclear activities.[71] Specifically, the *E-Cadherin-catenin complex* is a type of adherens junction that plays an important role in maintaining epithelial integrity.[69] Disruption of the E-cadherin/ catenin complex leads to a decrease in cell-cell junction adhesion and increases cell migration and invasiveness.[73] *Kim et al.* (2011) demonstrated that E-cadherin/ catenin complex functions as an upstream regulator of the Hippo cascade and YAP/TAZ in mammalian cells.[73] Another EMT associated protein that regulates the Hippo cascade and YAP/TAZ is the key cell polarity determinant, Scribble. When Scribble is localized to the membrane, it acts as an adaptor to assemble a protein complex consisting of MST, LATS and YAP or TAZ, which promotes the phosphorylation and inactivation of YAP and TAZ.[74,75] EMT triggers Scribble delocalization from the membrane and localization in the cytoplasm, which inactivates the Hippo cascade inducing YAP/ TAZ activity.[74,75] Not only does EMT induce YAP and TAZ, but YAP and TAZ promote EMT in both cancer and non-cancerous cell phenotypes.[76]

1.2.3 Mechanotransduction and YAP activity

In the body, the mechanical environment of a cell varies depending on the type of tissue, the composition and stiffness of the surrounding substrate, and the amount of space available. In order to adapt to their environments, cells have the ability to sense their three-dimensional environment by interpreting physical forces, such as shear, tensile, and compression stress. These forces can be generated in response to physical properties like substrate stiffness, cell contractility, and forces generated by adjacent cells. These mechanical cues have important roles in cell fate

decisions regarding proliferation, survival, and differentiation as well as regeneration and wound repair.[77] Defects in the cells ability to respond to mechanical cues and/ or inadequate remodelling of the extracellular space can cause various disease states; for example, fibrosis.[77] Cells respond to mechanical cues by the process of mechanotransduction. Mechanotransduction is the process of sensing and translating mechanical forces into biochemical signals, like activating signaling cascades and genes.[77] A cell uses both the Hippo-pathway and YAP/TAZ to sense and respond to mechanical stimuli such as cell density, cell area, tissue stretch, shear forces, and substrate stiffness. The ability of the cell's mechanical machinery, such as focal adhesions, the actin cytoskeleton, and cell-cell junctions to regulate YAP/TAZ will be discussed.

Mechanoresponsive structures in the cell, such as focal adhesions and cell-cell junctions regulate the Hippo-pathway and YAP/TAZ. Focal adhesions are mechanoresponsive structures that act as a bridge between integrins and the cell's actomyosin cytoskeleton to promote signaling. Integrins are transmembrane proteins that connect cells to their substrates. Focal adhesions are known to sense and respond to mechanical tension to promote cell spreading and migration based on substrate stiffness.[78] *Meng et al.* (2018) , discovered that focal adhesions inhibit the Hippo pathway and promote YAP/TAZ activity to increase proliferation and survival when cells are on stiffer substrates.[79] As well, *Meng et al.* (2018) compared gene expression profiles of HEK293A cells on stiff versus soft substrates and discovered that the majority of the mechano-responsive gene expression changes depended on YAP/TAZ and LATS1/2.[79] Therefore, Hippo signaling and YAP/TAZ play a central role in transcriptional regulation in response to changes in substrate stiffness. Later studies concluded that the ability of focal adhesion signaling to regulate the Hippo pathway and YAP/TAZ is driven by many complex pathways, such as FAK signaling.[80]

The actin cytoskeleton is known to be highly responsive to mechanical stress. *Gupta et al.* (2015) discovered that focal adhesions are involved in the mechanical regulation of the actin cytoskeleton.[81] On soft substrates, cells form smaller focal adhesions and the actin cytoskeleton turns fluid due to disorganization of fibers. However, on stiffer substrates focal adhesions form stable links with actin, which promotes solidification and orientation.[81] Interestingly, research has uncovered that the Hippo pathway and YAP/TAZ may be able to indirectly sense and respond to changes in the mechanical environment by monitoring the actin cytoskeleton. Therefore, focal adhesions may also affect YAP activity by their ability to regulate the actin cytoskeleton. For example, when *Dupont et al.* (2011) increased filamentous (F)-actin, by knock-down of actin cytoskeleton regulators, nuclear YAP/TAZ and YAP/TAZ targeted gene expression was increased.[68] Later, it was determined that disassembly or loss of F-actin filaments results in LATS1/2 phosphorylation and activation, which inhibits YAP as it sequesters it in the cytoplasm. Mechanistically, F-actin can influence YAP/TAZ activity through both Hippo pathway (LATS1/2)-dependent[82,83] and independent mechanisms[68]. Angiomotins (AMOT) in conjunction with neurofibromatosis 2 (NF2) are able to control Hippo-pathway and YAP activity in response to F-actin levels.[84] Angiomotins (AMOT) and neurofibromatosis 2 (NF2) are both up-stream regulators of the Hippo-pathway. AMOT is able to regulate YAP in both a Hippo pathway-dependent and independent manner; AMOTs are capable of inhibiting YAP through direct interaction or phosphorylation of LATS1/2.[85] A model has been proposed where high F-actin levels cause AMOT to bind to F-actin, which impairs AMOT ability to bind to YAP and promote LATS1/2 activity.[86] When F-actin levels decrease AMOT are free to inhibit YAP directly or by LATS1/2 activation. As well, AMOT can also bind to NF2, which stimulates NF2 association to LATS1/2. NF2's role is to recruit LATS1/2 to the plasma membrane, where it is activated by MST

kinases.[87(p2)] Lastly, F-actin disruption has been found to stimulate NF2 interaction to LATS1/2, which also inhibits YAP. In the next section, cell-cell junctions' ability to mechanically regulate YAP/TAZ through a process known as cell contact inhibition of proliferation will be discussed.

Finally, YAP/ TAZ not only respond to mechanical stimuli, but also function as mediators of a cell's mechanical response.[68] For example, YAP/TAZ are able to control cell fate in response to mechanical stimuli. *Dupont et al.* (2011) discovered that the ability of substrate stiffness to control cell-type specific differentiation in mesenchymal stem cells (MSCs) depends on the proper regulation of YAP/TAZ. MSCs will differentiate into distinct tissue types depending on their mechanical environment. MSCs cultured on a stiff matrix that mimics collagenous bone become osteogenic, whereas, on softer matrices MSCs differentiate into adipocytic lineages.[88] When *Dupont et al.* (2011) cultured MSCs depleted of YAP/TAZ on stiff substrates, the MSCs were unable to differentiate into an osteogenic lineage and instead underwent adipogenic differentiation, similar to MSCs grown on a soft substrate. Therefore, mechanotransduction is a major regulator of YAP activity.

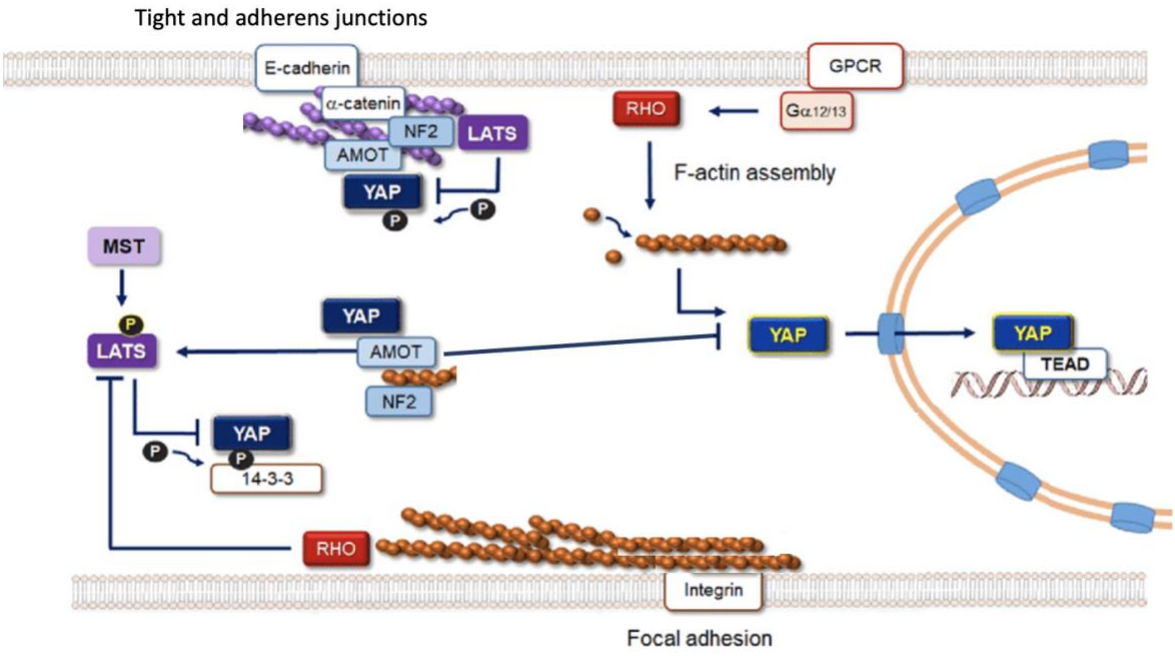

Figure 3: Overview of how mechanical signaling regulates YAP activity modified from Seo and Kim (2018).[89] Actin Filaments associated with the tight and adherens junctions negatively regulate YAP/TAZ activity, while stress fibers associated with focal adhesions promote nuclear YAP/TAZ localization. The activation of RHO GTPases either by GPCRs or from mechanical stimuli at focal adhesion promote F-actin assembly and YAP/TAZ nuclear localization. Oppositely, F-actin capping and severing factors inhibit the activity of YAP/TAZ. AMOT and NF2 cause both cytoplasmic retention and phosphorylation of YAP/ TAZ by LATS.

1.2.4 Cell Density and YAP Activity

Zhao et al. (2007) discovered that YAP and TAZ are regulated by contact inhibition of proliferation (CIP).[66] CIP is a property where non-malignant cells at high-cell density cease proliferation and cell division when they occupy all the space allocated to them upon reaching confluence.[90] CIP is a well-known property of normal differentiated tissues and needs to be tightly regulated for proper tissue morphogenesis.[73] Contact inhibition is overcome in rapidly growing tissues during embryonic development, tissue regeneration, and wound healing.[73] Pathologically, loss of CIP is a hallmark of cancer, as it leads to uncontrolled cell growth and increase the ability

of cells to invade host tissues.[90] *Zhao et al. (2007)* showed that YAP and TAZ are nuclear and active in non-malignant cells growing at low density but become mostly cytoplasmic in confluent cultures.[66] It was also found that the Hippo pathway is activated in the course of CIP.[66]

Aragona et al. (2013) uncovered a two-step mechanism of how cell-cell contact affects YAP/ TAZ activity. The first step is when cells make contact with each other, the E-cadherin/ catenin complex triggers LATS activation and YAP/TAZ phosphorylation. However, this contributed to only about 30% of growth inhibition and YAP/TAZ relocation to the cytoplasm, which led to the conclusion that cell-cell contact partially inhibits YAP/TAZ activity through Hippo-signaling but leaves a sufficient amount of active YAP/TAZ for proliferation. Therefore, for YAP/TAZ nuclear exclusion to occur a secondary mechanical inhibitory step is needed. As the cells continue to proliferate, cell crowding in a monolayer causes individual cells to be boxed into a smaller area. This reduced cell spreading impairs YAP/TAZ by a mechanical pathway, similar to the effects seen when single cells are plated on a small or soft extracellular matrix. *Aragona et al.* (2013) came to the conclusion that the remodelling of the F-actin cytoskeleton mediated by F-capping and severing proteins Cofilin, CapZ, and Gesolin caused an inhibition in YAP/TAZ activity in a mechanical nature. Finally, Aragon et al. also discovered that cells have the ability to "read" the architectural topology of a tissue as patterns of mechanical stress and translate this into differences in YAP/TAZ activity. Tissue conformation, as in the rigidity of the extracellular matrix, may use YAP/TAZ-mediated mechanotransduction to template the patterns of cell proliferation and growth arrest within an epithelial monolayer.[71,91] In conclusion when cells are at low density and are flat/ well-spread on a stiff extracellular matrix, YAP/TAZ localize to the nucleus and are transcriptionally active. However, when cells are round/ compact at high-cell

density or plated on a soft matrix with minimum adhesion area to the extracellular matrix, YAP/TAZ are re-distributed to the cytosol and are inactive.[90]

In this section some of the main mechanisms of regulating YAP, that are important to this thesis have been discussed. These mechanisms include the Hippo pathway, EMT, mechanotransduction, and contact inhibition of cell proliferation. One problem for research investigating mechanical regulation of YAP, has been that each one of the YAP/TAZ regulatory pathways likely affects multiple other YAP/TAZ pathways. Therefore, mechanical regulation of YAP/TAZ is very complex. Some pathways that mechanically regulate YAP have been discussed, but there are many other mechanical mechanisms that are outside the scope of this thesis. This thesis will briefly investigate the effect of stiffness and cell density mechanical signaling on retinoids in embryonic epicardial cells.

1.3 The Role of the Epicardium, YAP, and RA-signaling During Cardiac Development

1.3.1 Heart Anatomy and Function

The mammalian heart is a complex muscle that pumps blood through three divisions of the circulatory system: the coronary, pulmonary, and systemic.[2] Coronary circulation takes blood directly from the aorta and has intrinsic vessels that serve the heart. Pulmonary circulation pumps blood to the lungs to be oxygenated and then returns the oxygenated blood to the heart to be pumped through the rest of the body through systemic circulation. In one day alone the heart contracts 108,000 times and pumps 14,000 liters of blood.[93] A typical heart is approximately the size of your fist and is similar to a pinecone shape as it has a broad superior surface that tapers to the inferior tip, the apex. The heart is located within the thoracic cavity, medially between the lungs in a space known as the mediastinum. The heart is separated from other mediastinal

structures by being encompassed within a tough membrane known as the pericardial sac, which surrounds the pericardial cavity.

As seen in Figure 4, the pericardium is a double layered membranous sac covering the heart.[94] The heart is invested in the visceral pericardium, also known as the epicardium. The epicardium is a macroscopic layer of simple squamous epithelium called the mesothelium, which is fused to the heart and is the first layer of the heart wall. There are three layers to the heart wall, from superficial to deep: epicardium, myocardium, and endocardium. The myocardium is the middle and thickest layer and composed largely of cardiac muscle cells built upon a framework of collagenous fibers, blood vessels, and nerves that supply and regulate the heart respectively. The innermost layer is the endocardium and it lines the chambers where blood circulates and lines the valves.

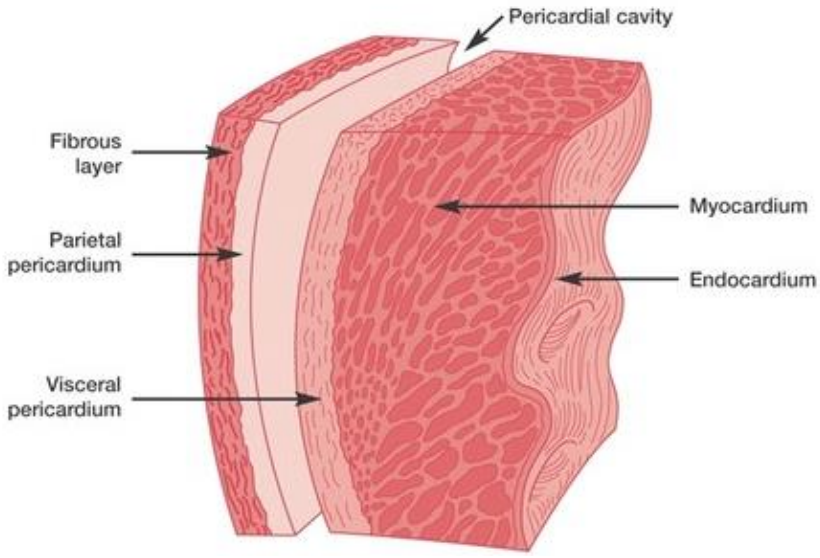

Figure 4: Illustration of the anatomy of the heart wall.[95]

1.3.2 Heart Development- The Epicardium

The human heart is the first functional organ to develop, as it begins to form at days 18-19 after fertilization and arises from the mesoderm.[96] The mesoderm is one of the three primary germ layers that differentiates to give rise to all tissues and organs. Early in development, the heart is simply a tube-like organ, referred to as the heart tube and is only built of only endothelial and myocardial cell lineages.[94,97] Interestingly, majority of other cell lineages present in the mature heart originate from progenitor cell populations outside the heart tubule. The epicardium is not present at the tubular heart stage as it is derived from a cauliflower-like extra-cardiac mesothelial cell cluster known as the proepicardium. The proepicardium arises from the pericardial coelomic mesothelium, which is a structure that buds out of the septum transversum in close proximity to the primitive heart tube and liver.[98,99] The proepicardium is heterogenous; the outer layer contains cuboidal epithelial cells expressing Wilm's tumour 1 (WT1) and the inner core has extracellular matrix harbouring several mesenchymal and endothelial cell types. Commonly WT1 with T-box transcription factor (Tbx18) and the basic helix-loop-helix transcription factor (Tcf21) are used to identify the proepicardium.[100] To understand the importance of the proepicardium, studies have impaired the proepicardium during development by microsurgical or genetic inhibition and this resulted in reduced proliferation of cardiomyocytes and a thin-walled myocardium.[97,101]

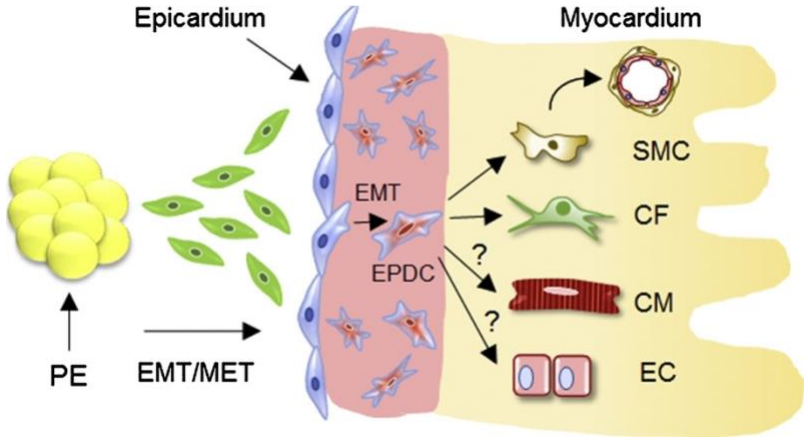

Figure 5: Formation of the epicardium and epicardial cell lineages during embryonic heart development from *Smits et al.* (2017).[94] The pro-epicardium (PE) undergoes EMT and migrates to the heart. Once PE cells cover the heart, they undergo MET to transform into epicardial cells creating a single layer epicardium. Next, epicardial cells will undergo a second round of EMT to migrate into the sub epicardial space (pink layer) and differentiate into epicardial derived cells (EPDCs). EPDCs will continue to migrate into the myocardium where they differentiate into vascular smooth muscle cells (SMCs) that form blood vessel and cardiac fibroblasts (CF) that help maintain the integrity and rigidity of the heart. The differentiation of EPDCs into cardiac myocytes (SM) and endothelial cells (EC) is still up for debate in literature.

Once the heart tube begins to loop, proepicardial cells undergo a process of epithelial to mesenchymal transition (EMT) and translocate to the heart. As seen in Figure 5, the proepicardial cells will adhere, migrate and proliferate by undergoing a reverse process of mesenchymal to epithelial transition (MET) to form a squamous epithelial layer around the heart, known as the epicardium. The epicardium completely covers the heart around E11.5 in mouse[46] and week 5 during human cardiac development.[103] The intimate relationship of epicardium to myocardium and nascent coronary vasculature uniquely position it to regulate myocardial growth and coronary vessel development.[104] Once the epicardium covers the developing heart it will start to produce paracrine factors that support myocardial growth.[105] These factors provide an essential exchange of signals between the epicardium and the myocardium so that the coronary vessels can properly develop, and the heart muscle can differentiate.[106] For example, *Stuckmann et al.* (2003)

established a E10 day old chick embryo heart slice culture and observed that a blockade of either retinoic acid or erythropoietin signaling in the epicardium inhibits cardiac myocyte proliferation and survival. This study also noted that retinoic acid and erythropoietin do not act directly on myocardial cells rather induce other factors that regulate proliferation of cardiomyocytes.[105]

Some of the cells within the epicardium will undergo a second round of EMT and form mesenchymal cells known as epicardium derived cells (EPDCs).[70] Many myocardial- and epicardial-derived growth factors regulate epicardial EMT, such as Transforming growth factor β (TGFβ)[107], Platelet Derived Growth Factor (PDGF)[108], and Fibroblast Growth Factor (FGF).[109] EPDCs will then invade the subepicardial matrix (Pink layer in Figure 5). From the subepicardium, EPDCs will migrate into the myocardial interstitium where they can be differentiated into several lineages of the heart.

Intense investigation has also focused on the fate of EPDCs. As illustrated in Figure 5, it is known that EPDCs become vascular smooth muscle cells (SMCs) that form the coronary arteries and interstitial fibroblasts of the myocardium and endocardial cushions.[110] Cardiac fibroblasts (CFs) are the main cell type that synthesize and maintain the ECM in the heart and provide the support for all heart structures and cell types.[111] *Dettman et al.* (1998), demonstrated the epicardial origin of CFs by grafting LacZ stained quail epicardial cells onto chicken hearts.[112] In vivo tracking found that the LacZ stained quail epicardial cells invaded the sub-epicardial space and myocardium, before forming the vascular smooth muscle cells of the coronary walls, as well as perivascular and intramyocardial fibroblasts.[112] Studies in recent years have used genetic fate-mapping in mice to confirm that a large portion of EPDCs differentiate into vascular smooth muscle cells and cardiac fibroblasts.[94,110] The differentiation of cardiac endothelial cells (ECs) and cardiomyocytes (CMs) from EPDCs is still up for debate.

It is quite clear that the epicardium is essential for cardiac development as it contributes both EPDC and paracrine factors that contribute to the myocardium and eventually the angiogenesis and overall structure of the heart. For the rest of this section, we will discuss the role of both epicardial RA-signaling and Hippo signaling for EPDC fate determination and proper cardiac development.

1.3.3 The Role of Epicardial Retinoic Acid in Heart Development

The embryonic epicardium is a major source of cardiac RA by expressing the main embryonic RA biosynthetic enzyme retinaldehyde dehydrogenase type II (RALDH2).[113,17] The embryonic epicardium also produces RARs and RXRs and is capable of active RA signaling.[52,114] Studies from mouse models have shown RA signaling plays a role in epicardial EMT mediated by WT1.[115,116] *Guadix et al.* (2011) showed that when *Wt1* was knocked out in epicardial cells, there was a decreased expression of *Raldh2* both in vivo and in vitro. As well, the *Wt1*-null epicardial cells showed a reduction in the synthesis of RA confirming the decrease in RALDH2. Further *Guadix et al.* (2011) demonstrated that Raldh2 is a direct transcriptional target of WT1 in epicardial cells. Since *Wt1*-null epicardial RA levels were significantly reduced, *Guadix et al.* (2011) investigated whether the RA decrease actually affected RA-related receptors known to be important for epicardial and EPDC development such as RXRα, PDGFRα and PDGFRβ. PDGFRβ-positive EPDCs migrate out of the epicardium and differentiate into VSMCs and pericytes. PDGFRα-positive EPDCs contribute to the coronary and interstitial fibroblast populations. PDGFRα and PDGFRβ mRNA and protein levels were downregulated in the absence of *Wt1*, but only *Pdgfra* expression was rescued by the addition of RA to *Wt1*-null epicardial cells.[116] Therefore, *Guadix et al.* (2011) discovered that WT1 is critical for the regulation of

RALDH2 during epicardial activity during embryonic development. *Gise et al.* (*Von* 2011) confirmed the findings of *Guadix et al.* (2011) by also observing a decrease in Raldh2 gene and protein expression when *Wt1* was knocked out in the mouse embryonic heart.[115] As well, *Raldh2* loss of function resulted in abnormalities of cardiac growth and coronary development similar to those in *Wt1*-null embryos.[117] The above studies indicate that there is a definite link between epicardial EMT and RA-signaling because of the link between RA-signaling enzymes and epicardial EMT promoting factors such as WT1, PDGFRα, and PDGFRβ. Another epicardial derived factor that can be regulated by RA-signaling is fibroblast growth factor 9 (FGF9).[109] When Lavine et al. (2005) treated both organ culture and primary epicardial cells with RA there was an upregulation in Fgf9 expression.[109]

Wang et al. (2018) discovered that both deficiency and excess of RA affect the migration of EPDCs *in vivo*. To create an RA deficient model, mouse embryos were subjected to treatment with WIN, which is a pharmacological inhibitor of RALDH2. WIN treated embryos did not survive past E14.5 and had many cardiac deformations such as reductions in ventricular coverage and density of coronary vessels, altered vessel morphology, and impaired recruitment of epicardial-derived mural cells.[57] The epicardial cells and EPDCs of the WIN treated vs DMSO control embryos were immunostained with the epicardial markers WT1, PDGFRα, and PDGFRβ. At E14.5 WIN-treated embryos showed a 50% reduction in WT1-positive infiltrating EPDCs in the myocardium compared to control embryos; this suggested that WIN delayed the migration of EPDCs. Similarly, both PDGFRα and PDGFRβ- positive EPDCs remained confined in the epicardial epithelium and subepicardial space, while they migrated to the myocardium in the controls. Next, *Wang et al.* (2018) investigated an RA excess genetic mouse model *Dhrs3*$^{-/-}$, which lacks the DHRS3 enzyme that maintains RA homeostasis by converting the RA precursor,

retinaldehyde, to retinol.[41] *Dhrs3*$^{-/-}$ embryos accumulate excess RA at E14.5 and also display cardiac malformations and embryonic lethality.[41] Interestingly the *Dhrs3*$^{-/-}$ embryos have the same heart malformations seen in the WIN-treated embryos.[57] Alternatively, there was a 2-fold increase in the WT1-positive infiltrating EPDCs in the myocardium of *Dhrs3*$^{-/-}$ embryos compared to wild type littermates; this suggested that excess RA in *Dhrs3*$^{-/-}$ hearts altered migration ability and or timing of the invasions of EPDCs. As well there was an increase and deeper myocardial localization of PDGFRα and PDGFRβ- positive EPDCs, however, the epithelial marker, *Cdh1*, was downregulated in E13.5 *Dhrs3*$^{-/-}$ hearts compared to the *Dhrs*$^{+/+}$ littermates. Together this indicated that EPDCs in *Dhrs3*$^{-/-}$ embryos migrate earlier, or more efficiently than the control littermates and thus are found localized deeper within the myocardium; which is the exact opposite to the WIN-treated embryos.

Another observation made by *Wang et al.* (2018) was that inhibition of RA synthesis impairs the response of epicardial cells to PDGFBB. When PDGFBB, an agent known to stimulate epicardial EMT as a ligand for PDGFRα and PDGFRβ, was added to the embryonic epicardial cell line, MEC1, it stimulated cytoskeletal reorganization, loss in expression of the epithelial marker, ZO-1 and accumulation of F-actin. If RA-synthesis was blocked with WIN before PDGFBB was added to the MEC1 cells, the WIN treatment counteracted the ZO-1 changes seen with just MEC1 treated with PDGFBB. Alternatively, *Wang et al.* (2018) activated RA-signaling in MEC1 cells by treatment with pan-RAR agonist TTNPB and observed that RA-signaling facilitates cytoskeletal arrangement. When TTNPB was added to MEC1 cells, there was active expression of ZO-1 found on the cell membrane, accumulation of F-actin polymerization, downregulation of epithelial marker Cdh1, and upregulation of the mesenchymal marker Cdh2 and the positive epicardial EMT-positive regulator Axin2; which was all consistent of cytoskeletal rearrangement. Finally, after

inducing cytoskeletal reorganization with TTNPB in MEC1 cells, *Wang et al.* (2018) performed transcriptome profiling to survey the expression of a wide array of genes. This analysis revealed that RA signaling affects a multitude of pathways in MEC1 cells, including many implicated in the formation and differentiation of EPDCs, such as cell cycle, focal adhesion, and Hippo signaling.[56] In conclusion, *Wang et al.* (2018) confirmed that RA-signaling is critical for epicardial EMT during heart development. The next section will discuss the role of the Hippo-pathway, specifically YAP in the development and differentiation of EPDCs.

1.3.4 The Role of Epicardial YAP in Heart Development

Singh et al. (2016) discovered a critical role for YAP/ TAZ activity in the epicardium during cardiac development. First, they discovered that Hippo signaling components are expressed in the developing mouse pro-epicardium and epicardium.[118] YAP immunohistochemistry was performed on embryonic hearts at ages E9.5 to E12.5.[118] At E9.5 YAP was noted in the pro-epicardium, where it co-localized with TBX18.[118] At the later ages YAP was expressed in the epicardium and co-localized with WT1 expressing epicardial cells. Next, RT-qPCR gene expression analysis performed on RNA harvested from embryonic epicardial explants revealed that YAP, TAZ, and TEAD1-3 are expressed in epicardial cells; however, TEAD 4 was barely detectable. As well, with the embryonic epicardium explants, western blotting demonstrated that Hippo kinases LATS1 and LATS2 are expressed in epicardial cells.[118]

Next *Singh et al*. (2016) created an epicardial *Yap* and *Taz* deleted mouse model to determine the role of YAP and TAZ in the epicardium. Conditional $Yap^{flox/flox}$ and $Taz^{flox/flox}$ alleles were crossed with a $Sema3d^{GFPCre/+}$ knockin mouse, thereby targeting Cre-recombinase to the pro-epicardium and epicardium.[118] SEMA3d is expressed by many pro-epicardial progenitors.

Breeding of *Sema3d*$^{GFPCre/+}$: *Yap*$^{flox/+}$*:Taz*$^{flox/+}$ *and Sema3d*$^{GFPCre/+}$: *Yap*$^{flox/flox}$*:Taz*$^{flox/flox}$ revealed that epicardial inactivation of *Yap* and *Taz* are embryonically lethal at E11.5 and E12.5.[118] As well, Yap played the dominant role as loss of both *Yap* alleles in a *Taz* heterozygous background is lethal, while loss of *Taz* in *Yap* heterozygous background produced viable mice.[118] Next immunostaining at E11.5 for cardiac marker MF-20 showed that the myocardium was thin and fragmented in the mutant *Yap* and *Taz* hearts but not in the controls.[118] Immunostaining with Ki67 showed a significant reduction in epicardial cell proliferation compared to the controls.[118] However, the E10.5 mice mutant was not physiologically different from its control and the epicardium was intact, suggesting that YAP and TAZ are not required for the initial migration of proepicardial cells in the heart.[118] To determine that the reduced myocardial thickness in the mutants was due to impaired epicardial-myocardial signaling, the expression of paracrine factors known to regulate myocardial growth was observed. Significantly lower expression of Fgf9, Raldh2, and Wnt5a was observed in the mutants when compared to the controls.[118] As well, Singh *et al*. used a inducible *Wt1*$^{CreERT2/+}$ mouse to allow for the assessment of older *Yap*$^{flox/flox}$*:Taz*$^{flox/flox}$ epicardial-deleted embryos. Cre-recombinase activity was induced at E11.5, and E15.5 *Wt1*$^{CreERT2/+:}$ *Yap*$^{flox/flox:}$*Taz*$^{flox/flox}$ showed fewer primitive vessels than the control indicating that Yap and Taz are required for patterning and/or remodelling of the coronary vasculature.[118] As well, further experiments with this same model indicated a significant reduction in migrating EPDCs and reduced epicardial contribution to endothelial cells, smooth-muscle cells, and fibroblasts' suggesting a defect or delay in fate determination.[118] Finally, *Singh et al*. discovered that there is TEAD binding sequences in the promoters of both *Tbx18* and *Wt1* and YAP strongly activates both *Wt1* and *Tbx18*. In conclusion Singh *et al*. found that YAP and TAZ regulate epicardial cell proliferation, EMT, and cell fate specification, in part by regulating Tbx18 and Wt1 expression.[118]

Alternatively, from *Singh et al.* (2016), *Xiao et al.* (2018) created an upregulated epicardial YAP activity model by knocking out *Lats1/2* in the epicardium of embryonic mice using the $Wt1^{CreERT2}$ allele called *Lats1/2* conditional knockout (CKO). *Lats1/2* CKO embryos did not survive past E15.5 and their heart at E14.5 had reduced vessel coverage and density when compared to the control embryos.[61] Further to ensure the coronary vasculature defects was due to an increase in YAP activity from genetic knockout of *Lats, Xiao et al.* (2018) genetically reduced *Yap* and *Taz* in the *Lats1/2* CKO embryos by generating a $Wt1^{CreERT2}$:$Lats1/2^{f/f}$: $Yap/Taz^{f/+}$ mouse model.[61] When *Yap* and *Taz* were genetically reduced in the *Lats1/2* CKO embryos, they were viable past E15.5 without major coronary vasculature defects indicating that LATS1/2 kinases are required for normal coronary vessel development by restricting YAP activity.[61]

Next *Xiao et al.* (2018) used drop-sequencing to profile cardiac tissue from control and *Lats1/2* CKO E13.5 and E14.5 embryos with 18,166 single cells. A designated cluster 20 (C20) in the *Lats1/2* CKO epicardium showed statistically significant enrichment compared to the control.[61] C20 possessed a gene intermediate between that of fibroblasts and the epicardium, as C20 cells expressed Tcf21, which is essential for epicardial-derived fibroblast development.[119] As well, immunofluorescent data showed that C20 cells are localized to the sub-epicardial space.[61] Further drop-sequencing data discovered a reduction in cardiac fibroblasts in E14.5 *Lats1/2* CKO hearts.[61] The drop sequencing data in total suggested a defect in epicardial-to-fibroblast transition.[61] Another interesting finding from the drop-sequencing profile was gene ontology (GO) analysis found that C20 cluster was enriched for YAP-TEAD direct target genes and genes involved in ECM organization, regulation of cell migration, and blood vessel development. To validate the drop-sequencing data *Xiao et al.* (2018) performed immunofluorescent experiments based on epicardial markers expressed in the C20 population of cells. PDGFR-α, a marker for fibroblasts

and the sub-epicardium mesenchyme was expressed in a single layer within the E14.5 control subepicardium, while in *Lats1/2* CKO hearts PDGFR-α was expressed in a several-layer thick subepicardium containing C20 cells.[61] Another experiment by *Xiao et al.* (2018) was to lineage trace epicardial-derived lineages by using *Rosa26*^{mTmG} reporter. Concurrent labelling of the E14.5 *Wt1*^{CreERT2} lineage with *Rosa26*^{mTmG} and PDGFR-α to mark cardiac fibroblasts, revealed by both immunofluorescence and fluorescence-activated cell sorting (FACS) that there was a reduction in epicardial-derived fibroblasts; which supported the drop-sequencing results.[61] As well, coronary artery smooth muscle differentiation was also examined with the same techniques but targeting PDGFR-β, to mark vascular smooth muscle cells.[61] This experiment uncovered that there was a reduction of E14.5 epicardial-derived smooth muscle cell progenitors, suggesting that smooth muscle lineage differentiation from the epicardium was diminished in *Lats1/2* CKO hearts. The drop-sequencing and immunofluorescence data together suggested that without *Lats1/2* activity, epicardial cells undergo EMT and transform into EPDCs, but EPDC differentiation to fibroblasts and vascular smooth muscle cells is impaired.[61] Therefore, the findings of both *Singh et al.* (2016) and *Xiao et al.* (2018) revealed that YAP activity is required for proper cardiac development because both upregulated and downregulated *Yap* genetic mouse models had defective development of the myocardium and coronary vasculature.[118,61]

1.5 Hypothesis and Aims

Research suggests that epicardial-derived RA plays important roles in cardiac developmental and regenerative processes, but many of the mechanistic details are still missing.[56] So far this thesis has discussed how both YAP and RA-signaling are critical for proper epicardial EMT progression and EPDC cell fate determination. Interestingly, *Xiao et al.* (2018) discovered a

potential link between YAP and RA-signaling by observing TEAD motifs in the *Dhrs3* gene within the mouse embryonic heart. As well, in the MEC1 epicardial cell line, YAP showed specific binding to the *Dhrs3* loci when YAP chromatin immunoprecipitation combined with qPCR at TEAD motifs were analyzed. Furthermore, *Dhrs3* was upregulated in *Lats1/2* CKO heart model. Therefore, *Xiao et al.* (2018) proposed a model where YAP upregulates *Dhrs3*, which causes impaired fibroblast differentiation by reducing RA formation and signaling. However, this model is still speculative as the impact of YAP on RA-signaling was never properly assessed. Therefore, the interaction of RA-signaling and YAP in the epicardium need to be carefully evaluated to discover the exact role of epicardial-derived RA in cardiac fibroblast differentiation. Understanding the relationship between RA-signaling and YAP may also provide insight into how epicardial EMT and EPDC cell fate is regulated, which could unlock new regenerative tools. Furthermore, since YAP is a mediator in many regulatory pathways, new mechanistic ways to regulate RA-signaling may be discovered; such as mechanotransduction, EMT, cell density, etc.

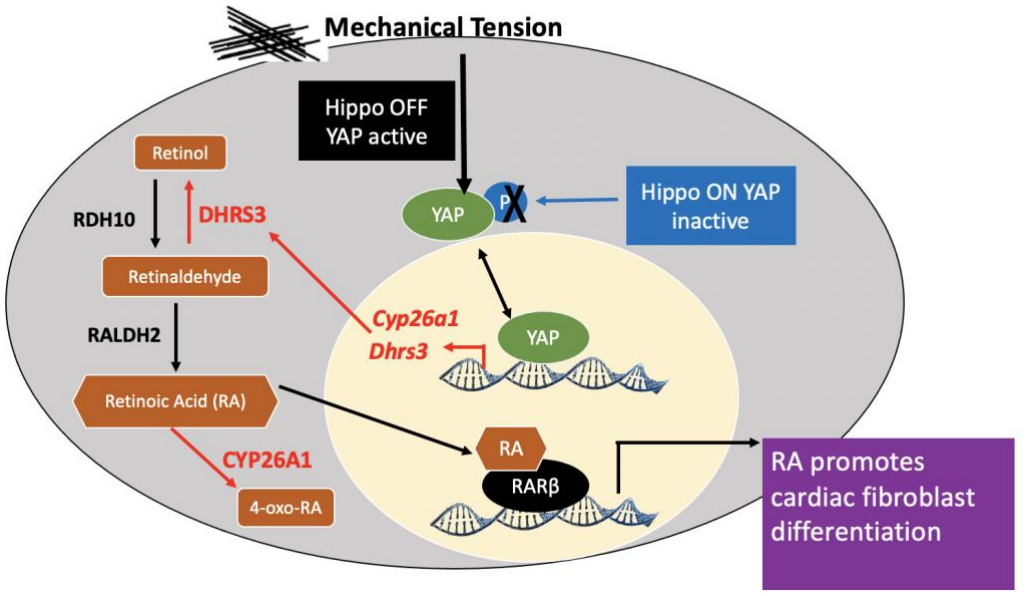

Figure 6: Hypothetical mechanistic overview of how YAP may regulate epicardial RA-signaling in embryonic cardiac development.

A hypothetical model was created in Figure 6 where YAP regulates the transcription of enzymes involved in the RA-signaling pathway to maintain appropriate levels of RA needed for proper EPDC differentiation and cardiac development. It is hypothesized that YAP affects RA-signaling in the epicardium during embryonic development. The first aim will focus on the effect of Yap on retinoid gene expression. The second aim will investigate the effect of Yap on the metabolism of Vitamin A.

In the first aim, reverse transcription, quantitative real time PCR (RT-qPCR) will be used to assess how active and supressed YAP will affect the level of expression of known retinoid enzymes and receptors such as *Dhrs3*, *Raldh2*, *Cyp26a1*, *Cyp26b*1and *Rarb*. To over express YAP a constitutively active form of YAP, YAP25SA, will be transfected into MEC1 cells and the expression of retinoid enzymes will be compared to the non-transfection control. YAP25SA is a mutant form of YAP that has all of its serines mutated to alanines so that is can avoid phosphorylation and stay constitutively active.[66] Alternatively, we will downregulate the activity of YAP by transfecting MEC1 cells with YAP small interfering RNA (siRNA) and by chemical inhibition with the YAP-TEAD inhibitor Verteporfin. For the second aim, the Gal4-RAR/5xUAS-Gaussia luciferase reporter will be used to measure how YAP affects the metabolism of vitamin A. The Gal4-RAR/5xUAS-Gaussia luciferase reporter detects RA when RA binds to the RAR in the Gal4-RAR fusion protein, which then activates the expression of Gaussia luciferase within the cell.[34] The Gal4-RAR/5xUAS-Gaussia luciferase reporter and constitutively active YAP25SA will be transiently co-transfected into MEC1 cells to observe if YAP25SA has an effect on the metabolism of retinol to retinoic acid. Finally, preliminary data on the effect of cell density and mechanical tension on RA-signaling will be discussed for future perspectives.

2. Methods

2.1 Cell Culture

The two cell lines investigated in this thesis are mouse embryonic epicardial (MEC1)[120] cells and primary mouse embryonic fibroblast (NIH3T3)[121] cells. The cells were cultured in complete Dulbecco's modified Eagle media (DMEM, Hyclone, Fisher Scientific) supplemented with 10% fetal bovine serum (FBS, Hyclone, Fisher Scientific,), and 100 μg/mL streptomycin and 100 U/mL penicillin (1% A+A, Life Technologies). Cell cultures were maintained in T75 flasks and incubated at 37°C, 5% CO2 and 100% humidity. MEC1 cells were sub-cultured onto a new T75 flasks every 2-3 days and NIH3T3 cells were cultured every 3-4 days. Cells were harvested using 3 mL of 1x 0.25% Trypsin-EDTA (CORNING, Fisher Scientific) for 3 minutes in an incubator at 37°C, 5% CO2 and 100% humidity to release the cells from the culture dish. Once the cells were released, 3 mL of complete DMEM media was added to de-activate the trypsin and then they were collected by centrifugation at 1000 RPM for 5 min. After centrifugation, the cells were resuspended in fresh complete DMEM media. A 1:10 and 1:8 fraction of cells was plated in a T-75 flask for MEC1 and NIH3T3 respectively in 10 mL of complete media.

2.2 Mycoplasma Treatment

Mycoplasma contamination has been shown to induce a number of cellular changes, which include decreased transfection efficiency.[122] Since this thesis methodically used transfections, MEC1 (Figure 6) and NIH3T3 cells (Supplementary Figure 1) were tested for mycoplasma infection using a PCR mycoplasma detection kit (abm). To test the cells for mycoplasma, the PCR mycoplasma detection kit (#G238, abm) exact protocol was followed and the MJ Mini 48-Well Personal Thermal Cycler (BioRad) was used. PCR samples were run through a 2% agarose gel to visually detect mycoplasma. The MEC1 cells unfortunately tested positive for mycoplasma so the

cells underwent a 2-week Plasmocin treatment (InvivoGen). The treatment consisted of adding 12.5 μg/ml of Plasmocin to the cell culture media every 3-4 days. After 2 weeks, the MEC1 cells were re-tested for mycoplasma and Plasmocin successfully treated the MEC1 cells from mycoplasma infection. To prevent recontamination, Plasmocin Prophylactic was added to the culture media for the MEC1 cells and the MEC1 cells were routinely checked.

Figure 7: Mycoplasma detection and treatment in MEC1 cells. MEC1 cells were tested for mycoplasma infection with a PCR mycoplasma detection kit (abm) to ensure a high transfection efficiency in subsequent experiments. PCR samples were run through a 2% agarose gel to visually detect mycoplasma. The MEC1 cell laboratory stocks tested positive for mycoplasma infection, so the MEC1 cells underwent a 2-week Plasmocin treatment (Invivogen). The treatment consisted of adding 12.5μg/ml of Plasmocin to the cell culture media every 3-4 days. After 2 weeks, the MEC1 cells were re-tested for mycoplasma and tested negative. Lane 1 and 5 depict the negative and positive mycoplasma controls from the PCR mycoplasma detection kit (abm). Lane 2 shows the Plasmocin treated MEC1 cells. Lane 3 illustrates the media used for cell culture. Finally, Lane 4 shows a MEC1 stock not treated with Plasmocin as another positive control.

2.3 Verteporfin Experiment

Verteporfin is a non-specific YAP-TEAD inhibitor.[118] MEC1 cells were split for assay into a 6-well plate at 80,000 cells per well. The next day, based off publications, two working solutions consisting of 5 μM of Verteporfin (NOVUS BIOLOGICALS)[118] or DMSO as a vehicle control were made by adding either 10 μL of the 5 mM Verteporfin stock solution or 10 μL of DMSO to 10 mL supplemented DMEM media. All the previous media was removed from the MEC1 cells and then three wells were treated separately with 3 mL of the Verteporfin working solution and another three wells were treated separately with 3 mL of the DMSO vehicle control solution to create three technical triplicates per sample. The treated MEC1 cells were placed in an incubator at 37°C, 5% CO2 and 100% humidity. After 48 hours mRNA was extracted from each of the six samples and RT-qPCR was performed on 20-30ng of cDNA, to observe the gene expression of known epicardial markers, down-stream targets of YAP and retinoid enzymes; refer section 2.6 for the RT-qPCR procedure. The experiment was then repeated on three different days to create biological triplicates (N=3).

2.4 Transfection Experiments

2.4.1 YAP siRNA

MEC1 cells were plated into four wells of a 6-well plate (30,000 cells/well). A low cell density was optimized to prevent cell-cell contact diminishing YAP-signaling during the experiment. The next day, the 6-well plate RNAimax (Thermofisher Scientific) protocol was followed. Three Eppendorf tubes were used to create three separate working solutions. The first working solution contained 36 μL of the RNAiMAX lipofectamine reagent and 600 μL of serum-free Opti-MEM media (Thermofisher Scientific) for all 4 samples. The second working solution

was for the Negative siRNA control samples and consisted of 60 pmol of Negative Control #1 Silencer Select siRNA (Ambion, Thermofisher Scientific) (30pmol/ sample) and 300 μL Opti-MEM media. The third working solution was the Yap siRNA samples and was made of 60 pmol of Yap1 Silencer Select siRNA (Ambion, Thermofisher Scientific) (30pmol/ sample) and 300 μL of Opti-MEM media. Next 300 μL of the first RNAiMAX lipofectamine working solution was added to the Negative siRNA control and Yap siRNA working solutions and resuspended gently a few times to form lipofectamine-DNA complexes for 20 minutes. Within the 20-minute wait period, the MEC1 cells were washed with Opti-MEM media to remove any FBS that could interfere with the efficiency of the transfection. After the 20 minute wait period, two wells were separately transfected with 300 μL of the Negative siRNA control-lipofectamine solution and another two wells were separately transfected with 300 μL of the YAP siRNA- lipofectamine solution to create technical duplicates of each sample. The solutions were added dropwise, and the plate was rocked gently for 5 minutes to ensure equal layering onto the MEC1 cells. Next, 500 μL of additional Opti-MEM media was added onto the cells to prevent them from drying out, and the MEC1 cells were incubated at 37°C, 5% CO2 and 100% humidity. After 5-6 hours an equivalent amount (800 μL) of DMEM media only supplemented with 20% FBS was added to the samples to form a 10% FBS solution for optimal growth and returned to the incubator. After 48 hours, mRNA was extracted separately from all samples to observe the expression of retinoid enzymes and down-stream targets of YAP transcripts by RT-qPCR; refer to section 2.6 for the RT-qPCR procedure. This experiment was repeated on three different days (N=3).

2.4.2 YAP25SA Time Point Experiment

MEC1 cells were split for transfection into a 12-well plate (50,000 cells/well for 6- and 12-hour time points and 40,000 cells/ well for 24-hour time point); to allow similar confluency since

cell density effects the expression of YAP. The next day the DNAfectin Plus Transfection Reagent (abm) protocol for a 12-well plate was followed. Two Eppendorf tubes were used to create the 2 separate working solutions for two different sample types: control and pCMV-flag YAP25SA (#27371, addgene). pCMV-flag YAP25SA is a constitutively active, mutant form of YAP that has serines at positions: 61, 109, 127, 128, 131, 163, 164, and 381 mutated to alanine to prevent phosphorylation and deactivation.[66] The YAP25SA working solution contained 4800 ng of the pCMV-flag YAP25SA plasmid (800 ng/sample) and 15 μL of DNAfectin reagent in 600 uL of Opti-MEM. The control working solution contained 15 μL of DNAfectin reagent in 600 μL of Opti-MEM. All solutions in each tube were resuspended gently, and the DNA was allowed to mix with the DNAfectin for 20 minutes. Within the 20-minute wait period, the MEC1 cells were washed with Opti-MEM media to remove any FBS that could interfere with the transfection. After 20 minutes, the control or pCMV-flag YAP25SA DNA-DNAfectin solutions were added to six wells of MEC1 cells dropwise each (100 μL/ sample) to create 12 samples and the plate was rocked gently for 5 minutes to ensure equal layering onto the MEC1 cells. Next, 200 μL of additional Opti-MEM media was added to each sample to prevent the MEC1 cells from drying out and the samples were incubated at 37°C, 5% CO2 and 100% humidity. After 5-6 hours an equivalent amount (300μL) of DMEM media only supplemented with 20% FBS was added to each sample to create a 10% FBS solution optimal for growth and the samples were returned to the incubator. After 6 hours mRNA was extracted from 4 samples to create 6-hour control and pCMV-flag YAP25SA technical duplicates. RNA was isolated from separate sets of wells at 12 and 24 hours post treatment for a total of 12 samples (3 timepoints and 4 technical repeats/timepoint). RT-qPCR was performed on 20-30 ng of cDNA to observe the gene expression of enzymes and receptors

involved in RA-signaling and downstream targets of YAP; the RT-qPCR procedure is in section 2.6. The experiment was performed in biological triplicates (N=3).

2.4.3 YAP25SA and YTIP Experiment

MEC1 cells were split for transfection into a 12-well plate (30,000 cells/well for 6 wells); a low cell confluency was optimized to prevent cell-cell contact diminishing YAP-signaling. The next day the DNAfectin Plus Transfection Reagent (ABM) protocol for a 12-well plate was followed. Three Eppendorf tubes were used to create the 3 separate working solutions for the following 3 different samples: control, YAP25SA, and YAP25SA+ YTIP-GFP. The first working solution for the YAP25SA+ YTIP-GFP technical duplicates contained 1600 ng of pCMV-flag YAP25SA (#27371, addgene), 1600 ng YTIP-GFP (#42238, addgene) plasmids (800 ng/ sample) and 5 μL of DNAfectin in 200 μL of serum free Opti-MEM media. YTIP (YAP1-TEAD Interfering Peptide)-GFP is a peptide that inhibits YAP from interacting to TEAD-1. YTIP contains expressed GFP fused to a region of YAP1 sufficient to bind to TEAD, specifically at amino acid residues 47-155 of YAP1 to interfere with YAP1-TEAD1 interaction.[70] The second working solution for the YAP25SA technical duplicates contained 1600 ng of pCMV-flag YAP25SA (#27371, addgene) plasmid (800 ng/ sample) and 5 μL of DNAfectin in 200 μL Opti-MEM media. The third working solution for the control technical duplicates contained 5 μL of DNAfectin in 200 μL Opti-MEM media. All samples were resuspended gently, and the DNA was allowed to mix with the DNAfectin for 20 minutes. Within the 20-minute wait period, the MEC1 cells were washed with Opti-MEM to remove any FBS that could interfere with the transfection. After 20 minutes, the control, YAP25SA, or YAP25SA+YTIP-GFP working solutions were added dropwise to two wells each, and the plate was rocked gently for 5 minutes to ensure equal layering onto the MEC1 cells. Next, 200 μL of additional Opti-MEM media was added to each well to prevent the cells from drying

out and the cells were incubated at 37°C, 5% CO2 and 100% humidity. After 5-6 hours an equivalent amount (300 μL) of DMEM media only supplemented with 20% FBS was added to each sample to create a 10% FBS solution optimal for growth, and the samples were returned back to the incubator. After 24 hours the MEC1 cells transfected with YTIP-GFP were checked for GFP expression using the Zoe Fluorescent Cell Imager (Bio-Rad) to ensure the co-transfection worked. Afterwards, mRNA was extracted from each of the 6 total samples and RT-qPCR was performed on about 20-30 ng of cDNA to observe the expression of RA-signaling enzyme and downstream targets of YAP transcripts; the RT-qPCR procedure is in section 2.6. The experiment was performed in five biological replicates (N=5).

2.5 Mechanical Tension Experiment

Ten wells of two 6-well plates and ten 2kPa and 30kPa plates (ExCellness) were coated with 10μg/mL of plasma fibronectin (Cat#5050, Advanced BioMatrix) overnight. The 2kPa and 30kPa plates were chosen because they are within embryonic and adult heart physiological range and the 6-well plate was used as a very stiff control.[123] To prevent the YAP-signal from being decreased due to cell-cell contact inhibition, the 12, 24, 48, 72, 96 hour time-points had a different number of MEC1 cells plated: 60,000, 40,000, 20,000, 10,000, and 10,000 respectively. MEC1 cells were incubated at 37°C, 5% CO2 and 100% humidity throughout the experiment. The experiment was performed in technical duplicates (six samples per time point). After 12, 24, 48, 72, and 96 hours the samples were harvested in RNALater (Thermofisher Scientific). In total, there were 30 samples and mRNA was extracted from all of the samples following section 2.7 protocol. RT-qPCR was performed with 15ng of cDNA across all time-points to observe how mechanical tension effects the expression of RA-signaling enzyme and downstream targets of YAP transcripts (RT-qPCR protocol is in section 2.7). The experiment was performed only once (N=1) as a preliminary

investigation, and upon discussions with my committee this thesis became instead focused on the relationship between YAP and RA-signaling in MEC1 cells (Supplementary Figure 4 and 5).

2.6 Preparing Samples for RT-qPCR

2.6.1 RNA Extraction

RNA was isolated from samples using the PureLink RNA mini kit (Ambion, Thermofisher Scientific, Cat#1218301BA). Fresh lysis buffer was prepared by 2-β-mercaptoethanol to the lysis buffer. Any media was removed from the samples and they were washed with PBS. Then, 350 μL of lysis buffer was added to each sample and a cell scraper was used to remove the cells from the plate. To further lyse the cells, a 21-gauge needle attached to a syringe was used and each sample was aspirated 5-10 times. The exact PureLink RNA mini kit procedure was then followed to recover the RNA. To elute the RNA, 75 μL of RNase-Free water was used. RNA was stored in -80°C until further use. A nanodrop was used to measure the concentration and purity of the RNA in each sample.

2.6.2 RT-qPCR

Next, the same concentration of RNA was treated with DNase and reverse-transcribed into complementary DNA (cDNA) using 5X All-in-One RT MasterMix with AccuRT Genomic DNA Removal Kit (abm, Cat#G492) for all samples. A no reverse transcription (no RT) control was made by taking 1 μL of DNase treated RNA and adding 1.33 μL of water, so that the concentration of the samples and no RT control would be equivalent. The No RT controls were put through the same steps as the cDNA samples except no 5X RT solution was added as it contained the reverse transcription enzyme.

Quantitative real-time PCR analysis using the SensiFAST SYBR No-ROX kit (Bioline, Frogga Bio, Cat# 4367659) was performed on an CFX Connect Real Time PCR Detection System (Bio-Rad). The primer sequences for each target gene are listed in Table 1. The amplified regions of all used primer sets have been mapped and validated by UCSC In-Silico PCR database [Dec. 2011 (GRCm38/mm10), mouse genome] and the products were examined by a 2% agarose gel electrophoresis to confirm the specificity of the primers.

This assay was optimized by first determining the annealing temperature of each primer; this was done by testing identical reactions containing a fixed primer concentration of 400 nM, across a range of annealing temperatures by using a temperature gradient block. Next to optimize this assay, the efficiency of all of the primers were determined, which were 88-110% efficiency. The cycling procedure used consisted of a 2 minute 95°C polymerase activation step, followed by a 5 second 95°C denaturation step, and then a 30 second 60°C annealing and extension step. After the 40 cycles of qPCR, a melt curve was also added onto the cycling procedure to ensure only one product was being amplified. The relative fold change of each target gene was calculated using the $2^{-\Delta\Delta Ct}$ method. First the target gene was normalized to the geometric mean of the reference genes: *Gapdh* and *Hprt1* (unless otherwise stated) and then treatment groups were normalized to control groups.

Table 1: Primer Sequences for RT-qPCR

Gene	Forward Sequence	Reverse Sequence
Gapdh	GTCAAGCTCATTTCCTGGTATG	CTTGCTCAGTGTCCTTGCTG
Hprt1	TCAGTCAACGGGGGACATAAA	GGGGCTGTACTGCTTAACCAG
Yap	TACTGATGCAGGTACTGCGG	TCAGGGATCTCAAAGGAGGA
Ctgf	GGGCCTCTTCTGCGATTTC	ATCCAGGCAAGTGCATTGGTA
Ankrd1	TGCGATGAGTATAAACGGACG	GTGGATTCAAGCATATCTCGGAA
Rarb	CAAGCTCCAAGAACCACTGC	ATTACACGTTCGGCACCTTTC
Cyp26a1	GAACATTCGCGCCAAGATCC	TTAGTGCCTGCATATCCAGCC
Cyp26b1	CCGTGAGAAGCTGCAGTGTA	GGGTTCCATCCTTCAGCTCC
Dhrs3	GTGAACAATGCCGCTGTGGT	GAAGGGCCTGGTTTTGTTGC
Raldh2	CAGAGAGTGGGAGAGTGTTCC	CACACAGAACCAAGAGAGAAGG

2.7 Two-hybrid Gal4-RAR;UAS-tk-Gaussia luciferase reporter system

A stable two-hybrid Gal4-RAR;UAS-tk-Gaussia luciferase reporter system was attempted to be constructed in NIH3T3 and MEC1 cells. This sensitive RA-reporter system expresses Gal4-RAR and a Gaussia luciferase under the control of a promoter containing five copies of the upstream activating sequence (UAS) so that when RA binds to Gal4-RAR, Gaussia luciferase is transcribed. Gaussia luciferase possesses a natural secretory signal, which upon expression is secreted into the medium, this makes cell lysing in order to assay Gaussia luciferase activities not necessary.[124] Therefore the Gaussia luciferase in the media can be measured to qualitatively determine the amount of RA in the cells. For the two-hybrid Gal4-RAR;UAS-tk-Gaussia luciferase reporter system to work, three components are needed: RA, pCS2p+Gal4-RAR and pGluc-mini-tk-2-UAS plasmids. pCS2p+Gal4-RAR is a construct expressing a fusion of the DNA-binding domain of the GAL4 protein (aa 1–147) to the ligand binding domain (aa 156–457) of zebrafish RARαb under the control of a CMV promoter and was obtained as a kind gift from Joshua Waxman (University of Cincinnati/Cincinnati Children's Hospital) and has been previously described by D'Aniello et al. 2013.[125] pGluc-mini-tk-2-UAS is a construct expressing Gaussia luciferase under

the control of the HSV thymidine kinase minimal promoter and was generated by cloning 5 tandem copies of upstream activating sequences (UAS) in the Bgl2 site of the pGluc-mini-TK-2 plasmid (New England Biolabs).

To detect the amount of luciferase, 20 μL of supernatant from each sample was added to a 96-well, white-opaque, falcon plate and mixed with 50 μL of the BioLux Gluc Assay solution from the BioLux Gluc Assay Kit (E3300, New England BioLabs) and then quickly measured. The Optima FLUOstar machine was used to detect the Gaussia luciferase signal using the luminometer set to 8 seconds of integration. As well, a blank sample was created by mixing 20 μL of supernatant from any sample and adding 50 μL of BioLux Gluc assay buffer, without the enzyme. For all reported data, the blank has been subtracted from the RFU value.

2.7.1 Constructing a stable Gal4-RAR;UAS-tk-Gaussia luciferase reporter system in MEC1 cells.

Since pGluc-mini-tk-2-UAS and pCS2p+Gal4-RAR plasmids contain a G418 antibiotic resistant gene that allow for selection and isolation of stable clones by culturing in the presence of G418 antibiotic (Fisher Scientific, Waltham, MA), the concentration of G418 to select stable MEC1 cell clones needed to be optimized by a kill curve. To create a kill curve, 10,000 MEC1 cells were plated in a 24-well plate and treated with ten different concentrations of G418: 4000 μg/ml, 2000 μg/ml, 1000 μg/ml, 500 μg/ml, 250 μg/ml, 125 μg/ml, 62.5 μg/ml, 31.3 μg/ml, 15.6 μg/ml, and 0 μg/ml. The media was changed every 2-3 days to allow continued growth, with the same concentrations of G418. The cells were allowed to grow, and observations were taken every 2-days. After 10 days the cells were counted, using a hemocytometer, to create a G418 kill curve (Supplementary Figure 6).

To construct the stable two-hybrid Gal4-RAR;UAS-tk-Gaussia luciferase reporter system, first, 60,000 MEC1 cells were transfected with 2 μg of the pGluc-mini-tk-2-UAS plasmid using DNAfectin (ABM) 6-well plate protocol. The pGluc-mini-tk-2-UAS- MEC1 cells were then selected by cell culture with complete medium containing 1 mg/mL of G418 for two weeks. Next, the pGluc-mini-tk-2-UAS- MEC1 were isolated into clones by plating three 96-well plates with a 0.5 cell/ well concentration in 1 mg/mL of G418 complete media.

Once there were enough cells, the next step was to test if the four pGluc-mini-tk-2-UAS-MEC1 stable clones expressed the pGluc-mini-tk-2-UAS gene. The day before transfection, 20,000 pGluc-mini-tk-2-UAS- MEC1 cells/ well of each clone were plated. Then 400ng of pCS2p+Gal4-RAR was transiently transfected into pGluc-mini-tk-2-UAS- MEC1 stable clones using DNAfectin (ABM) 24-well plate protocol. After 5-6 hours an equivalent amount of DMEM media supplemented with 20% FBS was added to each sample to create a 10% FBS solution optimal for growth and the samples were returned to the incubator. The next day the clones were treated with 10 nM of TTNPB or DMSO for 48 hours. TTNPB is an analog of retinoic acid that potently and selectively activates retinoic acid receptors.[56] The BioLux Gaussia Luciferase Kit protocol and the Optima FLUOstar machine was used to detect the Gaussia luciferase signal; following the protocol in section 2.6. Results are illustrated in Supplementary Table 2.

2.7.2 Constructing a stable Gal4-RAR;UAS-tk-Gaussia luciferase reporter system in NIH3T3 cells.

A stable two-hybrid Gal4-RAR;UAS-tk-Gaussia luciferase reporter system was also attempted to be constructed in NIH3T3 cells. First, NIH3T3 cells were transfected with pGluc-mini-tk-2-UAS and then isolated and selected to create clones of a pGluc-mini-tk-2-UAS- NIH3T3 cell line. As illustrated in Table 4, twelve clones of pGluc-mini-tk-2-UAS- NIH3T3 were isolated.

To test if the NIH3T3 clones expressed pGluc-mini-tk-2-UAS, 30,000 cells/ well for each clone was plated in a 24-well plate. The next day, 400 ng of pCS2p+Gal4-RAR was transiently transfected into the clones using DNAfectin (ABM) 24-well plate protocol. After 5-6 hours an equivalent amount of DMEM media supplemented with 20% FBS was added to each sample to create a 10% FBS solution optimal for growth and the samples were returned to the incubator. The next day the clones were treated with 10 nM of TTNPB or DMSO in complete media for 48 hours. The BioLux Gaussia Luciferase Kit protocol and the Optima FLUOstar machine was used to detect the Gaussia luciferase signal; following the protocol in section 2.6. Results are illustrated in Supplementary Table 3.

After a pGluc-mini-tk-2-UAS- NIH3T3 clone was confirmed to express pGluc-mini-tk-2-UAS, it was transfected with pCS2p+Gal4-RAR plasmid to create the two-hybrid Gal4-RAR;UAS-tk-Gaussia luciferase reporter system. The reporter system clones were isolated to create another stable cell line. However, no stable clones were able to be isolated.

2.7.3 Gal4-RAR virus protocol

Both MEC1 cells and pGluc-mini-tk-2-UAS- NIH3T3 cells were virally infected with a virus that was packaged with pMX-IG-Gal4-RAR. First, 30,000 MEC1 cells per well and 50,0000 pGluc-mini-tk-2-UAS- NIH3T3 cells per well, were plated to fill their own 6-well plates. Previously, the Gal4RAR virus was determined to be at a concentration of $4x10^8$ IU/mL, so 0, 2, 10, 20, 100, and 500 μL of virus was added per well that contained 1 mL of complete media for both plates. Also, 20 μL of 0.8 mg/mL of polybrene was added to all the wells. After 24 hours, the media containing the virus was removed from each well and new complete media with 1mg/mL of G418 was added to each well. Since the virus expressed GFP, Zoe Fluorescent cell imager was used to determine which sample expressed the most GFP to ensure the viral infection worked. It

was determined that the sample treated with 100 μL and 500 μL of virus worked the best for NIH3T3 and MEC1 cells respectively as illustrated in Supplementary Figure 7. Next, 0.5 cells per well were plated in all wells of four 96 well plates containing complete media treated with 10% conditioned media from the respective cell culture and 1mg/mL of G418 to isolate monoclonal, stable clones infected with the virus. Conditioned media was created by removing the media from the respective cell's culture and centrifuging it. Unfortunately, after four weeks, no stable pGluc-mini-tk-2-UAS- NIH3T3 cells that expressed GFP were isolated.

However, 12 virally infected MEC1 clones expressing GFP were isolated and checked for expression of viral Gal4-RAR. 20,000 virally infected MEC1 cells/ well of each clone were plated in a 24- well plate. The next day, 400ng of pGluc-mini-tk-2-UAS were transiently transfected into the virally infected MEC1 cells/ well following the DNAfectin (ABM) 24-well plate protocol. After 5-6 hours an equivalent amount of DMEM media supplemented with 20% FBS was added to each sample to create a 10% FBS solution optimal for growth and the samples were returned to the incubator. The next day the clones were treated with 10 nM of TTNPB or DMSO for 48 hours. The BioLux Gaussia Luciferase Kit protocol and the Optima FLUOstar machine was used to detect the Gaussia luciferase signal; following the protocol in section 2.6. Results are illustrated in Supplementary Table 1.

2.7.4 Transient Transfection of YAP25SA and theGal4-RAR;UAS-tk-Gaussia luciferase reporter system

MEC1 cells were reverse co-transfected with pGluc-mini-tk-2-UAS and pCS2p+Gal4-RAR reporter plasmids at 400 ng each, per well, using Lipofectamine 2000 (ThermoFisher) in Opti-MEM (Invitrogen), and seeded at 150,000 cells per well in a 24-well cell culture plate to create a total of nine samples. An additional 400ng of pCMV-flag YAP25SA (#27371, addgene)

was reverse co-transfected into three of the samples: sample 7-9. The DNA-lipofectamine complexes were mixed in the 24-well plate for 20 minutes before the cells were seeded to increase transfection efficiency. After three hours an equivalent amount to the total transfection volume of 20% FBS supplemented media was added to the samples to create a final concentration of 10% FBS for optimal cell growth. The transfected MEC1 cells were placed in an incubator at 37°C, 5% CO2 and 100% humidity. Next, 24 hours post- transfection, three treatment groups were created by (1) adding DMSO to only the reporter samples to create a reporter control and (2) adding 6 μM of retinol to samples containing only the reporter and (3) the reporter with YAP25SA. The concentration of ROL was verified through UV-visual spectrophotometry and using Beer's Law calculation based on the absorbance of 3 μL of retinol in 3 mL of hexane where the extinction coefficient ε=51,700 at 325nm for retinol in hexane. A time course experiment was then completed by measuring the Gaussia luciferase signal of all the samples at 2, 12, 24 and 48 hours. To do this, the samples were swirled to ensure optimal distribution of Gaussia luciferase signal and 20 μL of supernatant from each sample and at each time point was added to a 96-well, white-opaque, falcon plate and mixed with 50μL of the BioLux Gluc assay solution from the BioLux Gaussia Luciferase Assay Kit (E3300, New England BioLabs). The Optima FLUOstar plate reader was used to detect the Gaussia luciferase signal using the luminometer set to 8 seconds of integration. The experiment was performed in biological triplicates (N=3) but only the least significant replicate is showed in Figure 14. The analysis of the biological replicates is illustrated in Supplementary Figure 3.

2.8 Data Analysis

All experiments were completed in technical duplicates or triplicates and repeated on three different days to create three biological replicates, unless stated otherwise. Technical replicate is defined as replicates completed on the same day and time but processed and analyzed separately.

Biological replicates are defined as repeating the experiment and technical replicates on different days. Technical replicates were averaged so that comparisons could be made between biological replicates, unless otherwise stated. Excel was used to compute all experimental fold changes. To calculate the relative fold change of target genes the $2^{-\Delta\Delta Ct}$ method was used. First target genes were normalized to the housekeeping genes: *Gapdh* and *Hprt1* and then treatment groups were normalized to control groups. GraphPad Prism was used for all statistical analysis. Any outliers were determined by using a Grubbs test. For assays containing two experimental groups, the statistical analysis was performed using paired Student's t-test between groups. For tests that contain more than two experimental groups, a one- way ANOVA with repeated measures was performed followed by a Tukey's post-hoc analysis. To assess the affects that two independent variables had on a dependent variable, a two-way ANOVA with repeated measures was used. The data were represented as means ± standard deviation and any significant differences were denoted as: *$p<0.05$ vs. control, **$p<0.01$ vs. control, ***$p<0.001$ vs. control and ****$p<0.001$ vs. control.

3. RESULTS

3.1 MEC1 cells phenotypically and genetically express epicardial characteristics and retinoid enzymes.

The epicardium is the main source of RA-signaling in the heart during embryonic development and it is critical for cytoskeletal re-arrangement and differentiation of epicardial cells into vascular smooth muscle cells and fibroblasts within the myocardium.[56,57] However, very little of the underlying mechanisms that regulate RA-signaling in the epicardium is known.[61] Therefore, we began our investigation of the role of YAP on the expression of enzymes and receptors involved in RA-signaling using a well-characterized epicardial cell-line, MEC1, derived from the ventricular epicardium of E13.5 embryos of the ICR/CD1 outbred mouse strain.[120] The MEC1 cell line was chosen because both Wang *et al*. (2018) and Xiao *et al.* (2018) utilized this exact cell line when studying the embryonic epicardium for YAP and RA-signaling. MEC1 cells retained many of the features of resting embryonic epicardial cells, such as their cobblestone epithelial morphology with tight cell-to-cell contact when mimicking physiological conditions such as being seeded on a plate with 2kPa mechanical tension and fibronectin (Supplementary Figure 4). Also illustrated in Figure 8, the MEC1 cells genetically expressed the epicardial markers: *Wt1, Tbx18, and Raldh2,* and the retinoid enzymes: *Rarb, Dhrs3, Cyp26a1 and Cyp26b1*.

3.3 Understanding how inhibition of YAP activity affects the gene expression of enzymes and receptors involved in RA-signaling in MEC1 cells

To understand the effects of YAP on the expression of RA-signaling enzyme transcripts in the embryonic epicardium, the activity of YAP was chemically (Figure 8) and genetically (Figure 9) inhibited in MEC1 cells. Throughout this thesis both the expression levels of connective tissue growth factor (*Ctgf)* and Ankyrin Repeat Domain 1 (*Ankrd1)* were measured as a control to verify changes in YAP activity because they are known direct targets of TEAD.[126]

3.3.1 Chemical inhibition of YAP results in slight changes in the expression of epicardial markers, YAP down-stream targets, and retinoid enzymes

Verteporfin is a compound that non-specifically inhibits the interaction of YAP with the TEAD transcription factors.[118,127] The first controls used to ensure Verteporfin was inhibiting YAP and TEAD interaction were the epicardial markers *Wt1* and *Tbx18* as they have shown to be affected by Verteporfin treatment. As illustrated in Figure 8A, the treatment of MEC1 cells with Verteporfin non-significantly decreased *Wt1* and *Tbx18* expression by 0.62-fold (P=0.118) and 0.44-fold (P=0.2055) respectively when compared to the mean of the DMSO control. Figure 8B illustrates that treatment of MEC1 cells with Verteporfin caused a decreased trend of *Ctgf* expression by 0.55-fold (P=0.097) when compared to the DMSO control. However, the expression of *Ankrd1* was essentially unchanged by being non-significantly increased by 1.11-fold (P= 0.112). Figure 8C illustrates the effects of Verteporfin on *Rarb*, *Dhrs3*, *Cyp26a1*, *Cyp26b1*, and *Raldh2*. Treatment of MEC1 cells with Verteporfin led to a decreased trend of *Cyp26a1* expression by 0.54-fold (P=0.277), *Cyp26b1* expression by 0.87-fold (P=0.189), and *Raldh2* expression by 0.85-fold (P=0.183) when compared to the DMSO control. There was no change in *Rarb* and *Dhrs3* expression as they displayed a 0.32-fold (P=0.376) and 0.33-fold (P=0.378) difference between

Verteporfin and DMSO treatment respectively. Attempts to chemically inhibit the interaction of YAP and TEAD with Verteporfin did not have a significant influence on the expression of YAP-targets or retinoid enzymes and receptors in MEC1 cells. Due to the lack of significant observable changes, it was decided to genetically inhibit YAP with YAP siRNA to observe the effects on RA-signaling.

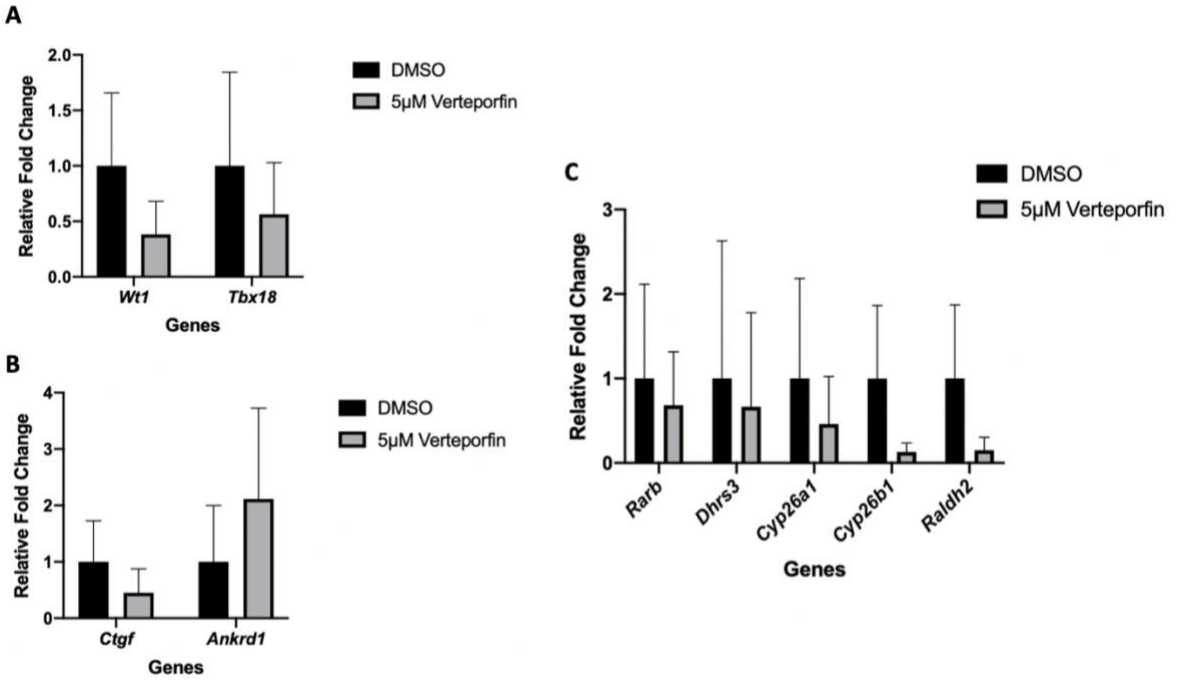

Figure 8: Verteporfin does not have any significant effects on the transcription of epicardial markers, known YAP down-stream targets and retinoid enzyme and receptors in MEC1 cells. Verteporfin was proposed to act as a non-specific YAP-TEAD inhibitor. MEC1 cells were either treated with Verteporfin or DMSO as a vehicle control. After 48 hours, total RNA was extracted and then RT-qPCR was performed. The $2^{-\Delta\Delta Ct}$ method was used to measure the level of expression of (A) *Wt1* and *Tbx18*; (B) *Ctgf* and *Ankrd1*; (C) *Rarb*, *Dhrs3*, *Cyp26a1*, *Cyp26b1* and *Raldh2*. This experiment was repeated on three different days to create biological replicates (N=3). Each graph shows the mean relative fold change and error bars indicate the standard deviation between biological replicates N=3. A student paired t-test was used for all comparisons and any significant differences were denoted as: *$p<0.05$ vs. DMSO.

3.3.2 Down-regulation of YAP activity mediated by YAP siRNA affects the expression of Cyp26 family enzyme transcripts

For genetic inhibition of YAP, MEC1 cells were transfected with YAP siRNA or Negative siRNA as a control. After 48 hours, mRNA was isolated from the samples and RT-qPCR was performed. As illustrated in Figure 9A, transfection of MEC1 cells with YAP siRNA resulted in a significant decrease in expression of *Yap* by 0.88-fold (P=0.016) when compared to the mean of the Negative siRNA samples. Therefore, *Yap* expression was successfully knocked down. However, there was only a decreasing trend in the expression of *Ctgf* and *Ankrd1* by 0.51-fold (P=0.082) and 0.53-fold (P=0.0585) respectively, when the mean of the Yap siRNA samples were compared to the mean of the Negative siRNA samples; but it did not reach statistical significance. Next, the effects of knocking down YAP on the gene expression of retinoid enzymes: *Cyp26a1*, *Cyp26b1*, *Rarb*, and *Dhrs3* was observed. As illustrated in Figure 9B, the transfection of MEC1 cells with YAP siRNA resulted in a modest but significant decrease in the expression of *Cyp26b1* by 0.53-fold (P=0.046) and there was a decreasing though not significant trend in the expression of *Cyp26a1* by 0.37-fold (P=0.162) and *Raldh2* by 0.82-fold (P=0.343) when MEC1 cells were transfected with YAP siRNA compared to Negative siRNA. YAP knockdown also did not seem to alter the expression of *Rarb* and *Dhrs3* as there was a 0.03-fold (P=0.817) and 0.144-fold (P=0.355) difference respectively when the mean of the YAP siRNA samples was compared to the mean of the Negative siRNA samples. Therefore, it was determined that treatment of MEC1 cells with YAP siRNA did have a very modest impact on the expression of *Cyp26b1*. However, since the changes observed were minimal, overall, it can be concluded that YAP-knockdown does not appear to affect YAP targets or the expression of the retinoid enzymes we investigated in MEC1 cells. The average CT values of the Negative siRNA samples across all of biological replicates for *Rarb, Dhrs3, Cyp26a1*, *Cyp26b1* and *Raldh2* were 26.40, 26.25, 29.33, 31.37, 34.07

respectively. The expression of *Raldh2* was below a reliable level of detection once transfected with YAP siRNA. As well, since *Cyp26a1* was had a higher expression in MEC1 cells than *Cyp26b1*, it was decided to only measure changes in the expression of *Rarb, Dhrs3* and *Cyp26a1* moving forward.

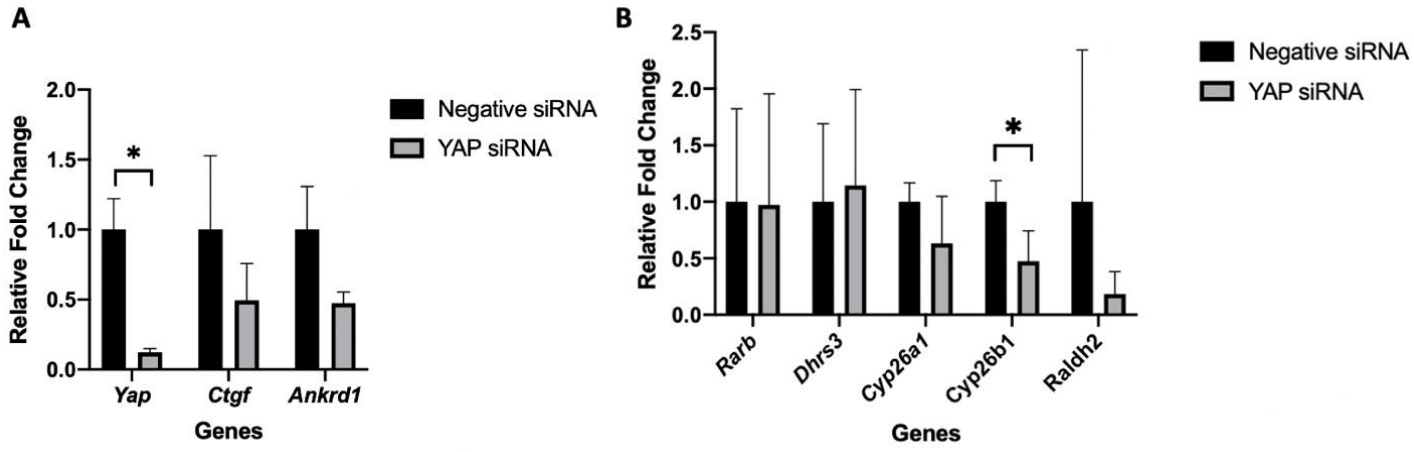

Figure 9: siRNA-mediated downregulation of YAP is associated with the regulation of YAP downstream targets and RA-signaling enzyme transcripts. MEC1 cells were either transfected with YAP siRNA or Negative siRNA as a control. After 48hours total RNA was extracted and RT-qPCR was performed. The $2^{-\Delta\Delta Ct}$ method was used to measure the level of expression of (A) *Yap, Ctgf* and *Ankrd1* and (B) *Rarb, Dhrs3, Cyp26a1, Cyp26b1* and *Raldh2*. Each graph shows the mean fold change values and error bars indicate the standard deviation between Negative siRNA and YAP siRNA. A student paired t-test was used for all comparisons and any significant differences were denoted as: *$p<0.05$ vs. Negative siRNA.

3.4 Upregulation of YAP activity affects the expression of RA-signaling enzyme transcripts

Cell-cell contact has potent inhibitory effects on YAP activity[66], therefore, the levels of active YAP are already quite low in a rapidly growing culture such as MEC1. It was thus reasoned that further suppression of YAP by chemical (Veteporfin) or genetic (siRNA) means may not be able to realistically affect the expression of YAP targets in cell culture conditions. The next approach employed a constitutively active YAP25SA to overcome the inhibitory effects of cull culture conditions on YAP activity and allow us to interrogate the effect of YAP on YAP-target gene expression and perhaps allow us to study the effects of YAP on RA-signaling.

To overcome problems in suppressing YAP activity via chemical or genetic means, we overexpressed a constitutively active form of YAP, pCMV-flag YAP25SA, also known as YAP25SA. YAP25SA is a mutant form of YAP that has its serine sites mutated to alanine to avoid phosphorylation, which constitutively upregulates YAP activity.

3.4.1 A constitutively active form of YAP, YAP25SA, affects the expression of RA-transcripts.

For genetic upregulation of YAP, MEC1 cells were transfected with either YAP25SA or treated with DNAfectin as a control. Total RNA was isolated at 6, 12 and 24 hours post transfection and RT-qPCR was performed. It is important to note that when calculating the relative fold change of target genes, the YAP25SA treatment group was normalized to the control group within the time point to only observe the changes caused by transfection of YAP25SA; because YAP is influenced by many mechanisms that vary naturally overtime, such as proliferation regulators.[71] Although a two way ANOVA showed that there were no significant differences in expression of known YAP targets *Ctgf* (Figure 10A) and *Ankrd1* (Figure 10B) for both time and treatment with

YAP25SA, there was an observational increased trend in *Ctgf* and *Ankrd1* expression at six hours when treated with YAP25SA and then trended towards reduced expression over time. In Figure 11C the time dependent changes in the expression of *Ctgf* and *Ankrd1* were investigated by comparing only the 6, 12 and 24 hour DNAfectin control samples to determine if the YAP25SA time course protocol itself had any effects on the activity of YAP. As depicted in Figure 10C, there was a significant increase in Ankrd1 expression of 2.73-fold (P=0.024) from 6 to 12 hours. On the other hand, there was a significant decrease in the expression of Ankrd1 by 2.12-fold (P=0.039) from 12 to 24 hours. There was only a fold change of 0.61 (P=0.351) for *Ankrd1* expression when the 24-hour time-point was compared to the 6-hour time point. There were no significant differences in *Ctgf* expression across the time course control samples; however, the expression of *Ctgf* had the exact same trends as *Ankrd1*. Therefore, it was determined that both *Ctgf* and *Ankrd1* did fluctuate in expression for the control samples during the time course experiments.

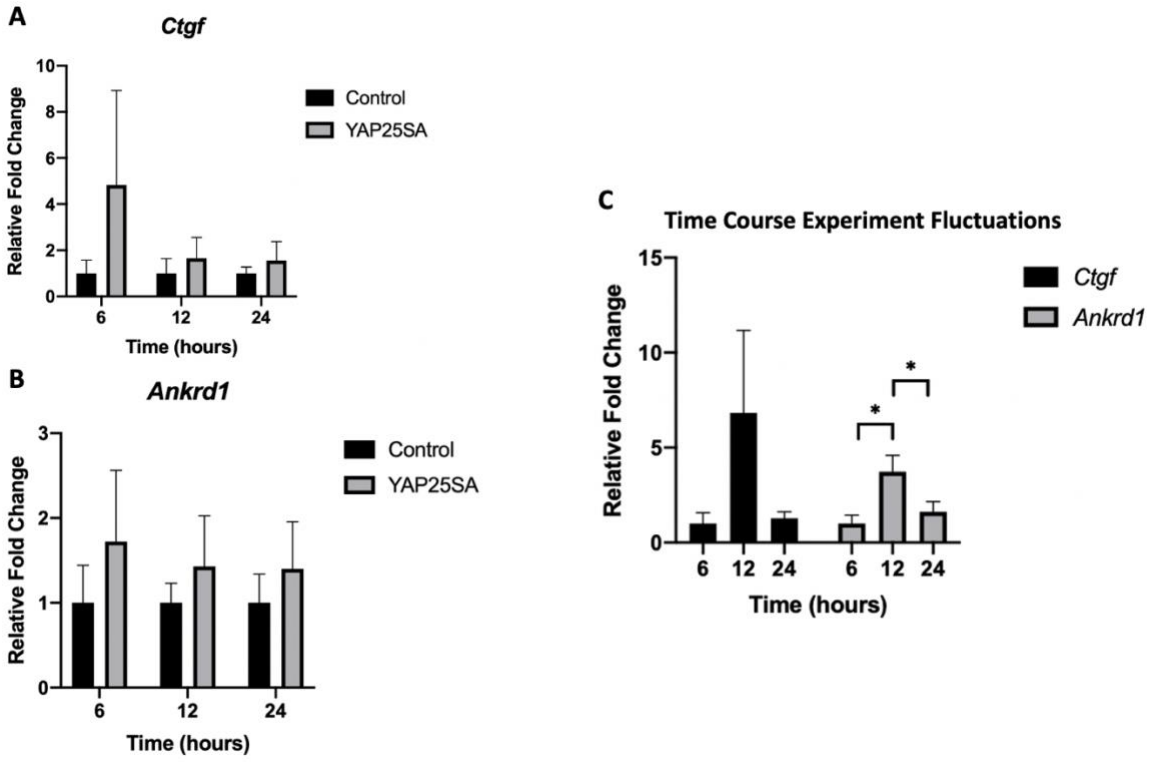

Figure 10: Transfection of a constitutively active form of YAP, YAP25SA, is associated with a trend towards increased expression in known YAP downstream targets: *Ctgf* and *Ankrd1*. MEC1 cells were transfected with YAP25SA or only treated with DNAfectin as a control. Total RNA was isolated at 6, 12 and 24 hours post transfection and the expression of (A) *Ctgf* and (B) *Ankrd1* were analyzed by RT-qPCR. The level of expression was quantified by the $2^{-\Delta\Delta Ct}$ method. The YAP25SA samples were normalized to the DNAfectin controls within their time-points. A two-way ANOVA with repeated measures followed by post hoc test revealed that there were no significant differences in the expression of *Ctgf* (P=0.167) or *Ankrd1* (P=0.210) for time and treatment with YAP25SA. (C) Time dependent changes in expression for *Ctgf* and *Ankrd1* were measured by comparing the DNAfectin control samples across the time course. The level of expression was quantified by the $2^{-\Delta\Delta Ct}$ method and by normalizing the 12-, and 24- hour DNAfectin to the 6- hour DNAfectin samples. A one-way ANOVA with repeated measures revealed there was a significant difference in the expression of *Ankrd1* (P=0.005) but not for *Ctgf* (P=0.052) across the time points. Significant differences are denoted as: *p<0.05, **p<0.01, ***p<0.001. Each graph shows the mean fold change values of the biological replicates (N=3) and error bars indicate the standard deviation.

Next, the level of expression of *Rarb* (Figure 11A), *Dhrs3* (Figure 11B), and *Cyp26a1* (Figure 11C) were measured to investigate if an upregulation in YAP activity had an effect on RA-signaling. As illustrated in Figure 11A, a two-way ANOVA with repeated measures did not show that there was a significant difference in *Rarb* expression between time and treatment with YAP25SA; however, there may have been a downwards trend in the expression of *Rarb* when YAP25SA was transfected into the MEC1 cells. A Tukey's post hoc test revealed that the expression of *Rarb* was significantly decreased by 0.59-fold (P=0.008), 0.4-fold (P=0.032), 0.36-fold (P=0.043) for 6-, 12-, and 24- hours respectively, when compared to the controls within the time-point. As well, there were only slight increases in *Rarb* expression of 0.19-fold (P=0.296) and 0.22-fold (P=0.194) for the 12- and 24-hour YAP25SA samples when compared to the 6-YAP25SA sample. This trend suggests that transfection of YAP25SA may slightly lower the expression of *Rarb* at six hours and the fold changes may gradually re-cooperate overtime.

In Figure 11B, at 6- and 12- hours post-transfection the mean of the YAP25SA samples displayed a modest but significant decrease in *Dhrs3* expression of 0.62-fold (P=0.002) and 0.33-fold (P=0.023) respectively, when compared to the controls within their time-point. However, 24 hours post-transfection with YAP25SA did not display a significant difference compared to its control, as there was only 0.07-fold decrease (P=0.742). Additionally, there was a significant increase in *Dhrs3* expression of 0.29-fold (P=0.038) and 0.54-fold (P=0.004) for the 12- and 24-hour YAP25SA samples respectively, when compared to the 6-hour YAP25SA control. This data suggests that transfection of YAP25SA has a minimal effect on the expression of *Dhrs3* in MEC1 cells at six hours and this change gradually diminishes overtime.

Finally, as depicted in Figure 11C, at 6- hours post-transfection the mean of the YAP25SA samples displayed a significant increase in *Cyp26a1* expression of 37.8-fold (P=0.001) when

compared to the 6- hour control. At 12- and 24- hours post YAP25SA transfection, there was an increased trend in *Cyp26a1* expression of 5.57-fold (P=0.518) and 3.3-fold (P=0.857) respectively, when compared to the control within their time-points. Additionally, there was a significant decrease in *Cyp26a1* expression for the 12- and 24-hour YAP25SA samples of 32.2-fold (P=0.003) and 34.5-fold (P=0.002) respectively, when compared to the 6-hour YAP25SA samples.

The same control samples for the 6-, 12- and 24- hour time points were analyzed alone to determine if the YAP25SA time course protocol itself had any effects on the expression of YAP downstream targets and RA-signaling transcripts. As illustrated in Figure 11D, both *Rarb* and *Dhrs3* significantly decreased in expression by 0.78-fold (P=0.027) and 0.86-fold (P=0.018) respectively from 6 to 12 hours. Both *Rarb* and *Dhrs3* had an increased trend of 0.44-fold (P=0.187) and 0.41-fold (P=0.266) respectively from 12 to 24 hours. However, there was still only a 0.34-fold (P=0.334) and 0.45-fold (P=0.183) decrease when the 24-hour controls were compared to the 6-hour controls. Interestingly both *Rarb* and *Dhrs3* had the complete opposite pattern from *Ctgf* and *Ankrd1*. Meanwhile, there were no differences in the expression of *Cyp26a1* across all control samples.

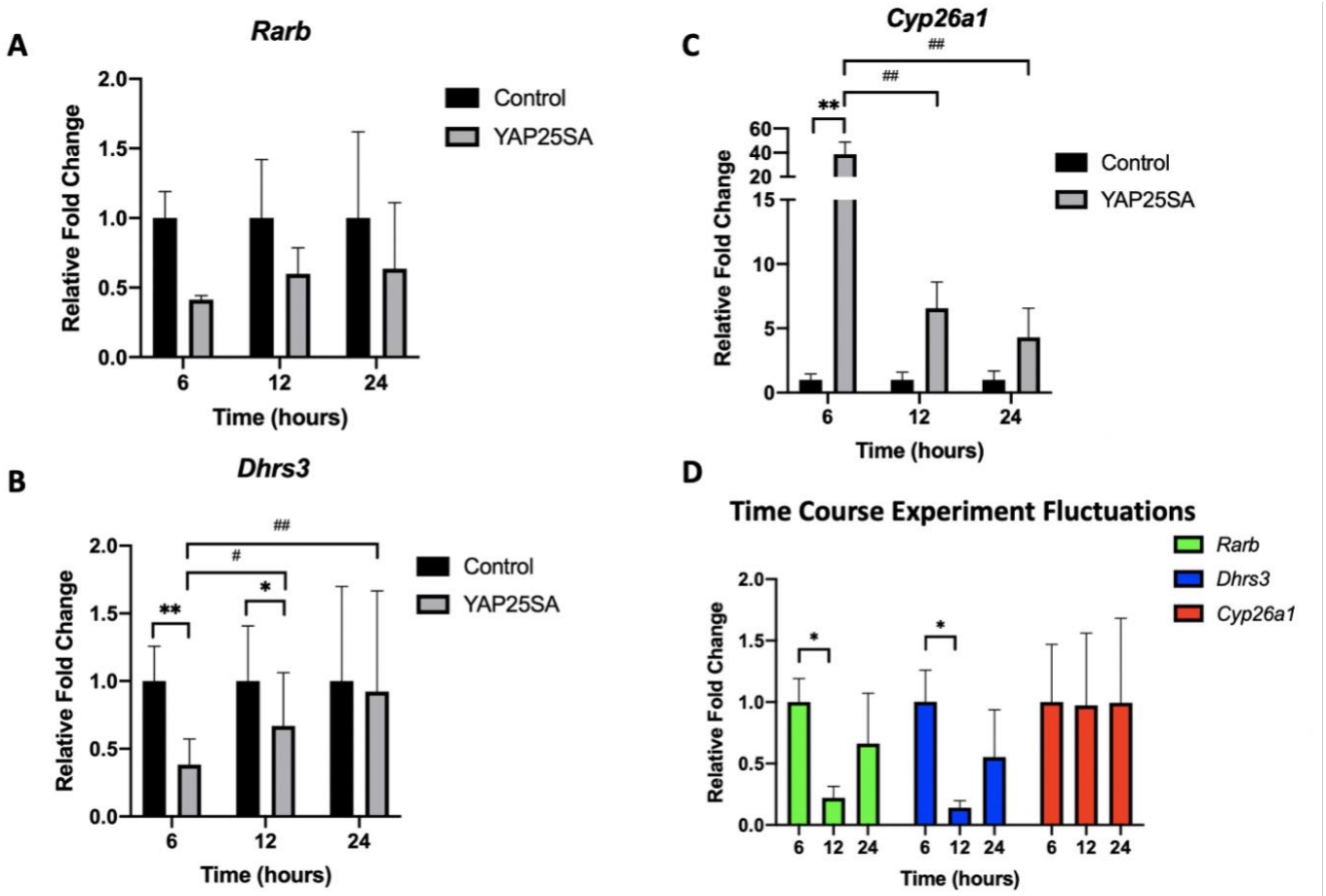

Figure 11: Transfection of a constitutively active form of YAP, YAP25SA, affects RA- signaling. MEC1 cells were transfected with YAP25SA or only treated with DNAfectin as a control. Total RNA was isolated at 6, 12 and 24 hours post transfection and the expression of (A) *Rarb* (B) *Dhrs3* (C) *Cyp26a1* were analyzed by RT-qPCR. The level of expression was quantified by the $2^{-\Delta\Delta Ct}$ method. The averaged YAP25SA samples were normalized to the DNAfectin controls within their time-points. Significant differences are indicated as *p<0.05 vs. control, **p<0.01 vs. control. A two-way ANOVA with repeated measures followed by post hoc test revealed there were significant differences in the expression of *Dhrs3* (P=0.006) and *Cyp26a1* (P=0.002) across time and treatment with YAP25SA; but not for *Rarb* (P=0.188). Significant differences between the time points were denoted as #p<0.05 vs. 6-hours, ##p<0.01 vs. 6-hours. D) Time dependent changes in expression for *Rarb*, *Dhrs3* and *Cyp26a1* were measured by comparing the DNAfectin control samples across the time course. The level of expression was quantified by the $2^{-\Delta\Delta Ct}$ method and by normalizing the 12-, and 24- hour DNAfectin to the 6- hour DNAfectin samples. A one-way ANOVA with repeated measures revealed that there were significant differences in the expression of *Rarb* ($F(2, 6) = 6.44$, P=0.032) and *Dhrs3* ($F(2, 6) = 7.67$, P=0.022) during the time course experiment, but not for *Cyp26a1* ($F(2, 6) = 0.001$, P=0.998). A Tukey's test was performed to determine any significant differences in the expression of RA-signaling targets between the control samples across the time course experiment, denoted as: *p<0.05, **p<0.01, ***p<0.001. Each graph shows the mean fold change and error bars indicate the standard deviation between the biological replicates N=3.

3.4.2 YAP25SA affects RA-signaling through TEAD.

To explore if YAP25SA affects RA-signaling transcripts through a TEAD mechanism, the YTIP-GFP plasmid was used in conjunction with the YAP25SA plasmid. YTIP-GFP is a peptide that outcompetes endogenous TEAD for binding with YAP, therefore interfering with YAP-TEAD signaling and expressing GFP.[70] This experiment consisted of comparing three groups to each other: DNAfectin control, YAP25SA and YAP25SA+ YTIP-GFP. MEC1 cells were either treated with just the DNAfectin solution, transfected with pCMV-flag YAP25SA plasmid or co-transfected with pCMV-flag YAP25SA and YTIP-GFP plasmids. As illustrated in Figure 12, the MEC1 cells treated with the (A) DNAfectin as the control and (B) transfected with YAP25SA did not express GFP, as expected. The MEC1 cells were successfully co-transfected with (C) YAP25SA + YTIP-GFP expressed GFP as they fluoresced green. Next, total RNA was extracted from all six samples and RT-qPCR was performed. There was a significant increase in the expression of both *Ctgf* and *Ankrd1* of 1.782-fold (P=0.007) and 1.040-fold (P=0.0008) respectively when the YAP25SA group was compared to the control group; which indicated that the MEC1 cells were successfully transfected with YAP25SA. As well, there was a significant decrease in the expression for both *Ctgf* and *Ankrd1* of 2.02-fold (P=0.004) and 1.33-fold (P=0.0001) respectively when the MEC1 cells were co-transfected with YAP25SA + YTIP-GFP versus just YAP25SA. Finally, there was no difference between the control and YAP25SA+ YTIP-GFP group as there was only a non-significant 0.24-fold (P=0.840) and a 0.29-fold (P=0.261) difference in the expression of *Ctgf* and *Ankrd1* respectively. This data together suggests that the YTIP-GFP peptide prevented the increased expression of both *Ctgf* and *Ankrd1* caused by YAP25SA, indicating that YAP25SA works through a TEAD mechanism to affect YAP downstream targets in MEC1 cells.

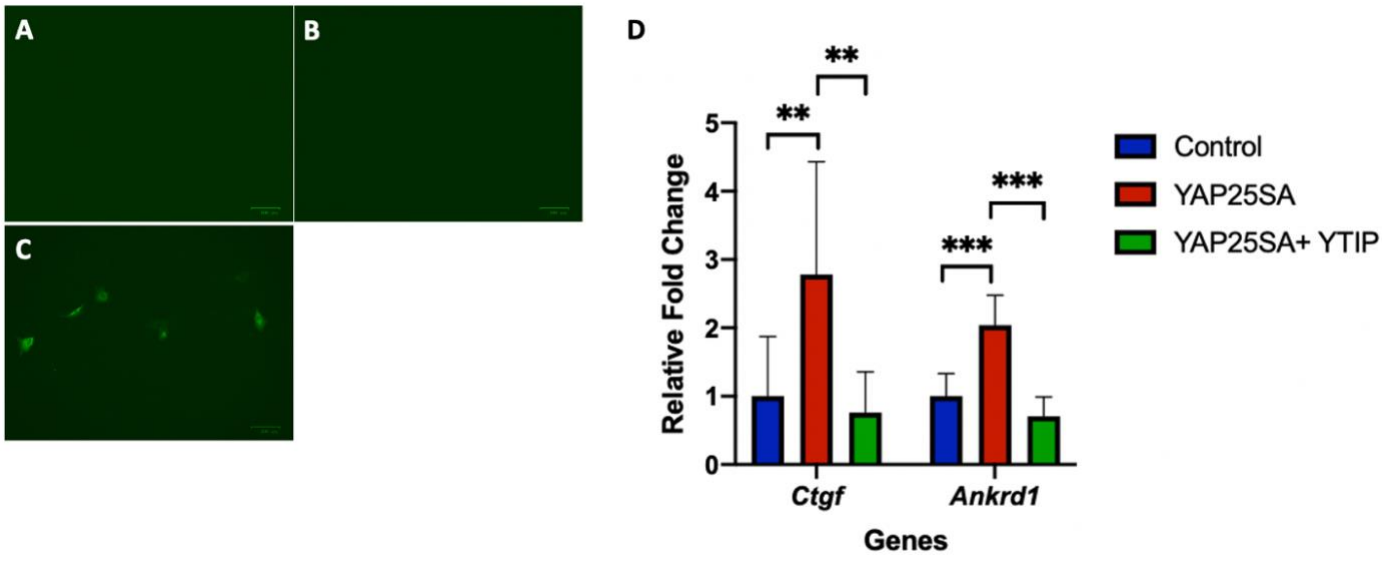

Figure 12: The transcriptional effects YAP25SA are inhibited by concomitant YTIP transfection suggesting that YAP2S5A operated through a TEAD mechanism in embryonic epicardial cells. MEC1 cells were transfected with YAP25SA, YAP25SA+YTIP-GFP or treated with the DNAfectin reagent as the control. After 24 hours, photos from each treatment: A) control, B) YAP25SA and C) YAP25SA+YTIP-GFP were taken with the Zoe Fluorescent Cell Imager (BioRad) to ensure the transfection worked. Next, D) total RNA was extracted and RT-qPCR was performed. Technical Replicates were averaged, and the $2^{-\Delta\Delta CT}$ method was used to calculate the relative fold change by first normalizing the gene of interest to the gene of reference and then the averaged YAP25SA or YAP25SA+YTIP-GFP samples were normalized to the control samples. The experiment was completed in five biological replicates (N=5) and any outliers were determined by using a Grubbs Test. A one-way ANOVA with repeated measures revealed that there was a significant difference in the expression of both *Ctgf* (P=0.003) and *Ankrd1* (P=0.0001) across the three groups. A Tukey's multiple comparisons post hoc test was performed to determine any significant differences between the treatments, denoted as: *p<0.05, **p<0.01, ***p<0.001. The data is reported as mean fold change and error bars indicate a standard deviation.

Next, the same experiment was conducted to see if YAP25SA affects the gene expression of: *Rarb*, *Dhrs3*, and *Cyp26a1* through a TEAD mechanism (Figure 13). The expression of *Cyp26a1* followed the same pattern as *Ctgf* and *Ankrd1*, as there was a significant increase in the expression of *Cyp26a1* of 9.12-fold (P<0.0001) and 2.37-fold (P=0.024) for the YAP25SA and YAP25SA+YTIP-GFP groups respectively, when compared to the control group. Oppositely, when YTIP-GFP was co-transfected with YAP25SA it caused a decrease in the expression of *Cyp26a1* by 3.37-fold (P<0.0001) compared to the YAP25SA group. This data together suggests that the constitutively active YAP25SA increases the expression of *Cyp26a1* through a TEAD-1 mechanism in MEC1 cells, because the YTIP-GFP peptide abrogated the effects of YAP25SA on *Cyp26a1*.

Interestingly, *Rarb* and *Dhrs3* displayed an opposite pattern of induction by YAP in comparison with *Cyp26a1* in Figure 13. There was a very modest decrease in the expression of *Rarb* by 0.24-fold (P=0.014) and a similar though not statistically significant trend of 0.22-fold (P=0.067) for *Dhrs3* when the MEC1 cells were transfected with YAP25SA compared to the control. The expression of *Rarb* and *Dhrs3* remained significantly decreased when the MEC1 cells were co-transfected with YAP25SA+ YTIP-GFP compared to the DNAfectin control by 0.33-fold (P=0.037) and 0.30-fold (P=0.039) respectively. As well, there was no significant difference in the expression of both *Rarb* and *Dhrs3* when comparing YAP25SA+ YTIP-GFP group to the YAP25SA group as the fold change was only 0.05-fold (P=0.683) and 0.03-fold (P=0.901) respectively. This data suggests that the YTIP-GFP peptide did not block the effects that the constitutively active YAP25SA had on the expression of *Rarb* and *Dhrs3* in MEC1 cells; but it is hard to draw a meaningful conclusion given the small magnitude of changes in expression of *Rarb* and *Dhrs3* after YAP2S5A transfection.

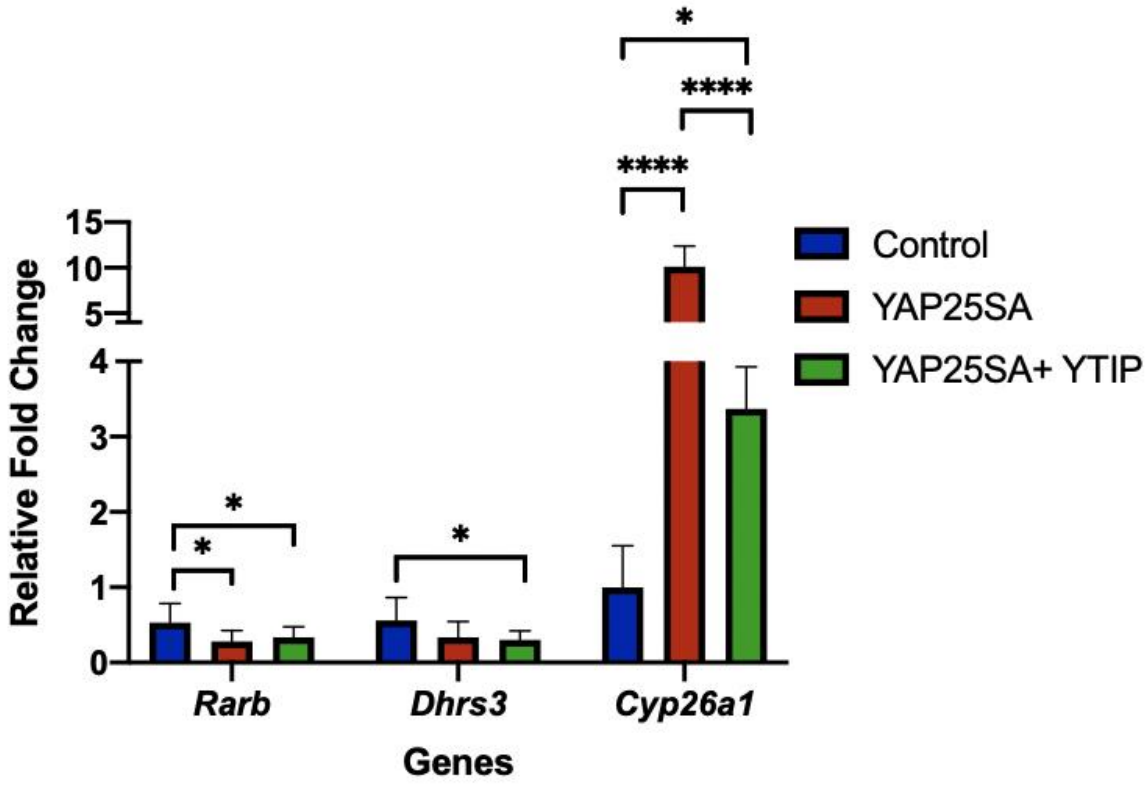

Figure 13: YAP25SA affects RA-signaling through a TEAD mechanism in embryonic epicardial cells. MEC1 cells were transfected with YAP25SA, YAP25SA+YTIP or treated with the DNAfectin reagent as the control in technical duplicates. After 24 hours mRNA was extracted from each of the 6 total samples and RT-qPCR was performed. Technical Replicates were averaged, and the $2^{-\Delta\Delta CT}$ method was used to calculate the relative fold change by first normalizing the gene of interest to the gene of reference and then the averaged YAP25SA or YAP25SA+YTIP samples were normalized to the control samples. The experiment was completed in five biological replicates (N=5) and any outliers were determined using the Grubbs test. A one-way ANOVA with repeated measures revealed that there were significant differences in the expression of *Rarb* (P=0.034), *Dhrs3* (P=0.013) and *Cyp26a1* (P<0.0001) across the three groups. A Tukey's multiple comparisons post hoc test was performed to determine any significant differences between the samples, denoted as: *p<0.05 vs. control, **p<0.01 vs. control, ***p<0.001 vs. control. The data represents the mean fold change and the error bars indicate a standard deviation between the biological replicates.

3.5 Upregulation of YAP activity with YAP25SA, increases RA signaling in MEC1 cells.

The second aim of this thesis was to determine how YAP affects the metabolism of vitamin A. A method used to qualitatively determine the amount of RA in a cell is based on a two-hybrid Gal4-RAR;UAS-tk-Gaussia luciferase reporter system. This sensitive RA-reporter system expresses Gal4-RAR chimeric receptor and a Gaussia luciferase reporter under the control of a promoter containing five copies of the upstream activating sequence (UAS), so that when RA binds to Gal4-RAR, Gaussia luciferase is transcribed and can be measured.[124] To assess if YAP25SA had an effect on the metabolism of retinol (ROL) to RA, the Gal4-RAR;UAS-tk-Gaussia reporter was transiently transfected in MEC1 cells and then three treatment groups were created: (1) DMSO as the control to assess the reporter, (2) ROL as the experimental control and (3) ROL and co-transfection with YAP25SA. Gaussia luciferase was measured from the same samples at 2-, 12-, 24- and 48-hour time points. This experiment was conducted by transfecting and treating each sample as separate events in technical triplicates. The technical triplicates were repeated on separate days to create biological replicates (N=3) that could confirm the patterns observed. Figure 14 shows the analysis of only technical triplicates from the biological replicate with the least significant result, defined as the representative experiment. A representative experiment was chosen by the showing the biological replicate with the highest error bars, since the P-values from the two-way ANOVA with repeated measures were $P< 0.0001$ for all biological replicates. It was decided to only report the least significant result across the biological replicates because this experiment is based off the published protocol by Shannon *et al.* 2020, who also presented their data this way.[34] However, the analysis conducted on all of the biological replicates from different days is illustrated in Supplementary Figure 3.

Figure 14A illustrates the Gaussia luciferase signal patterns throughout the entire time course. The two-hybrid Gal4-RAR;UAS-tk-Gaussia luciferase reporter system was successfully transfected into MEC1 cells as more Gaussia luciferase was transcribed after the addition of ROL. Specifically, there was a significant increase when ROL was added to the two-hybrid Gal4-RAR; UAS-tk-Gaussia luciferase reporter by 10.66-fold (P=0.024), 12.97-fold (P=0.007) and 18.58-fold (P=0.0004) at 12-, 24- and 48- hours respectively when compared to the DMSO control group (Figure 14B).

Interestingly, transfecting YAP25SA into the transient two-hybrid Gal4-RAR; UAS-tk-Gaussia luciferase reporter system resulted in significantly more RA binding to Gal4-RAR and a slower plateau in the signal when compared to the reporter treated with only ROL ($P<0.001$) in MEC1 cells (Figure 14A). Specifically co-transfection of the two-hybrid Gal4-RAR; UAS-tk-Gaussia luciferase reporter system with YAP25SA+ ROL resulted in a significant increase by 9.82-fold (P=0.036), 33.71 fold ($P<0.0001$) and 54.40-fold ($P<0.0001$) at 12-, 24- and 48- hours respectively when compared to the reporter just treated with ROL. Therefore, it was concluded that YAP25SA causes ROL to be converted more efficiently to RA and results in more RA available to bind to the Gal4-RAR in the two-hybrid Gal4-RAR; UAS-tk-Gaussia luciferase reporter system in MEC1 cells. There were no significant differences between all three groups at the 2-hour time point. Therefore, it took longer than two hours for Guassia to be transcribed and secreted after the metabolism of ROL to RA.

Differences in Guassia luciferase were also investigated between time points. The reporter showed the biggest significant increase in Gaussia luciferase by 18.23-fold (P=0.001) from 2 to 48 hours, which confirmed the high stability of Gaussia luciferase as it accumulates overtime. The reporter co-transfected with YAP25SA and treated with ROL had an even bigger significant

increase by 72.03-fold ($P<0.0001$) from 2 to 48 hours. Further confirming that YAP25SA causes there to be more ROL converted to RA. As well, there was a significant increase of 26.30-fold ($P<0.0001$) in Gaussia luciferase from 24 to 48 hours only when the MEC1 two-hybrid Gal4-RAR; UAS-tk-Gaussia luciferase reporter was co-transfected with YAP25SA. Although there was an increase of 5.61- fold ($P=0.401$) for the reporter just treated with ROL, it was not significantly different from the DMSO group. This result also confirmed the trends observed in Figure 14A, as YAP25SA caused the Gaussia luciferase signal to not plateau as quickly.

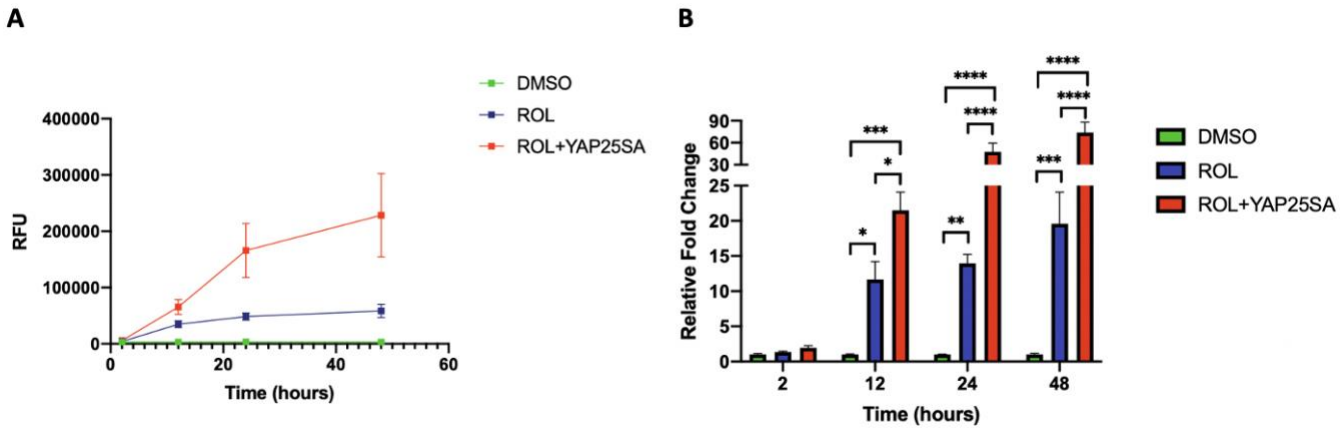

Figure 14: YAP25SA affects the metabolism of ROL to RA in MEC1 cells. MEC1 cells were either reverse co-transfected with pGluc-mini-tk-2-UAS and pCS2p+Gal4-RAR reporter plasmids as a control or pGluc-mini-tk-2-UAS, pCS2p+Gal4-RAR and pCMV-flag YAP25SA plasmids. The next day, half of the MEC1 cells reverse co-transfected with pGluc-mini-tk-2-UAS and pCS2p+Gal4-RAR were treated with DMSO, as the vehicle control to verify the reporter system, and half with 6μM of ROL to the experimental control. The pGluc-mini-tk-2-UAS, pCS2p+Gal4-RAR, and YAP25SA reverse co-transfected MEC1 cells were treated with 6μM of ROL. Each treatment group contained three technical replicates defined as three separate wells were transfected and assayed separately at the same time. A time course experiment was then completed on each of the technical replicates by measuring the Gaussia luciferase signal at 2, 12, 24 and 48 hours after DMSO or ROL was added with a luminometer. (A) shows the mean RFU values for each group across the time course. Error bars indicate a standard deviation between the technical replicates. (B) Relative fold change was calculated by first subtracting the RFU of the blank sample from all of the samples and then dividing the mean of each treatment group by the mean of the DMSO control group. A two-way ANOVA with repeated measures revealed that there was a significant difference between the three groups across both time and treatment ($P<0.0001$). A Tukey's multiple comparisons post hoc test was performed to determine any significant differences between the groups, denoted as: *$p<0.05$, **$p<0.01$, ***$p<0.001$. The data represents the mean fold change and the error bars indicate a standard deviation between the technical replicates. The experiment was performed in biological triplicates (N=3) but only the least significant replicate is showed in Figure 14. The analysis of the biological replicates is illustrated in Supplementary Figure 3.

4. DISCUSSION

The proper regulation of both YAP and RA-signaling is critical for epicardial EMT and the infiltration and differentiation of epicardial cells into fibroblasts and VSMCs of the myocardium.[56,57,61,118] Dysregulation of either epicardial YAP or RA-signaling leads to embryonic lethality. [56,57,61,118] Although YAP and RA-signaling are involved in overlapping developmental processes, the relationship between YAP and RA-signaling has not been thoroughly investigated. Therefore, the goal of this thesis was to explore if YAP activity regulates RA-signaling in the embryonic epicardium. MEC1 cells were used as the model for the embryonic epicardium. MEC1 cells were determined to be a suitable model as they phenotypically (Supplementary Figure 4) and genetically expressed embryonic epicardial characteristics. Specifically, the MEC1 cells expressed *Wt1, Tbx18,* and *Raldh2* (Figure 8), which are genes expressed by the embryonic epicardium. Unfortunately, the MEC1 cells were contaminated with mycoplasma and had to go through several passages of Plasmocin treatment before experiments were conducted. Epicardial cells differentiate into other cellular types, such as EPDCs, fibroblasts or VSMCS and therefore the MEC1 cells may have lost some epicardial characteristics due to them being passaged many times before conducting the transfection experiments.[94] A giant limitation to this study is the unfortunate fact that the experiments with the MEC1 cells could not be conducted at an earlier passage to ensure epicardial characteristics.

4.1 The effects of YAP activity on retinoid gene transcription

4.1.1 Downregulating YAP activity affects the transcription of epicardial markers, retinoid receptors and enzymes.

First, the effects of decreasing the activity of YAP on the expression of YAP targets and retinoid enzymes and receptors was investigated utilizing Verteporfin and YAP siRNA.

Verteporfin is used as a photosensitizer for photodynamic therapy and is used to treat neovascularization caused by age-related macular degeneration, pathologic myopia, and presumed ocular histoplasmosis.[128] Verteporfin also has been found to non-specifically inhibit the interaction of YAP with the TEAD transcription factors; therefore inhibiting YAP activity.[118,127] When MEC1 cells were treated with Verteporfin *Ctgf* expression non-significantly decreased in trend and *Ankrd1* was essentially unchanged (Figure 8). Although there was a non-significant decrease in *Ctgf* expression we were not able to reproduce the inhibitory effect of Verteporfin on Yap-TEAD signaling in MEC1 cells. The effects that Verteporfin has been shown to repress *Ctgf* and *Ankrd1* in a dosage dependent manner in other cell lines.[129] A possible reason why Verteporfin did not have significant effects on known targets in MEC1 cells was because we conducted the experiment in light. Other groups have reported that Verteporfin inhibits YAP activation when cells are maintained in dark conditions [130,131], and therefore this experiment should be repeated in conditions of no light. Although it is hard to draw conclusions due to the lack of significance, our data tracks with a possible decrease in epicardial markers as reported by Singh *et al.* (2016) in relation Verteporfin causing suppression of *Tbx18* and *Wt1*.[118] Although, YAP has been found to strongly regulate both *Wt1* and *Tbx18* expression,[118] we did not observe a strong regulation in MEC1 cells.

Treatment of MEC1 cells with Verteporfin non-significantly decreased *Cyp26a1*, *Cyp26b1* and *Raldh2* expression (Figure 8). Meanwhile, there was no change in expression of *Rarb* and *Dhrs3*. Singh *et al.* (2016) also concluded that Hippo signaling components are strongly expressed in the epicardium and are required for the expression of some epicardial derived growth factors, such as *Raldh2*.[118] This could explain our observed trend in *Raldh2* expression but more work is required to make this conclusion. Previously, *Martien* (2015) showed that TEAD binds to multiple regions of *Raldh2* and overexpressing YAP promoted *Raldh1* expression, which is in the aldehyde

dehydrogenase family.[132] As well, *Guadix et al*. (2011) showed that when *Wt1* was knocked out in epicardial cells, there was a decreased expression of *Raldh2* both *in vivo* and *in vitro*; and that *Raldh2* is a direct transcriptional target of WT1 in epicardial cells.[116] Therefore, it is possible that Verteporfin may decrease *Raldh2* expression directly by interfering with YAP-binding to *Raldh2* or indirectly by inhibiting YAP which reduces *Wt1* expression which lastly causes a decrease in *Raldh2*. In summary, attempts to chemically inhibit the interaction of YAP and TEAD with Verteporfin did not have a significant influence on the expression of epicardial markers, YAP-targets or retinoid enzymes and receptors in MEC1 cells. Due to the non-significant changes observed, it was decided to also genetically inhibit YAP with YAP siRNA to observe the effects on RA-signaling.

Transfection of MEC1 cells with YAP siRNA resulted in a significant decrease in expression of *Yap* by 0.88-fold (P=0.016), but *Ctgf* and *Ankrd1* only displayed a not statistically significant decreased trend when compared to the mean of the Negative siRNA samples. Therefore, although *Yap* was successfully knocked down, its activity may already be low because of the extensive cell-cell contact present in a rapidly growing culture.[66,90] The lack of effect of YAP knockdown in relation to the YAP downstream target gene expression in MEC1 cells could be a result of the very low level of YAP activity in continuously passaged cells. As well, although the MEC1 cells were transfected at the lowest possible confluency to try to prevent cell contact from diminishing YAP activity, the MEC1 cells grew rapidly and started to make contact at 48 hours post transfection. Therefore, the successful knockdown of *Yap* and only a slight knockdown in its targets may be explained by cell contact related reductions in YAP activity, which obscure any effect of further reductions.

Despite these limitations, it is interesting to note that the effects of YAP siRNA on the expression of retinoid enzymes reflected the same trends seen with the Verteporfin treatment. As illustrated in Figure 9B, the transfection of MEC1 cells with YAP siRNA resulted in a modest decrease in the expression of *Cyp26b1* and a non-significant decreased trend in the expression of *Cyp26a1* and *Raldh2*. YAP-knockdown also did not seem to alter the expression of *Rarb* and *Dhrs3*. Although *Cyp26b1* showed a slight decrease in expression when MEC1 cells were transfected with YAP siRNA, overall, inhibiting YAP activity in MEC1 cells with Verteporfin and YAP siRNA does not appear to considerably affect YAP targets or the expression of the retinoid enzymes and receptors. A large standard deviation between biological replicates in treatment groups across genes was also observed, which increase the likelihood of a Type II error (false negative) (Figure 8 and 9). Therefore, this assay may need to be further optimized. As well, for the YAP siRNA data, it should be noted that the CT values of *Raldh2* were quite low in the 34-40 range. The lower CT values could be due to the MEC1 cells starting to lose epicardial characteristic from undergoing multiple passages because RALDH2 is expressed primarily by quiescent epicardial cells.[116] Potentially, if YAP could be maintained at higher activity, it would be possible to revisit the effect of Verteporfin and YAP siRNA on the expression of retinoid enzymes and receptors in MEC1 cells. In the next section, we tried to overcome the potential low YAP activity in cultured MEC1 cells by upregulating YAP expression, to investigate if there could be a potential relationship between YAP activity and the expression of retinoid enzymes in the embryonic epicardium.

4.1.2 The constitutively active YAP25SA activity affects the transcription of retinoid enzymes through a TEAD mechanism

To overcome problems in suppressing YAP activity via chemical or genetic means, we explored an alternative approach by forcing the expression of a constitutively active form of YAP, YAP25SA in MEC1 cells.[66] It was reasoned that given the known inhibitory effects of cell contact on YAP activity[66], it is possible that constitutively active YAP25SA will overcome these inhibitory effects and lead to recordable changes in YAP down-stream target gene expression and perhaps allow us to study the effects of YAP on retinoid enzyme and receptor gene expression and more generally on RA-signaling. We acknowledge that we are employing a relatively artificial paradigm by overexpression of a constitutively active form of YAP, however, for these initial studies, this approach allows us to evaluate possible effects of YAP in RA signaling.

Transfection of MEC1 cells with YAP25SA lead to an increase in YAP activity as both *Ctgf* and *Ankrd1* expression increased when compared to the control group (Figure 12D). Our results correspond to Kim et al. (2019) findings that the YAP25SA mutant is able to increase the expression of *Ctgf*.[133] Further, to verify YAP25SA lead to an increase in YAP activity we employed a competitive inhibitor of YAP-TEAD binding, YTIP-GFP. YTIP-GFP is a peptide that outcompetes endogenous TEAD for binding with YAP, therefore interfering with YAP-TEAD signaling.[70] When MEC1 cells were co-transfected with both YAP25SA and YTIP-GFP it completely counteracted the increased expression of *Ctgf* and *Ankrd1* caused by YAP25SA alone (Figure 12D). Therefore, YAP25SA affected *Ctgf* and *Ankrd1* expression through a TEAD dependent mechanism. YAP25SA was also found to affect the expression of *Ctgf* and *Ankrd1* in as quick as 6 hours post transfection (Figure 10A and B). The expression of *Ctgf* and *Ankrd1* may not have been significant in Figure 10 due to insufficient statistical power.

Six hours after MEC1 cells were transfected with YAP25SA there was a significant 37.8-fold increase in *Cyp26a1* expression (Figure 11C), which then diminished overtime. As well, YTIP-GFP counteracted the increase in *Cyp26a1* expression caused by transfection with YAP25SA alone, as YTIP-GFP co-transfected with YAP25SA was associated with only 3.37-fold increase in a *Cyp26a1* expression (Figure 13). Therefore, it was determined that YAP activity can regulate the expression of *Cyp26a1* through a YAP-TEAD mechanism. This is also important to establish because YAP also has TEAD independent effects. For example YAP can also bind to other transcription factors to regulate gene transcription, such as p73 RUNX2, NKX2-1, TBX5 and CTNNB1.[71,134–140]

Oppositely, both *Dhrs3* (Figure 11B) and *Rarb* (Figure 11A) had a trend of modest decrease in expression when YAP25SA was transfected after 6 hours and then their expression recovered over time; although, only the differences detected for the expression of *Dhrs3* were significant. Interestingly, YTIP-GFP did not counteract the effects caused by YAP25SA for *Dhrs3* expression (Figure 13). It is difficult to draw conclusions if YAP25SA affects the expression of *Dhrs3* and *Rarb* as the changes in magnitude were small. These results are in contrast to the results reported by *Xiao et al.* (2018). When *Xiao et al.* (2018) created an upregulated epicardial YAP activity model by knocking out *Lats1/2* in the epicardium of embryonic mice using the $Wt1^{CreERT2}$ allele called *Lats1/2* conditional knockout (CKO) they reported increased *Dhrs3* expression in the *Lats1/2* CKO heart model-and showed YAP binding to a TEAD motif near the *Dhrs3* locus.[61] This led the authors to suggest a relationship between YAP and *Dhrs3*.[61] Our results report the opposite result as increased YAP25SA activity seemed to potentially downregulate the expression of *Dhrs3* in MEC1 cells. However, we employed a different approach than the one used by Xiao et al. Unlike Xiao et al. 2018, we analyzed the effect of increased YAP activity on *Dhrs3 in vitro*, which could

also explain the differences in results, as other studies have noted that the changes in gene expression of retinoid enzymes can change when culturing on a standard cell culture plate versus plates that mimic more of a *in vivo* environment.[132,141] Therefore, more experiments are needed to confirm if there is a relationship between YAP activity and *Rarb* and *Dhrs3* expression. Next steps to properly assess this would be do conduct experiments either *in vivo* or in conditions that mimic the *in vivo* epicardial environment. The next section will explore if YAP25SA affects the metabolism of retinol to RA.

4.2 YAP activity affects the metabolism of retinol to retinoic acid.

4.2.1 Gaussia Luciferase Assay as a way to qualitatively measure the amount of RA

The gold standard of quantifying the amount of RA in a cell is by extraction and quantification via LC-MS/MS. LC-MS/MS offers the advantage of direct, absolute quantitation of RA that is applicable to cell lines and tissues and is very reproducible.[142,143] Limitations of this approach include requirement for access to expertise and expensive, specialized instrumentation which was not possible in the current environment of the pandemic.[34] To overcome the barriers of directly measuring the amount of RA associated with LC-MS/MS, the two-hybrid Gal4-RAR;UAS-tk-Gaussia luciferase reporter was utilized in this thesis. This sensitive RA-reporter system expresses Gal4-RAR chimeric receptor and a Gaussia luciferase reporter under the control of a promoter containing five copies of the upstream activating sequence (UAS), so that when RA binds to Gal4-RAR, Gaussia luciferase is transcribed and can be measured to qualitatively determine the activity of RA.[124]

The two-hybrid Gal4-RAR;UAS-tk-Gaussia luciferase reporter was attempted to be stably cloned into both MEC1 and NIH3T3 cell lines, but was unsuccessful (Supplementary Section 2). Although it would have been convenient to create a stable two-hybrid Gal4-RAR;UAS-tk-Gaussia

luciferase reporter, ourselves and other groups have found the transient transfections work well.[34,144] In order to construct a stable two-hybrid Gal4-RAR;UAS-tk-Gaussia luciferase reporter further optimizations are needed.

A limitation we identified with the two-hybrid Gal4-RAR;UAS-tk-Gaussia luciferase reporter, was that there was a temporal delay exposure to RA because there were no differences in RA activity detected 2 hours after the addition of retinol (Figure 14). The only differences in Gaussia luciferase signals across all three groups were observed at the 12- hour time point (Figure 14) and continued through the full 48 hours. This temporal delay in exposure was also observed in a study by *Shannon et al.* (2020). *Shannon et al.* (2020) reported that the luciferase levels in the two-hybrid Gal4-RAR;UAS-tk-Gaussia luciferase reporter assay showed an increase in signal starting at around 12 hours after adding retinol and continued through 96 hours. Interestingly, they also simultaneously measured the amount of RA in both the reporter cells and their media by LC-MS/MS. LC-MS/MS detected an increase in the production of RA from retinol after 0.5 hours in the cells and 0.1 hours in their media, which both continued to increase up until 12 hours with sustained, concentration dependent level of RA through 72 hours; confirming the temporal delay between exposure to RA and reporter signal.

4.2.2 YAP25SA increases the metabolism of retinol into RA in MEC1 cells

Transfection of YAP25SA caused a significant increase in the Gaussia luciferase signal when induced by retinol treatment as seen from 12 through 48 hours (Figure 14). This indicated that YAP25SA may cause more RA to be formed in MEC1 cells. This may be related to improved retinol uptake or conversion to RA, or decreased RA oxidation. Or perhaps, YAP25SA may have caused more RA binding to the Gal4RAR receptor or for a longer period of time (Figure 14). The

result of YAP25SA qualitatively increasing the metabolism of retinol to RA may even explain the induction of *Cyp26a1* expression seen in Figures 11C and Figure 13. This is because CYP26A1 is very responsive to RA.[43] Therefore, the increase in *Cyp26a1* expression seen in YAP25SA transfected MEC1 cells may in fact be due to YAP25SA causing more RA to be produced. *Shannon et al.* (2020) reported the very quick production of RA from retinol after 0.5 hours in the HEK293 cells and 0.1 hours in their media using LC-MS/MS. However, this cannot be confirmed with our findings because the two-hybrid Gal4-RAR;UAS-tk-Gaussia luciferase reporter has a temporal delay exposure to RA of 12 hours and so, it is difficult to determine if *Cyp26a1* expression could be increased from transfection of MEC1 cells with YAP25SA causing an increase in RA levels within 6 hours as depicted in Figure 11C. Use of LC-MS/MS would have allowed us to directly assess whether the induction of *Cyp26a1* is due to increased RA or due to some other mechanism. Therefore, despite advantages of the two-hybrid Gal4-RAR;UAS-tk-Gaussia luciferase reporter in that it can be applied to any cell line amenable to transfection, does not require cell lysis, and offers rapid and reproducible results, the limitations include transfection difficulty in some cell lines, a non-quantitative response, and a temporal delay exposure to RA.[34] The next section will explore if other regulatory mechanisms, such as mechanotransduction and cellular proliferation, have an effect on retinoid enzyme and receptor gene expression.

4.3 Mechanisms that regulate YAP may also regulate RA-signaling

4.3.1 Addition of FBS to serum-starved MEC1 cells affects RA-signaling transcripts in MEC1 cells

The main challenge of studying the effects of YAP25SA on RA signaling is derived from the many factors that may influence endogenous YAP activity. There are many mechanisms that regulate the activity of YAP, such as cell proliferation, EMT, mechanotransduction and many intra

cellular pathways.[71] Unfortunately, in the time course experiments, a major limitation was that it was hard to control for these outside regulatory mechanisms (Figure 10C). When the control samples were compared, it revealed that the experimental protocol did have significant effects on *Ankrd1, Rarb* and *Dhrs3* expression.

There was a significant increase in *Ankrd1* expression from 6 to 12 hours post transfection and *Ctgf* followed the same trend in expression (Figure 10C). These observed changes may have been due to the addition of FBS 6-hours post-transfection causing an increase in endogenous YAP activity. FBS was added 6-hours post transection because it interacts with the transfection efficiency, but it was also required in culture media to allow MEC1 cells to proliferate for the full 24-hour time course experiment. *Plouffe et al.* (2018) demonstrated that serum is a potent activator of YAP/TAZ activity as it activates G protein–coupled receptors to inactivate the Hippo pathway, resulting in dephosphorylated, nuclear, and transcriptionally active YAP and TAZ.[145] As well, *Plouffe et al.* (2018) reported that following serum stimulation, the expression of the known YAP targets *Ctgf* and *Cyr61* were induced in all cell lines except the YAP/TAZ KO cell line created by CRISPR-Cas9, which indicated that the induction of *Ctgf* and *Cyr61* by FBS is YAP/TAZ-dependent. Although *Ctgf* expression was not significantly increased like *Ankrd1* in MEC1 cells after addition of FBS, it did follow the same trend which corresponds to *Plouffe et al.* (2018) findings.

FBS contains retinol.[146] Therefore, we expected that after addition of FBS, *Cyp26a1, Dhrs3* and *Rarb* expression would increase as the MEC1 cells quickly metabolized retinol to RA as they are directly induced by RA.[36,38,41] Surprisingly, *Cyp26a1* expression was not affected by the addition of FBS at 6 hours, meanwhile both *Rarb* and *Dhrs3* significantly decreased in expression from 6 to 12 hours (Figure 11D). Therefore, the decrease in *Rarb* and *Dhrs3* may be due to other

mechanisms related to cellular proliferation caused by the addition of FBS. This would not be surprising because changes in *Cyp26a1*, *Dhrs3* and *Rarb* expression have been implicated in cancer progression, which involves unregulated cellular proliferation.[147,148,149(p1)] For example both *Dhrs*3 and *Rarb* have been shown to be under expressed and epigenetically silenced in breast cancer.[147,148] Meanwhile, primary breast cancers were found to over-express *Cyp26a1*. Further investigation is needed to determine how FBS may have influenced the expression of *Dhrs3* and *Rarb*, but not *Cyp26a1* in MEC1 cells.

4.3.2 Contact inhibition of proliferation and mechanical tension affects RA-signaling transcripts in MEC1 cells

Another potential confounding YAP regulatory mechanism that might have explained differences in transcript expression for the controls during the experiments conducted in Figures 10 and 11 was contact inhibition of proliferation (CIP). CIP is a property where non-malignant cells at high-cell density cease proliferation and cell division when they occupy all the space allocated to them upon reaching confluence.[66] It was observationally noted that at 24 hours, MEC1 cells made contact due to high cell density. MEC1 cells grow rapidly so CIP was a re-occuring factor in all experiments. For example, within 24 hours after plating only 40,000 MEC1 cells on a 12-well plate, they would be confluent (Figure 10C and 11D). Our results reflect that MEC1 cells are capable of CIP because *Ankrd1* expression significantly decreased between 12 and 24 hours as the cells reached a high confluency; which indicated a decrease in YAP activity associated with CIP (Figure 10C). Meanwhile, there was a non-significant slight increased trend in *Rarb* and *Dhrs3* expression from 12 to 24 hours (Figure 11D). These observations were also complimented by Supplementary Figures 4 and 5 because as MEC1 cells make contact both *Ctgf* and *Ankrd1* expression decreased in trend overtime, while *Rarb* and *Dhrs3* expression increased overtime. It

is well known in literature that YAP/TAZ are mediators of CIP.[66] When cells are seeded at a low density and are flat/ well-spread on a stiff extracellular matrix, YAP/TAZ localize to the nucleus and are transcriptionally active. However, when cells are round/ compact at high-cell density or plated on a soft matrix with minimum adhesion area to the extracellular matrix, YAP/TAZ are re-distributed to the cytosol and are inactive.[71] CIP may be a possible new regulatory mechanism for the RA-signaling pathway, but further experiments are needed to validate this observation. CIP is also a form of mechanotransduction as compact cells experience mechanical stress.[91]

Despite the shutdown, we conducted a preliminary experiment to investigate if mechanical tension influences epicardial YAP activity and RA-signaling by seeding MEC1 cells on plates of varying stiffness over a 96-hour time period. The 2kPa plate approximated embryonic heart stiffness[123], while the 30kPa plate mimicked a developed heart[150] and normal cell culture plates are equivalent to a mechanically stiff control. The observations recorded in Supplementary Figure 4, show that after 12 hours of culture under various substrate matrix conditions, MEC1 cells exhibited noticeable morphological differences. At 12 hours, the MEC1 cells were round on the 2kPa plate and then became flatter and more spread out as the plates became stiffer. Our results reflect the observations made by *Xiao et al.* (2018) who plated WT1-expressing primary epicardial cells on hydrogels of 4kPa and 20kPa stiffness. On the 4kPa matrix, the primary epicardial cells exhibited a spindle shape with YAP distributed equally to the nucleus and the cytoplasm. In contrast epicardial cells grown on a stiffer 20kPa matrix had a flat shape with increased nuclear YAP localization.[61] When we conducted RT-qPCR and calculated the fold change in mRNA expression by normalizing all the samples to the 2kPa, 12-hour control there were some preliminary trends noticed in Supplementary Figure 5. It should be noted that this is preliminary data and mean values are from the technical duplicates that were formed side by side and on the

same day but processed and analyzed separately (N=1) and therefore no significant conclusions could be formed. At 12 and 24 hours, the MEC1 cells may have had a higher *Ctgf* and *Ankrd1* expression when plated on the 30kPa and 6-well plates. This was expected as a stiffer matrix is known to increase YAP activity and nuclear localization. Our data supports *Xiao et al.* (2018) conclusions that mechanical tension is an upstream physiologic signal controlling Hippo/Yap activity in embryonic epicardial cells and increased nuclear YAP.

Rarb, *Dhrs3* and *Cyp26a1* expression seemed to be minimally higher on 30kPa and 6-well plates compared to the 2kPa plates within their time points. This observation supports Swift et al. (2013) conclusions that matrix elasticity is upstream of the RA pathway.[141] Swift et al. (2013) discovered that lamin-A, an intermediate filament protein compromising the major structural and mechanical components of the nuclear lamina directly regulates *Rarb* expression but not *Cyp26a1* expression. Further, Bioinformatics analysis of promoters for *LMNA* and chromatin-IP confirmed binding of RARs to *LMNA*. This is interesting because it was previously known that lamin-A transcription is regulated by the RA[151], but lamin-A itself might regulate the RA signaling pathway. As well, Swift et al. (2013) discovered that proper RA-signaling is required for Lamin-A to respond to mechanical stiffness. A mutated promoter construct (**Δ**-*LMNA*) that lacked four of six RAREs showed no significant response to RA. In mesenchymal stem cells (MSCs) with a lamin-A promoter driving GFP expression, there was an increase in expression on stiff matrix compared to soft matrix, while **Δ**-*LMNA* showed no significant difference. Also, lamin-A expression decreased with the addition of RA on a stiff matrix, but the effects were entirely suppressed on a soft matrix. Therefore, mechanical stiffness could have influenced the expression of *Dhrs3* and *Rarb* in MEC1 cells. As well, Yi et al. (2015) reported that mechanical force and tensile strain inhibit retinol metabolism by inhibiting Lecithin retinol acyltransferase (LRAT),

Cellular retinol-binding protein-1 (CRBP-1), retinyl ester hydrolase (REH), RARβ and RXRα mRNA and protein expression in hepatic stellate cells. Our preliminary data in Supplementary Figure 5, cannot conclude if mechanical tension influences RA-signaling expression in MEC1 cells because it is hard to draw meaningful conclusions due to the experiment only being conducted once (N=1). The relationship between mechanical tension and RA-signaling needs to be further investigated to delineate if there is a relationship between mechanical tension and RA-signaling. As well, future directives should be to investigate if mechanical tension can influence RA-signaling via YAP or other mechanisms such as lamin-A in MEC1 cells or primary epicardial cells. Furthermore, to expand on this thesis, the post translational effects of YAP activity on retinoid enzyme and receptor protein expression in MEC1 cells needs to also be investigated to gain a deeper understanding of the relationship between YAP and RA-signaling in the epicardium.

5. Conclusions

The goal of this thesis was to establish if there was a relationship between YAP activity and RA-signaling in MEC1 cells. First YAP activity was attempted to be inhibited through YAP siRNA and the YAP-TEAD inhibitor, Verteporfin. Verteporfin was unsuccessfully able to interrupt YAP and TEAD activity in MEC1 cells, as the expression of known targets: *Ctgf, Ankrd1, Wt1,* and *Tbx18* were not significantly affected. YAP siRNA was successfully able to knockdown the expression of *Yap* in MEC1 cells; however, its activity was not significantly affected because *Ctgf* and *Ankrd1* only decreased in a non-significant manner. Only *Cyp26b1* was significantly affected by YAP siRNA, as its expression levels decreased. However, due to YAP siRNA not being able to decrease the gene expression of known YAP downstream targets, no conclusions can be drawn. It was questioned whether the rapid growth of MEC1 cells causing contact inhibition of

proliferation, could decrease the activity of YAP to the point where the signal was too low to detect any changes in gene expression. Therefore, we decided to upregulate YAP activity in MEC1 cells using the YAP25SA plasmid that is constitutively active due to mutations in its phosphorylation sites. We were able to confirm a relationship between *Cyp26a1* expression and upregulated YAP activity as YAP25SA induced an increase in mRNA expression by 37.8-fold within 6 hours of transfection. As well, we were able to determine that YAP25SA affected *Cyp26a1* expression through TEAD mechanism. Because when MEC1 cells were co-transfected with YAP25SA and YTIP-GFP, a plasmid that blocks YAP-TEAD interaction, the induced effects of YAP25SA on *Cyp26a1* expression decreased. Although transfecting MEC1 cells with YAP25SA caused significant decreases in *Dhrs3* and *Rarb* expression, the changes were so minimal that no conclusion could be drawn. Therefore, we successfully established a relationship between *Cyp26a1* mRNA expression and YAP activity. Next, we investigated if YAP25SA had any effects on retinol metabolism using the two-hybrid Gal4-RAR;UAS-tk-Gaussia luciferase reporter system. It was determined that co-transfection of MEC1 cells with YAP25SA allowed more retinol to be converted to RA and for a longer period of time when compared to MEC1 cells transfected with only the reporter. Since *Cyp26a1* is directly induced by RA, it was proposed that YAP25SA may cause increased RA levels that then induce *Cyp26a1* mRNA expression. However, due to the temporal delay in RA we could not establish if *Cyp26a1* was induced directly by YAP or indirectly by YAP25SA causing increased RA production. Further experiments are needed to delineate how YAP25SA affected *Cyp26a1* expression as this may lead us to new mechanisms that can regulate RA-signaling. Especially since we were able to show that addition of FBS and contact inhibition of proliferation regulated YAP activity in MEC1 cells and may have had an influence on both *Dhrs3* and *Rarb* expression.

6. Future Implications

Understanding the relationship between RA and YAP signaling in the epicardium during embryonic development will help gain a deeper understanding into the mechanisms that allow for proper cardiac development. Since YAP is a mediator for many physiological processes ranging from mechanotransduction to cellular proliferation, establishing a relationship with RA-signaling could lead to new mechanisms of RA regulation. This is important because a dysregulation of either RA or YAP signaling can be fatal.[54,57,61] Therefore, the long-term implications of this research could help us to mitigate diseases caused by a dysregulation in epicardial RA-signaling. Specifically, current literature has investigated both epicardial RA and YAP signaling to understand the mechanisms that take place after a myocardial infarction to prevent subsequent heart failure. Research into heart failure is important because with increased technology more patients are surviving heart attacks, however the damage to a patient's heart gives later poor outcomes. During a myocardial infarction, the obstruction of blood flow causes sudden cessation of oxygen supply to regions of the cardiac muscle resulting in the death of mostly cardiomyocytes, endothelial cells and fibroblasts.[110] The adult mammalian-infarcted heart cannot regenerate the lost tissue and instead myofibroblasts replace the damaged myocardium with fibrotic tissue.[152,153] This leads to the creation of a non-contractile scar, which severely impairs cardiac function, eventually progressing to heart failure.[94] Heart failure occurs when abnormalities in heart function cause the pumping action of the heart to be reduced, resulting in less blood flow throughout the body and can be life threatening.[154] The prognosis for a patient is not good, as there are few therapeutic options and the adult human heart has limited regenerative capabilities.[154] Below is a detailed summary of the literature that investigated the role of the epicardium, YAP, and RA-signaling in heart regeneration.

6.1 The Pathological Role of the Adult Epicardium After Cardiac Injury

During embryonic development the epicardium is essential as it sends EPDCs and paracrine signals to the myocardium. However, the postnatal mammalian heart is a quiescent cell layer that downregulates many epicardial specific genes.[94,155] *Zhou et al.* (2011) showed this by using a tamoxifen inducible *Wt1*^{CreERT2} mouse crossed onto a Cre reporter line (*Rosa*^{mTmG}) to label WT1 cells at any point to track their fate by continuous expression of GFP. This experiment gave healthy adult mice tamoxifen injections for eight weeks and revealed no migration of WT1/GFP expressing cells into the myocardium.[155] However, when *Zhou et al.* (2011) treated adult *Wt1*$^{CreERT2/+}$*;Rosa26*$^{mTmG/+}$ mice with tamoxifen, then induced myocardial infarction (MI) by coronary artery ligation, there was an upregulation of embryonic epicardial genes *Wt1*, *Tbx18*, and *Raldh2*. As well, EPDCs of the adult heart after MI expressed markers of mesenchymal lineages including fibroblasts, myofibroblasts, and smooth muscle cells, which was confirmed by analysis of FACS-purified EPDCs with immunostaining and RT-qPCR. *Zhou et al.* (2011) concluded after MI, EPDCs are formed as a thickened layer on the surface of the heart that secrete paracrine factors and adopt fibroblast and smooth muscle cell fates.

6.2 The Pathological Role of the Epicardial RA-signaling After Cardiac Injury in a Zebra Fish Model

Unlike adult mammals, zebrafish have remarkable cardiac-regenerative capacity. After 20% resection of the ventricle, zebrafish can fully regenerate lost heart tissue by forming new coronary blood vessels to vascularize the regenerating myocardium.[156] Expression of the embryonic epicardial markers *Tbx18*, *Pdgfr*β and *Raldh2* is induced in the epicardium of adult regenerating hearts, suggesting that an embryonic gene expression program in the epicardium is activated in response to injury. RA-signaling in the epicardium has been found to be critical in

mediating the regeneration of the adult zebrafish heart. For example, Kikuchi *et al.* (2011) found that by day one post-trauma, the injured site becomes supplemented with *Raldh2*-expressing epicardial cells as cardiogenesis begins. Alternatively, induced transgenic inhibition of RARs or expression of an RA-degrading Cyp26 family of enzymes blocked regenerative cardiomyocyte proliferation.[157] Therefore, in the zebra fish model epicardial RA-signaling has a crucial role in their ability to regenerate the heart.

6.3 The Pathological Role of the Epicardial YAP After Cardiac Injury

Research has revealed that Hippo signaling and YAP play a role in the regulation of fibrosis, which is an excessive accumulation of extracellular matrix after MI.[158,159] *Liu et al.* (2015) found that both YAP and TAZ accumulate in the nuclei of fibroblasts grown on pathologically stiff matrices.[159] As well, knockdown of YAP and TAZ together *in vitro* reduced key fibroblast functions on pathologically stiff matrices, such as matrix synthesis, contraction, and proliferation.[159] In addition, immortalized fibroblasts that conditionally express active YAP or TAZ mutant proteins overcame soft matrix limitations on growth and promoted fibrosis when adoptively transferred to a mouse lung.[159] Therefore, the conclusions by Liu et al. (2015) demonstrate that YAP and TAZ are mechano-activated coordinators of the matrix-driven feedback loop that amplifies and sustains fibrosis. When fibroblasts are activated in injured tissues by inflammatory signals and stretch, it also leads to active YAP and TAZ by their nuclear accumulation.[159] Recently Xiao *et al.* (2019) discovered that the Hippo pathway is an integrated component of cardiac fibroblasts differentiation and activation in the adult mouse heart in normal homeostasis and injured models.[160,111] This was accomplished by genetically deactivating the Hippo pathway by conditionally deleting *Lats1/2* genes in cardiac fibroblasts using a fibroblast-

specific, adult inducible Cre strategy.[160] Conditional deletion of Hippo pathway kinases, *Lats1* and *Lats2*, in uninjured Cardiac fibroblasts lead to fibroblast activation in the endo- and epicardial regions of the heart.[160,111] Single cell transcriptomics showed that uninjured *Lats1/2* mutant cardiac fibroblasts spontaneously transitioned to a myofibroblast cell state.[160] Furthermore, integrated genome-wide analysis of *Yap* chromatin occupancy revealed that YAP directly activated myofibroblast cell identity genes and an array of genes encoding pro-inflammatory factors in the *Lats1/2* mutant cardiac fibroblasts.[160] Therefore, it was concluded that *Lats1/2* maintains the resting cardiac fibroblast cell state through restricting the YAP-induced injury response.[160,111] Next, Xiao *et al.* (2019) subjected *Lats1/2* CKO mouse model to myocardial infarction (MI) to understand the effects of *Lats1/2* depletion in cardiac fibroblasts in a disease setting. In comparison to the wild type mice, the *Lats1/2* CKO mice had prolonged cardiac fibroblast proliferation and an altered scar formation that lead to their lethality within 3 weeks.[160] Furthermore, Massons' trichrome staining of the injured area revealed less dense, noncompacted collagen content in the Lats1/2 CKO, suggesting that Hippo signaling was necessary for mature scar formation and the fully differentiated function of myofibroblasts.[160] Therefore, conditional deletion of Hippo pathway kinases, *Lats1/2*, in uninjured cardiac fibroblasts initiated a self-perpetuating fibrotic response that is exacerbated following MI.[160,111] The epicardium is an intriguing cell population to study because it is easily accessible, since it is located outside the heart allowing for less invasive procedures.[94] A better understanding of the relationship between RA- and YAP-signaling in the epicardium during cardiac development may suggest strategies to manipulate adult epicardial cells to facilitate myocardial regrowth and angiogenesis after cardiac injury.

7. References

1. Yokota S, Shirahata T, Yusa J, Sakurai Y, Ito H, Oshio S. Long-term dietary intake of excessive vitamin A impairs spermatogenesis in mice. *J Toxicol Sci*. 2019;44(4):257-271. doi:10.2131/jts.44.257

2. Clagett-Dame M, DeLuca HF. The role of vitamin A in mammalian reproduction and embryonic development. *Annu Rev Nutr*. 2002;22:347-381. doi:10.1146/annurev.nutr.22.010402.102745E

3. Conaway HH, Henning P, Lerner UH. Vitamin a metabolism, action, and role in skeletal homeostasis. *Endocr Rev*. 2013;34(6):766-797. doi:10.1210/er.2012-1071

4. Tan L, Wray AE, Ross AC. Oral Vitamin A and Retinoic Acid Supplementation Stimulates Antibody Production and Splenic Stra6 Expression in Tetanus Toxoid–Immunized Mice. *J Nutr*. 2012;142(8):1590-1595. doi:10.3945/jn.112.161091

5. Duester G. Retinoic Acid Synthesis and Signaling during Early Organogenesis. *Cell*. 2008;134(6):921-931. doi:10.1016/j.cell.2008.09.002

6. Hernandez RE, Putzke AP, Myers JP, Margaretha L, Moens CB. Cyp26 enzymes generate the retinoic acid response pattern necessary for hindbrain development. *Development*. 2007;134(1):177-187. doi:10.1242/dev.02706

7. Huang P, Chandra V, Rastinejad F. Retinoic Acid Actions Through Mammalian Nuclear Receptors. *Chem Rev*. 2014;114(1):233-254. doi:10.1021/cr400161b

8. Endo T, Mikedis MM, Nicholls PK, Page DC, de Rooij DG. Retinoic Acid and Germ Cell Development in the Ovary and Testis. *Biomolecules*. 2019;9(12). doi:10.3390/biom9120775

9. D'Ambrosio DN, Clugston RD, Blaner WS. Vitamin A metabolism: an update. *Nutrients*. 2011;3(1):63-103. doi:10.3390/nu3010063

10. Collins MD, Mao GE. Teratology of retinoids. *Annu Rev Pharmacol Toxicol*. 1999;39:399-430. doi:10.1146/annurev.pharmtox.39.1.399

11. Lohnes D, Mark M, Mendelsohn C, et al. Function of the retinoic acid receptors (RARs) during development (I). Craniofacial and skeletal abnormalities in RAR double mutants. *Development*. 1994;120(10):2723-2748.

12. Wilson JG, Warkany J. Malformations in the genito-urinary tract induced by maternal vitamin a deficiency in the rat. *American Journal of Anatomy*. 1948;83(3):357-407. doi:10.1002/aja.1000830303

13. Kaylor JJ, Cook JD, Makshanoff J, Bischoff N, Yong J, Travis GH. Identification of the 11-cis-specific retinyl-ester synthase in retinal Müller cells as multifunctional O-acyltransferase (MFAT). *PNAS*. 2014;111(20):7302-7307. doi:10.1073/pnas.1319142111

14. Travis GH, Golczak M, Moise AR, Palczewski K. Diseases caused by defects in the visual cycle: retinoids as potential therapeutic agents. *Annu Rev Pharmacol Toxicol*. 2007;47:469-512. doi:10.1146/annurev.pharmtox.47.120505.105225

15. Saari JC. Vitamin A metabolism in rod and cone visual cycles. *Annu Rev Nutr*. 2012;32:125-145. doi:10.1146/annurev-nutr-071811-150748

16. Ghyselinck NB, Duester G. Retinoic acid signaling pathways. *Development*. 2019;146(13). doi:10.1242/dev.167502

17. Moss JB, Xavier-Neto J, Shapiro MD, et al. Dynamic patterns of retinoic acid synthesis and response in the developing mammalian heart. *Dev Biol*. 1998;199(1):55-71. doi:10.1006/dbio.1998.8911

18. Rhinn M, Dolle P. Retinoic acid signalling during development. *Development*. 2012;139(5):843-858. doi:10.1242/dev.065938

19. West KP. Vitamin A Deficiency Disorders in Children and Women. *Food Nutr Bull*. 2003;24(4_suppl_1):S78-S90. doi:10.1177/15648265030244S104

20. Goodman DS. Vitamin A and retinoids in health and disease. *N Engl J Med*. 1984;310(16):1023-1031. doi:10.1056/NEJM198404193101605

21. Shimozono S, Iimura T, Kitaguchi T, Higashijima S-I, Miyawaki A. Visualization of an endogenous retinoic acid gradient across embryonic development. *Nature*. 2013;496(7445):363-366. doi:10.1038/nature12037

22. Green AS, Fascetti AJ. Meeting the Vitamin A Requirement: The Efficacy and Importance of β-Carotene in Animal Species. *ScientificWorldJournal*. 2016;2016. doi:10.1155/2016/7393620

23. Al Tanoury Z, Piskunov A, Rochette-Egly C. Vitamin A and retinoid signaling: genomic and nongenomic effects. *J Lipid Res*. 2013;54(7):1761-1775. doi:10.1194/jlr.R030833

24. Moriwaki H, Blaner WS, Piantedosi R, Goodman DS. Effects of dietary retinoid and triglyceride on the lipid composition of rat liver stellate cells and stellate cell lipid droplets. *J Lipid Res*. 1988;29(11):1523-1534.

25. Wongsiriroj N, Piantedosi R, Palczewski K, et al. The Molecular Basis of Retinoid Absorption. *J Biol Chem*. 2008;283(20):13510-13519. doi:10.1074/jbc.M800777200

26. Kawaguchi R, Zhong M, Kassai M, Ter-Stepanian M, Sun H. STRA6-Catalyzed Vitamin A Influx, Efflux, and Exchange. *J Membr Biol*. 2012;245(11):731-745. doi:10.1007/s00232-012-9463-1

27. Smith FR, Goodman DS. Vitamin A transport in human vitamin A toxicity. *N Engl J Med*. 1976;294(15):805-808. doi:10.1056/NEJM197604082941503

28. Muenzner M, Tuvia N, Deutschmann C, et al. Retinol-Binding Protein 4 and Its Membrane Receptor STRA6 Control Adipogenesis by Regulating Cellular Retinoid Homeostasis and Retinoic Acid Receptor α Activity. *Molecular and Cellular Biology*. 2013;33(20):4068-4082. doi:10.1128/MCB.00221-13

29. Yang Q, Graham TE, Mody N, et al. Serum retinol binding protein 4 contributes to insulin resistance in obesity and type 2 diabetes. *Nature*. 2005;436(7049):356-362. doi:10.1038/nature03711

30. Christensen HN. Is PQQ a significant nutrient in addition to its role as a therapeutic agent in the higher animal? *Nutr Rev*. 1994;52(1):24-25. doi:10.1111/j.1753-4887.1994.tb01351.x

31. Vogel S, Mendelsohn CL, Mertz JR, et al. Characterization of a New Member of the Fatty Acid-binding Protein Family That Binds All-trans-retinol. *J Biol Chem*. 2001;276(2):1353-1360. doi:10.1074/jbc.M005118200

32. Napoli JL. A gene knockout corroborates the integral function of cellular retinol-binding protein in retinoid metabolism. *Nutr Rev*. 2000;58(8):230-236. doi:10.1111/j.1753-4887.2000.tb01870.x

33. Ghyselinck NB, Båvik C, Sapin V, et al. Cellular retinol-binding protein I is essential for vitamin A homeostasis. *EMBO J*. 1999;18(18):4903-4914. doi:10.1093/emboj/18.18.4903

34. Shannon SR, Yu J, Defnet AE, et al. Identifying vitamin A signaling by visualizing gene and protein activity, and by quantification of vitamin A metabolites. *Methods Enzymol*. 2020;637:367-418. doi:10.1016/bs.mie.2020.03.011

35. Jiang W, Napoli JL. The Retinol Dehydrogenase Rdh10 Localizes to Lipid Droplets during Acyl Ester Biosynthesis. *J Biol Chem*. 2013;288(1):589-597. doi:10.1074/jbc.M112.402883

36. Sandell LL, Lynn ML, Inman KE, McDowell W, Trainor PA. RDH10 oxidation of Vitamin A is a critical control step in synthesis of retinoic acid during mouse embryogenesis. *PLoS One*. 2012;7(2):e30698. doi:10.1371/journal.pone.0030698

37. Harrison EH. Mechanisms involved in the intestinal absorption of dietary vitamin A and provitamin A carotenoids. *Biochim Biophys Acta*. 2012;1821(1):70-77. doi:10.1016/j.bbalip.2011.06.002

38. Niederreither K, McCaffery P, Dräger UC, Chambon P, Dollé P. Restricted expression and retinoic acid-induced downregulation of the retinaldehyde dehydrogenase type 2 (RALDH-2) gene during mouse development. *Mech Dev*. 1997;62(1):67-78. doi:10.1016/s0925-4773(96)00653-3

39. Dupé V, Matt N, Garnier J-M, Chambon P, Mark M, Ghyselinck NB. A newborn lethal defect due to inactivation of retinaldehyde dehydrogenase type 3 is prevented by maternal retinoic acid treatment. *PNAS*. 2003;100(24):14036-14041. doi:10.1073/pnas.2336223100

40. Fan X, Molotkov A, Manabe S-I, et al. Targeted disruption of Aldh1a1 (Raldh1) provides evidence for a complex mechanism of retinoic acid synthesis in the developing retina. *Mol Cell Biol*. 2003;23(13):4637-4648. doi:10.1128/mcb.23.13.4637-4648.2003

41. Billings SE, Pierzchalski K, Butler Tjaden NE, et al. The retinaldehyde reductase DHRS3 is essential for preventing the formation of excess retinoic acid during embryonic development. *FASEB J*. 2013;27(12):4877-4889. doi:10.1096/fj.13-227967

42. Feng L, Hernandez RE, Waxman JS, Yelon D, Moens CB. Dhrs3a regulates retinoic acid biosynthesis through a feedback inhibition mechanism. *Dev Biol*. 2010;338(1):1-14. doi:10.1016/j.ydbio.2009.10.029

43. Topletz AR, Tripathy S, Foti RS, Shimshoni JA, Nelson WL, Isoherranen N. Induction of CYP26A1 by Metabolites of Retinoic Acid: Evidence that CYP26A1 is an Important Enzyme in the Elimination of Active Retinoids. *Mol Pharmacol*. Published online January 1, 2014. doi:10.1124/mol.114.096784

44. Niederreither K, Abu-Abed S, Schuhbaur B, Petkovich M, Chambon P, Dollé P. Genetic evidence that oxidative derivatives of retinoic acid are not involved in retinoid signaling during mouse development. *Nat Genet*. 2002;31(1):84-88. doi:10.1038/ng876

45. Dong D, Ruuska SE, Levinthal DJ, Noy N. Distinct roles for cellular retinoic acid-binding proteins I and II in regulating signaling by retinoic acid. *J Biol Chem*. 1999;274(34):23695-23698. doi:10.1074/jbc.274.34.23695

46. Wang L, Li Y, Yan H. Structure-function relationships of cellular retinoic acid-binding proteins. Quantitative analysis of the ligand binding properties of the wild-type proteins and site-directed mutants. *J Biol Chem*. 1997;272(3):1541-1547. doi:10.1074/jbc.272.3.1541

47. Ruberte E, Friederich V, Morriss-Kay G, Chambon P. Differential distribution patterns of CRABP I and CRABP II transcripts during mouse embryogenesis. *Development*. 1992;115(4):973-987.

48. Nelson CH, Peng C-C, Lutz JD, Yeung CK, Zelter A, Isoherranen N. Direct protein-protein interactions and substrate channeling between cellular retinoic acid binding proteins and CYP26B1. *FEBS Lett*. 2016;590(16):2527-2535. doi:10.1002/1873-3468.12303

49. Zhong G, Ortiz D, Zelter A, Nath A, Isoherranen N. CYP26C1 Is a Hydroxylase of Multiple Active Retinoids and Interacts with Cellular Retinoic Acid Binding Proteins. *Mol Pharmacol*. 2018;93(5):489-503. doi:10.1124/mol.117.111039

50. Germain P, Chambon P, Eichele G, et al. International Union of Pharmacology. LX. Retinoic Acid Receptors. *Pharmacol Rev*. 2006;58(4):712-725. doi:10.1124/pr.58.4.4

51. Germain P, Chambon P, Eichele G, et al. International Union of Pharmacology. LXIII. Retinoid X Receptors. *Pharmacol Rev*. 2006;58(4):760-772. doi:10.1124/pr.58.4.7

52. Dollé P. Developmental expression of retinoic acid receptors (RARs). *Nucl Recept Signal*. 2009;7. doi:10.1621/nrs.07006

53. Pikarsky E, Sharir H, Ben-Shushan E, Bergman Y. Retinoic acid represses Oct-3/4 gene expression through several retinoic acid-responsive elements located in the promoter-enhancer region. *Mol Cell Biol*. 1994;14(2):1026-1038.

54. Sandell LL, Sanderson BW, Moiseyev G, et al. RDH10 is essential for synthesis of embryonic retinoic acid and is required for limb, craniofacial, and organ development. *Genes Dev*. 2007;21(9):1113-1124. doi:10.1101/gad.1533407

55. Rhinn M, Schuhbaur B, Niederreither K, Dollé P. Involvement of retinol dehydrogenase 10 in embryonic patterning and rescue of its loss of function by maternal retinaldehyde treatment. *Proceedings of the National Academy of Sciences of the United States of America*. 2011;108:16687-16692. doi:10.1073/pnas.1103877108

56. Wang S, Yu J, Jones JW, et al. Retinoic acid signaling promotes the cytoskeletal rearrangement of embryonic epicardial cells. *FASEB J*. 2018;32(7):3765-3781. doi:10.1096/fj.201701038R

57. Wang S, Huang W, Castillo HA, et al. Alterations in retinoic acid signaling affect the development of the mouse coronary vasculature. *Developmental Dynamics*. 2018;247(8):976-991. doi:10.1002/dvdy.24639

58. Sakai Y, Meno C, Fujii H, et al. The retinoic acid-inactivating enzyme CYP26 is essential for establishing an uneven distribution of retinoic acid along the anterio-posterior axis within the mouse embryo. *Genes Dev*. 2001;15(2):213-225. doi:10.1101/gad.851501

59. Lee LMY, Leung C-Y, Tang WWC, et al. A paradoxical teratogenic mechanism for retinoic acid. *Proc Natl Acad Sci U S A*. 2012;109(34):13668-13673. doi:10.1073/pnas.1200872109

60. Restricted expression and retinoic acid-induced downregulation of the retinaldehyde dehydrogenase type 2 (RALDH-2) gene during mouse development. *Mechanisms of Development*. 1997;62(1):67-78. doi:10.1016/S0925-4773(96)00653-3

61. Xiao Y, Hill MC, Zhang M, et al. Hippo signaling plays an essential role in cell state transitions during cardiac fibroblast development. *Dev Cell*. 2018;45(2):153-169.e6. doi:10.1016/j.devcel.2018.03.019

62. Harvey KF, Pfleger CM, Hariharan IK. The Drosophila Mst Ortholog, hippo, Restricts Growth and Cell Proliferation and Promotes Apoptosis. *Cell*. 2003;114(4):457-467. doi:10.1016/S0092-8674(03)00557-9

63. Boopathy GTK, Hong W. Role of Hippo Pathway-YAP/TAZ Signaling in Angiogenesis. *Front Cell Dev Biol*. 2019;7. doi:10.3389/fcell.2019.00049

64. Meng Z, Moroishi T, Guan K-L. Mechanisms of Hippo pathway regulation. *Genes Dev*. 2016;30(1):1-17. doi:10.1101/gad.274027.115

65. M P, F X, J A. MOBKL1A/MOBKL1B Phosphorylation by MST1 and MST2 Inhibits Cell Proliferation. Current biology : CB. doi:10.1016/j.cub.2008.02.006

66. Zhao B, Wei X, Li W, et al. Inactivation of YAP oncoprotein by the Hippo pathway is involved in cell contact inhibition and tissue growth control. *Genes Dev*. 2007;21(21):2747-2761. doi:10.1101/gad.1602907

67. M S. Yes-associated Protein (YAP65) Is a Proline-Rich Phosphoprotein That Binds to the SH3 Domain of the Yes Proto-Oncogene Product. Oncogene. Published August 1994. Accessed June 5, 2020. https://pubmed.ncbi.nlm.nih.gov/8035999/?dopt=Abstract

68. Dupont S, Morsut L, Aragona M, et al. Role of YAP/TAZ in mechanotransduction. *Nature*. 2011;474(7350):179-183. doi:10.1038/nature10137

69. Tian X, Liu Z, Niu B, et al. E-Cadherin/β-Catenin Complex and the Epithelial Barrier. Journal of Biomedicine and Biotechnology. doi:https://doi.org/10.1155/2011/567305

70. von Gise Alexander, Pu William T. Endocardial and Epicardial Epithelial to Mesenchymal Transitions in Heart Development and Disease. *Circulation Research*. 2012;110(12):1628-1645. doi:10.1161/CIRCRESAHA.111.259960

71. The Biology of YAP/TAZ: Hippo Signaling and Beyond | Physiological Reviews. Accessed June 5, 2020. https://journals.physiology.org/doi/full/10.1152/physrev.00005.2014?url_ver=Z39.88-2003&rfr_id=ori%3Arid%3Acrossref.org&rfr_dat=cr_pub++0pubmed&

72. Martin-Belmonte F, Perez-Moreno M. Epithelial cell polarity, stem cells and cancer. *Nat Rev Cancer*. 2011;12(1):23-38. doi:10.1038/nrc3169

73. Kim N-G, Koh E, Chen X, Gumbiner BM. E-cadherin mediates contact inhibition of proliferation through Hippo signaling-pathway components. *Proc Natl Acad Sci USA*. 2011;108(29):11930-11935. doi:10.1073/pnas.1103345108

74. Cordenonsi M, Zanconato F, Azzolin L, et al. The Hippo Transducer TAZ Confers Cancer Stem Cell-Related Traits on Breast Cancer Cells. *Cell*. 2011;147(4):759-772. doi:10.1016/j.cell.2011.09.048

75. Chen D, Sun Y, Wei Y, et al. LIFR is a breast cancer metastasis suppressor upstream of the Hippo-YAP pathway and a prognostic marker. *Nat Med*. 2012;18(10):1511-1517. doi:10.1038/nm.2940

76. Ltd TC of B. Hippo signalling in EMT and metastasis. *J Cell Sci*. 2014;127(7):e0704-e0704.

77. Dasgupta I, McCollum D. Control of cellular responses to mechanical cues through YAP/TAZ regulation. *J Biol Chem*. 2019;294(46):17693-17706. doi:10.1074/jbc.REV119.007963

78. Humphrey JD, Dufresne ER, Schwartz MA. Mechanotransduction and extracellular matrix homeostasis. *Nature Reviews Molecular Cell Biology*. 2014;15(12):802-812. doi:10.1038/nrm3896

79. Meng Z, Qiu Y, Lin KC, et al. RAP2 mediates mechanoresponses of the Hippo pathway. *Nature*. 2018;560(7720):655-660. doi:10.1038/s41586-018-0444-0

80. Lachowski D, Cortes E, Robinson B, Rice A, Rombouts K, Hernández AEDR. FAK controls the mechanical activation of YAP, a transcriptional regulator required for durotaxis. *The FASEB Journal*. 2018;32(2):1099-1107. doi:10.1096/fj.201700721R

81. Gupta M, Sarangi BR, Deschamps J, et al. Adaptive rheology and ordering of cell cytoskeleton govern matrix rigidity sensing. *Nature Communications*. 2015;6(1):7525. doi:10.1038/ncomms8525

82. Wada K-I, Itoga K, Okano T, Yonemura S, Sasaki H. Hippo pathway regulation by cell morphology and stress fibers. *Development*. 2011;138(18):3907-3914. doi:10.1242/dev.070987

83. Kim M, Kim M, Lee S, et al. cAMP/PKA signalling reinforces the LATS–YAP pathway to fully suppress YAP in response to actin cytoskeletal changes. *The EMBO Journal*. 2013;32(11):1543-1555. doi:10.1038/emboj.2013.102

84. Mana-Capelli S, Paramasivam M, Dutta S, McCollum D. Angiomotins link F-actin architecture to Hippo pathway signaling. *MBoC*. 2014;25(10):1676-1685. doi:10.1091/mbc.e13-11-0701

85. Leung CY, Zernicka-Goetz M. Angiomotin prevents pluripotent lineage differentiation in mouse embryos via Hippo pathway-dependent and -independent mechanisms. *Nat Commun*. 2013;4:2251. doi:10.1038/ncomms3251

86. Wang W, Huang J, Chen J. Angiomotin-like Proteins Associate with and Negatively Regulate YAP1. *J Biol Chem*. 2011;286(6):4364-4370. doi:10.1074/jbc.C110.205401

87. Yin F, Yu J, Zheng Y, Chen Q, Zhang N, Pan D. Spatial Organization of Hippo Signaling at the Plasma Membrane Mediated by the Tumor Suppressor Merlin/NF2. *Cell*. 2013;154(6):1342-1355. doi:10.1016/j.cell.2013.08.025

88. Engler AJ, Sen S, Sweeney HL, Discher DE. Matrix Elasticity Directs Stem Cell Lineage Specification. *Cell*. 2006;126(4):677-689. doi:10.1016/j.cell.2006.06.044

89. Seo J, Kim J. Regulation of Hippo signaling by actin remodeling. *BMB Rep*. 2018;51(3):151-156. doi:10.5483/BMBRep.2018.51.3.012

90. Pavel M, Renna M, Park SJ, et al. Contact inhibition controls cell survival and proliferation via YAP/TAZ-autophagy axis. *Nature Communications*. 2018;9(1):2961. doi:10.1038/s41467-018-05388-x

91. Aragona M, Panciera T, Manfrin A, et al. A Mechanical Checkpoint Controls Multicellular Growth through YAP/TAZ Regulation by Actin-Processing Factors. *Cell*. 2013;154(5):1047-1059. doi:10.1016/j.cell.2013.07.042

92. Molnar C, Gair J. 21.3. Mammalian Heart and Blood Vessels. In: *Concepts of Biology - 1st Canadian Edition*. BCcampus; 2019. Accessed April 23, 2020. https://opentextbc.ca/biology/chapter/21-3-mammalian-heart-and-blood-vessels/

93. OpenStax. 19.1 Heart Anatomy. In: *Anatomy and Physiology*. OpenStax; 2013. Accessed April 10, 2020. https://opentextbc.ca/anatomyandphysiology/chapter/19-1-heart-anatomy/

94. Smits AM, Dronkers E, Goumans M-J. The epicardium as a source of multipotent adult cardiac progenitor cells: Their origin, role and fate. *Pharmacological Research*. 2018;127:129-140. doi:10.1016/j.phrs.2017.07.020

95. Layers of the Heart, Pericarditis, and Endocarditis – HeartStrong|RN. Accessed July 9, 2020. https://heartstrongnurse.com/2017/06/20/layers-of-the-heart/

96. Merchiers EH, Dhont M, De Sutter PA, Beghin CJ, Vandekerckhove DA. Predictive value of earl embryonic cardiac activity for pregnancy outcome. *American Journal of Obstetrics and Gynecology*. 1991;165(1):11-14. doi:10.1016/0002-9378(91)90214-C

97. Männer J, Schlueter J, Brand T. Experimental analyses of the function of the proepicardium using a new microsurgical procedure to induce loss-of-proepicardial-function in chick embryos. *Developmental Dynamics*. 2005;233(4):1454-1463. doi:10.1002/dvdy.20487

98. Schlueter J, Brand T. Origin and fates of the proepicardium. *Aswan Heart Centre Science & Practice Series*. 2011;2011(2):11. doi:10.5339/ahcsps.2011.11

99. Maya-Ramos L, Cleland J, Bressan M, Mikawa T. Induction of the Proepicardium. *Journal of Developmental Biology*. 2013;1(2):82-91. doi:10.3390/jdb1020082

100. Cossette S, Misra R. The identification of different endothelial cell populations within the mouse proepicardium. *Developmental Dynamics*. 2011;240(10):2344-2353. doi:10.1002/dvdy.22724

101. Gittenberger-de Groot Adriana C., Vrancken Peeters Mark-Paul F.M., Bergwerff Maarten, Mentink Monica M.T., Poelmann Robert E. Epicardial Outgrowth Inhibition Leads to Compensatory Mesothelial Outflow Tract Collar and Abnormal Cardiac Septation and Coronary Formation. *Circulation Research*. 2000;87(11):969-971. doi:10.1161/01.RES.87.11.969

102. Vicente-Steijn R, Scherptong RWC, Kruithof BPT, et al. Regional differences in WT-1 and Tcf21 expression during ventricular development: implications for myocardial compaction. *PLOS ONE*. 2015;10(9):e0136025. doi:10.1371/journal.pone.0136025

103. Duim SN, Smits AM, Kruithof BPT, Goumans M-J. The roadmap of WT1 protein expression in the human fetal heart. *Journal of Molecular and Cellular Cardiology*. 2016;90:139-145. doi:10.1016/j.yjmcc.2015.12.008

104. Pérez-Pomares JM, de la Pompa JL. Signaling during epicardium and coronary vessel development. *Circ Res*. 2011;109(12):1429-1442. doi:10.1161/CIRCRESAHA.111.245589

105. Stuckmann I, Evans S, Lassar AB. Erythropoietin and retinoic acid, secreted from the epicardium, are required for cardiac myocyte proliferation. *Developmental Biology*. 2003;255(2):334-349. doi:10.1016/S0012-1606(02)00078-7

106. Olivey Harold E., Svensson Eric C. Epicardial–Myocardial Signaling Directing Coronary Vasculogenesis. *Circulation Research*. 2010;106(5):818-832. doi:10.1161/CIRCRESAHA.109.209197

107. Austin AF, Compton LA, Love JD, Brown CB, Barnett JV. Primary and immortalized mouse epicardial cells undergo differentiation in response to TGFβ. *Developmental Dynamics*. 2008;237(2):366-376. doi:10.1002/dvdy.21421

108. Mellgren Amy M., Smith Christopher L., Olsen Gregory S., et al. Platelet-Derived Growth Factor Receptor β Signaling Is Required for Efficient Epicardial Cell Migration and Development of Two Distinct Coronary Vascular Smooth Muscle Cell Populations. *Circulation Research*. 2008;103(12):1393-1401. doi:10.1161/CIRCRESAHA.108.176768

109. Lavine KJ, Yu K, White AC, et al. Endocardial and Epicardial Derived FGF Signals Regulate Myocardial Proliferation and Differentiation In Vivo. *Developmental Cell*. 2005;8(1):85-95. doi:10.1016/j.devcel.2004.12.002

110. Krainock M, Toubat O, Danopoulos S, Beckham A, Warburton D, Kim R. Epicardial Epithelial-to-Mesenchymal Transition in Heart Development and Disease. *J Clin Med*. 2016;5(2). doi:10.3390/jcm5020027

111. Johansen AKZ, Molkentin JD. Hippo signaling does it again: arbitrating cardiac fibroblast identity and activation. *Genes Dev*. 2019;33(21-22):1457-1459. doi:10.1101/gad.332791.119

112. Dettman RW, Denetclaw W, Ordahl CP, Bristow J. Common epicardial origin of coronary vascular smooth muscle, perivascular fibroblasts, and intermyocardial fibroblasts in the avian heart. *Dev Biol*. 1998;193(2):169-181. doi:10.1006/dbio.1997.8801

113. Pérez-Pomares JM, Phelps A, Sedmerova M, et al. Experimental studies on the spatiotemporal expression of WT1 and RALDH2 in the embryonic avian heart: a model for the regulation of myocardial and valvuloseptal development by epicardially derived cells (EPDCs). *Dev Biol*. 2002;247(2):307-326. doi:10.1006/dbio.2002.0706

114. Merki E, Zamora M, Raya A, et al. Epicardial retinoid X receptor alpha is required for myocardial growth and coronary artery formation. *Proc Natl Acad Sci USA*. 2005;102(51):18455-18460. doi:10.1073/pnas.0504343102

115. von Gise A, Zhou B, Honor LB, Ma Q, Petryk A, Pu WT. WT1 regulates epicardial epithelial to mesenchymal transition through β-catenin and retinoic acid signaling pathways. *Developmental Biology*. 2011;356(2):421-431. doi:10.1016/j.ydbio.2011.05.668

116. Guadix JA, Ruiz-Villalba A, Lettice L, et al. Wt1 controls retinoic acid signalling in embryonic epicardium through transcriptional activation of Raldh2. *Development*. 2011;138(6):1093-1097. doi:10.1242/dev.044594

117. Lin S-C, Dollé P, Ryckebüsch L, et al. Endogenous retinoic acid regulates cardiac progenitor differentiation. *Proc Natl Acad Sci U S A*. 2010;107(20):9234-9239. doi:10.1073/pnas.0910430107

118. Singh A, Ramesh S, Cibi DM, et al. Hippo signaling mediators Yap and Taz are required in the epicardium for coronary vasculature development. *Cell Rep*. 2016;15(7):1384-1393. doi:10.1016/j.celrep.2016.04.027

119. Acharya A, Baek ST, Huang G, et al. The bHLH transcription factor Tcf21 is required for lineage-specific EMT of cardiac fibroblast progenitors. *Development*. 2012;139(12):2139-2149. doi:10.1242/dev.079970

120. Li P, Cavallero S, Gu Y, et al. IGF signaling directs ventricular cardiomyocyte proliferation during embryonic heart development. *Development*. 2011;138(9):1795-1805. doi:10.1242/dev.054338

121. Copeland NG, Cooper GM. Transfection by exogenous and endogenous murine retrovirus DNAs. *Cell*. 1979;16(2):347-356. doi:10.1016/0092-8674(79)90011-4

122. Yin Z, Zhang Y, Liang S, Zhao S, Du J, Cheng B. Mycoplasma contamination-mediated attenuation of plasmid DNA transfection efficiency is augmented via L-arginine deprivation in HEK-293 cells. *J Zhejiang Univ Sci B*. 2019;20(12):1021-1026. doi:10.1631/jzus.B1900380

123. Majkut S, Idema T, Swift J, Krieger C, Liu A, Discher DE. Heart-Specific Stiffening in Early Embryos Parallels Matrix and Myosin Expression to Optimize Beating. *Current Biology*. 2013;23(23):2434-2439. doi:10.1016/j.cub.2013.10.057

124. *Retinoid Signaling Pathways*. Academic Press; 2020.

125. D'Aniello E, Rydeen AB, Anderson JL, Mandal A, Waxman JS. Depletion of Retinoic Acid Receptors Initiates a Novel Positive Feedback Mechanism that Promotes Teratogenic Increases in Retinoic Acid. *PLOS Genetics*. 2013;9(8):e1003689. doi:10.1371/journal.pgen.1003689

126. Avruch J, Zhou D, Fitamant J, Bardeesy N, Mou F, Barrufet LR. Protein kinases of the Hippo pathway: regulation and substrates. *Semin Cell Dev Biol*. 2012;23(7):770-784. doi:10.1016/j.semcdb.2012.07.002

127. Felley-Bosco E, Stahel R. Hippo/YAP pathway for targeted therapy. *Transl Lung Cancer Res*. 2014;3(2):75-83. doi:10.3978/j.issn.2218-6751.2014.02.03

128. Matsubara A, Nakazawa T, Husain D, et al. Investigating the Effect of Ciliary Body Photodynamic Therapy in a Glaucoma Mouse Model. *Invest Ophthalmol Vis Sci*. 2006;47(6):2498-2507. doi:10.1167/iovs.05-0959

129. Dong L, Lin F, Wu W, Liu Y, Huang W. Verteporfin inhibits YAP-induced bladder cancer cell growth and invasion via Hippo signaling pathway. *Int J Med Sci*. 2018;15(6):645-652. doi:10.7150/ijms.23460

130. Chen W-S, Cao Z, Krishnan C, Panjwani N. Verteporfin without light stimulation inhibits YAP activation in trabecular meshwork cells: Implications for glaucoma treatment. *Biochem Biophys Res Commun*. 2015;466(2):221-225. doi:10.1016/j.bbrc.2015.09.012

131. Liu-Chittenden Y, Huang B, Shim JS, et al. Genetic and pharmacological disruption of the TEAD–YAP complex suppresses the oncogenic activity of YAP. *Genes Dev*. 2012;26(12):1300-1305. doi:10.1101/gad.192856.112

132. Martien MF. BIDIRECTIONAL REGULATION OF YAP AND ALDH1A. :53.

133. Kim D-H, Choi H-I, Park JS, et al. Src-mediated crosstalk between FXR and YAP protects against renal fibrosis. *The FASEB Journal*. 2019;33(10):11109-11122. doi:https://doi.org/10.1096/fj.201900325R

134. Komuro A, Nagai M, Navin NE, Sudol M. WW domain-containing protein YAP associates with ErbB-4 and acts as a co-transcriptional activator for the carboxyl-terminal fragment of ErbB-4 that translocates to the nucleus. *J Biol Chem*. 2003;278(35):33334-33341. doi:10.1074/jbc.M305597200

135. Omerovic J, Puggioni EMR, Napoletano S, et al. Ligand-regulated association of ErbB-4 to the transcriptional co-activator YAP65 controls transcription at the nuclear level. *Exp Cell Res*. 2004;294(2):469-479. doi:10.1016/j.yexcr.2003.12.002

136. Strano S, Munarriz E, Rossi M, et al. Physical interaction with Yes-associated protein enhances p73 transcriptional activity. *J Biol Chem*. 2001;276(18):15164-15173. doi:10.1074/jbc.M010484200

137. Vitolo MI, Anglin IE, Mahoney WM, et al. The RUNX2 transcription factor cooperates with the YES-associated protein, YAP65, to promote cell transformation. *Cancer Biol Ther*. 2007;6(6):856-863. doi:10.4161/cbt.6.6.4241

138. Levy D, Adamovich Y, Reuven N, Shaul Y. The Yes-associated protein 1 stabilizes p73 by preventing Itch-mediated ubiquitination of p73. *Cell Death Differ*. 2007;14(4):743-751. doi:10.1038/sj.cdd.4402063

139. Rosenbluh J, Nijhawan D, Cox AG, et al. β-Catenin-driven cancers require a YAP1 transcriptional complex for survival and tumorigenesis. *Cell*. 2012;151(7):1457-1473. doi:10.1016/j.cell.2012.11.026

140. Mitani A, Nagase T, Fukuchi K, Aburatani H, Makita R, Kurihara H. Transcriptional coactivator with PDZ-binding motif is essential for normal alveolarization in mice. *Am J Respir Crit Care Med*. 2009;180(4):326-338. doi:10.1164/rccm.200812-1827OC

141. J S, Il I, A B, et al. Nuclear lamin-A scales with tissue stiffness and enhances matrix-directed differentiation. *Science*. 2013;341(6149):1240104-1240104. doi:10.1126/science.1240104

142. Jones JW, Pierzchalski K, Yu J, Kane MA. Use of Fast HPLC Multiple Reaction Monitoring Cubed for Endogenous Retinoic Acid Quantification in Complex Matrices. *Anal Chem*. 2015;87(6):3222-3230. doi:10.1021/ac504597q

143. Kane MA, Folias AE, Wang C, Napoli JL. Quantitative profiling of endogenous retinoic acid in vivo and in vitro by tandem mass spectrometry. *Anal Chem*. 2008;80(5):1702-1708. doi:10.1021/ac702030f

144. Allenby G, Bocquel MT, Saunders M, et al. Retinoic acid receptors and retinoid X receptors: interactions with endogenous retinoic acids. *PNAS*. 1993;90(1):30-34. doi:10.1073/pnas.90.1.30

145. Plouffe SW, Lin KC, Moore JL, et al. The Hippo pathway effector proteins YAP and TAZ have both distinct and overlapping functions in the cell. *J Biol Chem*. 2018;293(28):11230-11240. doi:10.1074/jbc.RA118.002715

146. Hengesbach LM, Hoag KA. Physiological Concentrations of Retinoic Acid Favor Myeloid Dendritic Cell Development over Granulocyte Development in Cultures of Bone Marrow Cells from Mice. *J Nutr*. 2004;134(10):2653-2659. doi:10.1093/jn/134.10.2653

147. Merino VF, Cho S, Nguyen N, et al. Induction of cell cycle arrest and inflammatory genes by combined treatment with epigenetic, differentiating, and chemotherapeutic agents in triple-negative breast cancer. *Breast Cancer Research*. 2018;20(1):145. doi:10.1186/s13058-018-1068-x

148. Sirchia SM, Ferguson AT, Sironi E, et al. Evidence of epigenetic changes affecting the chromatin state of the retinoic acid receptor β2 promoter in breast cancer cells. *Oncogene*. 2000;19(12):1556-1563. doi:10.1038/sj.onc.1203456

149. Osanai M, Sawada N, Lee G-H. Oncogenic and cell survival properties of the retinoic acid metabolizing enzyme, CYP26A1. *Oncogene*. 2010;29(8):1135-1144. doi:10.1038/onc.2009.414

150. Bhana B, Iyer RK, Chen WLK, et al. Influence of substrate stiffness on the phenotype of heart cells. *Biotechnol Bioeng*. 2010;105(6):1148-1160. doi:10.1002/bit.22647

151. Okumura K, Hosoe Y, Nakajima N. c-Jun and Sp1 family are critical for retinoic acid induction of the lamin A/C retinoic acid-responsive element. *Biochem Biophys Res Commun*. 2004;320(2):487-492. doi:10.1016/j.bbrc.2004.05.191

152. Castellan RFP, Meloni M. Mechanisms and Therapeutic Targets of Cardiac Regeneration: Closing the Age Gap. *Front Cardiovasc Med*. 2018;5. doi:10.3389/fcvm.2018.00007

153. Vanhoutte D, Schellings M, Pinto Y, Heymans S. Relevance of matrix metalloproteinases and their inhibitors after myocardial infarction: A temporal and spatial window. *Cardiovasc Res*. 2006;69(3):604-613. doi:10.1016/j.cardiores.2005.10.002

154. Heart failure. Heart and Stroke Foundation of Canada. Accessed April 24, 2020. https://www.heartandstroke.ca/en/heart/conditions/heart-failure/

155. Zhou B, Honor LB, He H, et al. Adult mouse epicardium modulates myocardial injury by secreting paracrine factors. *J Clin Invest*. 2011;121(5):1894-1904. doi:10.1172/JCI45529

156. Poss KD. Getting to the heart of regeneration in zebrafish. *Semin Cell Dev Biol*. 2007;18(1):36-45. doi:10.1016/j.semcdb.2006.11.009

157. Kikuchi K, Holdway JE, Major RJ, et al. Retinoic acid production by endocardium and epicardium is an injury response essential for zebrafish heart regeneration. *Dev Cell*. 2011;20(3):397-404. doi:10.1016/j.devcel.2011.01.010

158. Gourdie RG, Dimmeler S, Kohl P. Novel therapeutic strategies targeting fibroblasts and fibrosis in heart disease. *Nat Rev Drug Discov*. 2016;15(9):620-638. doi:10.1038/nrd.2016.89

159. Liu F, Lagares D, Choi KM, et al. Mechanosignaling through YAP and TAZ drives fibroblast activation and fibrosis. *Am J Physiol Lung Cell Mol Physiol*. 2015;308(4):L344-357. doi:10.1152/ajplung.00300.2014

160. Xiao Y, Hill MC, Li L, et al. Hippo pathway deletion in adult resting cardiac fibroblasts initiates a cell state transition with spontaneous and self-sustaining fibrosis. *Genes Dev*. 2019;33(21-22):1491-1505. doi:10.1101/gad.329763.119

8. Appendix: Supplementary Information

8.1 Supplementary Section 1

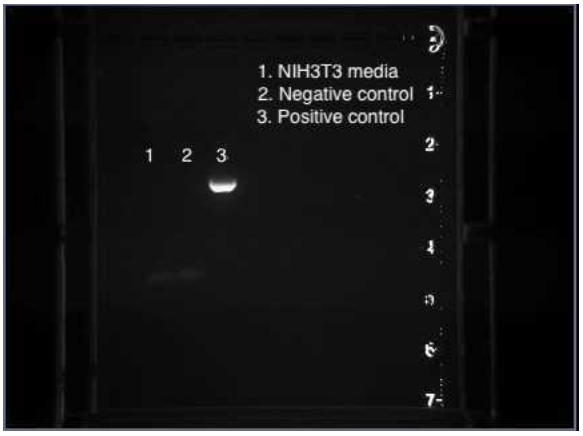

Supplementary Figure 1: NIH3T3 cells were not infected with mycoplasma.

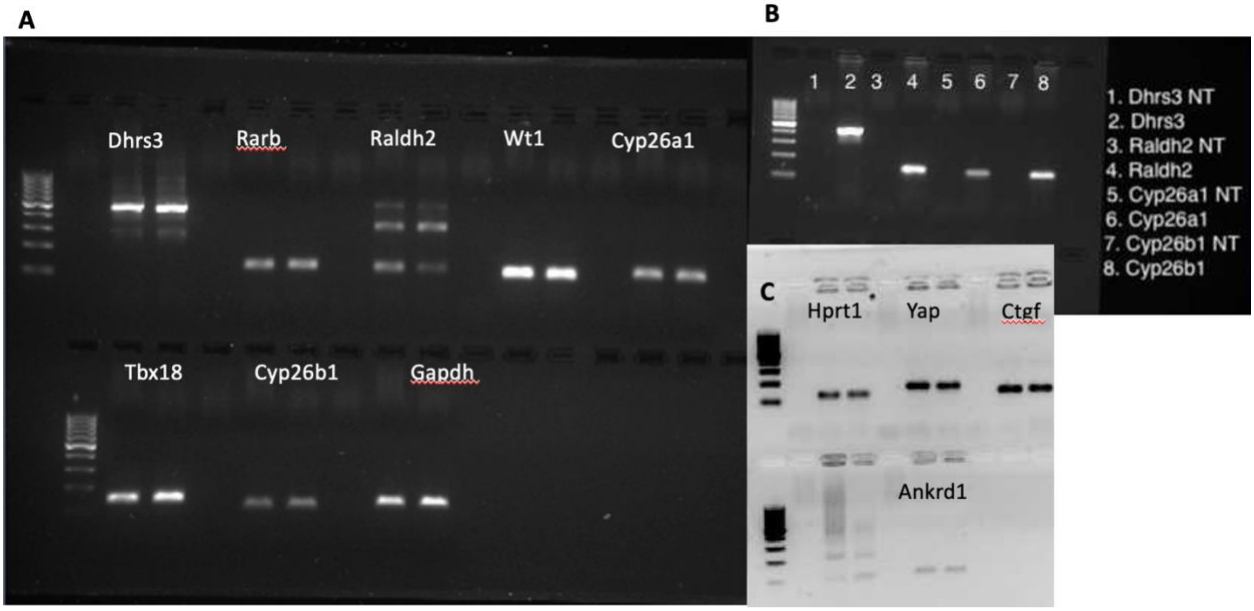

Supplementary Figure 2: The primers of each target genes after RT-qPCR run through a 2% agarose gel. (A) *Dhrs3, Rarb, Raldh2, Wt1, Cyp26a1, Tbx18, Cyp26b1,* and *Gapdh* are 499bp, 141bp, 136bp, 112bp, 125bp, 151bp, 119bp and 128bp respectively. There are two products for *Raldh2* because the primer amplifies both cDNA and genomic DNA at 34bp. (B) The same primers were re-run to ensure a single product was formed for both *Dhrs3* and *Raldh2* after optimization. NT means no template controls. (C) *Hprt1, Yap, Ctgf, Ankrd1* are 142bp, 180bp, 151bp, and 119bp respectively.

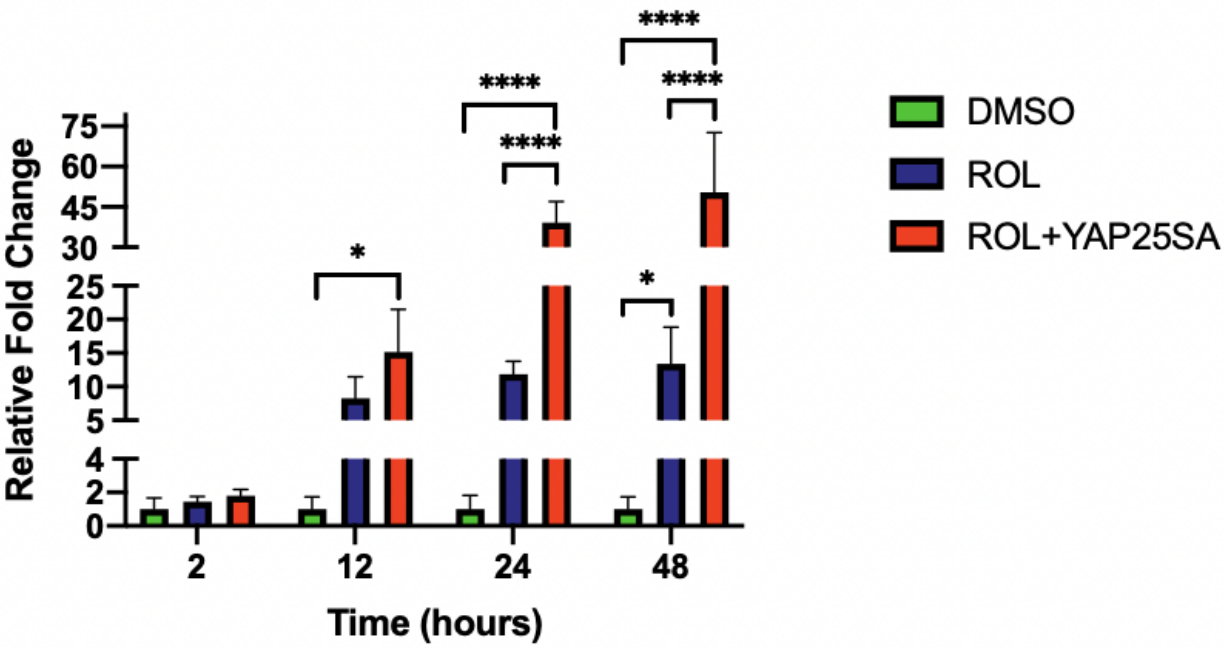

Supplementary Figure 3: YAP25SA affects the metabolism of ROL to RA in MEC1 cells. MEC1 cells were treated with three different groups: reverse co-transfected with pGluc-mini-tk-2-UAS and pCS2p+Gal4-RAR reporter plasmids and DMSO for the reporter control, reverse co-transfected with pGluc-mini-tk-2-UAS and pCS2p+Gal4-RAR reporter plasmids and ROL for the experimental control, and reverse co-transfected with pGluc-mini-tk-2-UAS, pCS2p+Gal4-RAR, YAP25SA and ROL. Each treatment group contained three technical replicates. A time course experiment was then completed on each of the technical replicates by measuring the Gaussia luciferase signal at 2, 12, 24 and 48 hours after DMSO or ROL was added with a luminometer. Relative fold change was calculated by first subtracting the RFU of the blank sample from all of the samples and then dividing the mean of each treatment group by the mean of the DMSO control group. This experiment was repeated on three different days (N=3). A two-way ANOVA with repeated measures was performed on the biological replicates and revealed that there was a significant difference between the three groups across both time and treatment with YAP25SA ($P<0.0001$). A Tukey's multiple comparisons post hoc test was performed to determine any significant differences between the groups, denoted as: *$p<0.05$, **$p<0.01$, ***$p<0.001$. The data represents the mean fold change and the error bars indicate a standard deviation between the biological replicates.

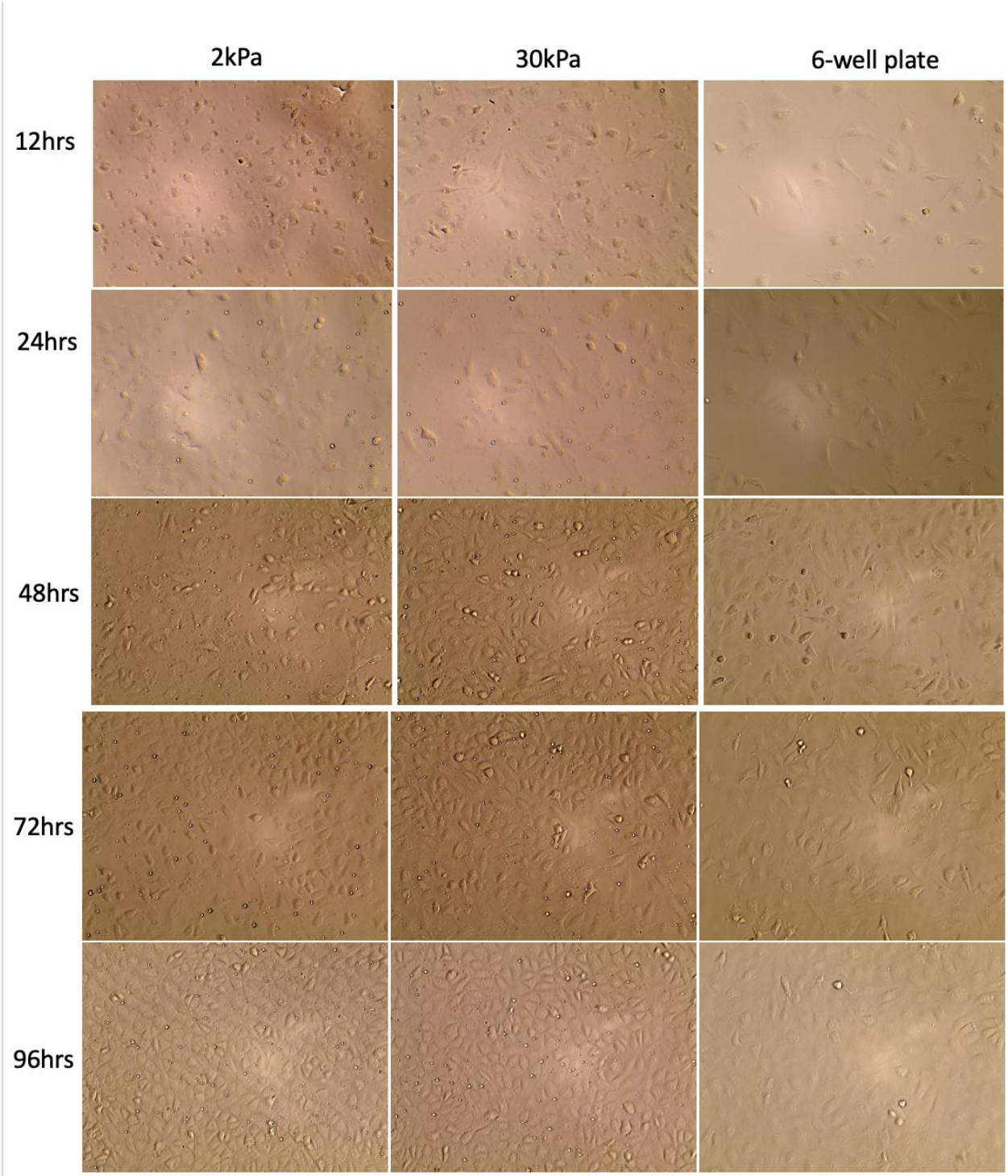

Supplementary Figure 4: MEC1 cells plated on plates varying in tension over a 96- hour time course experiment.

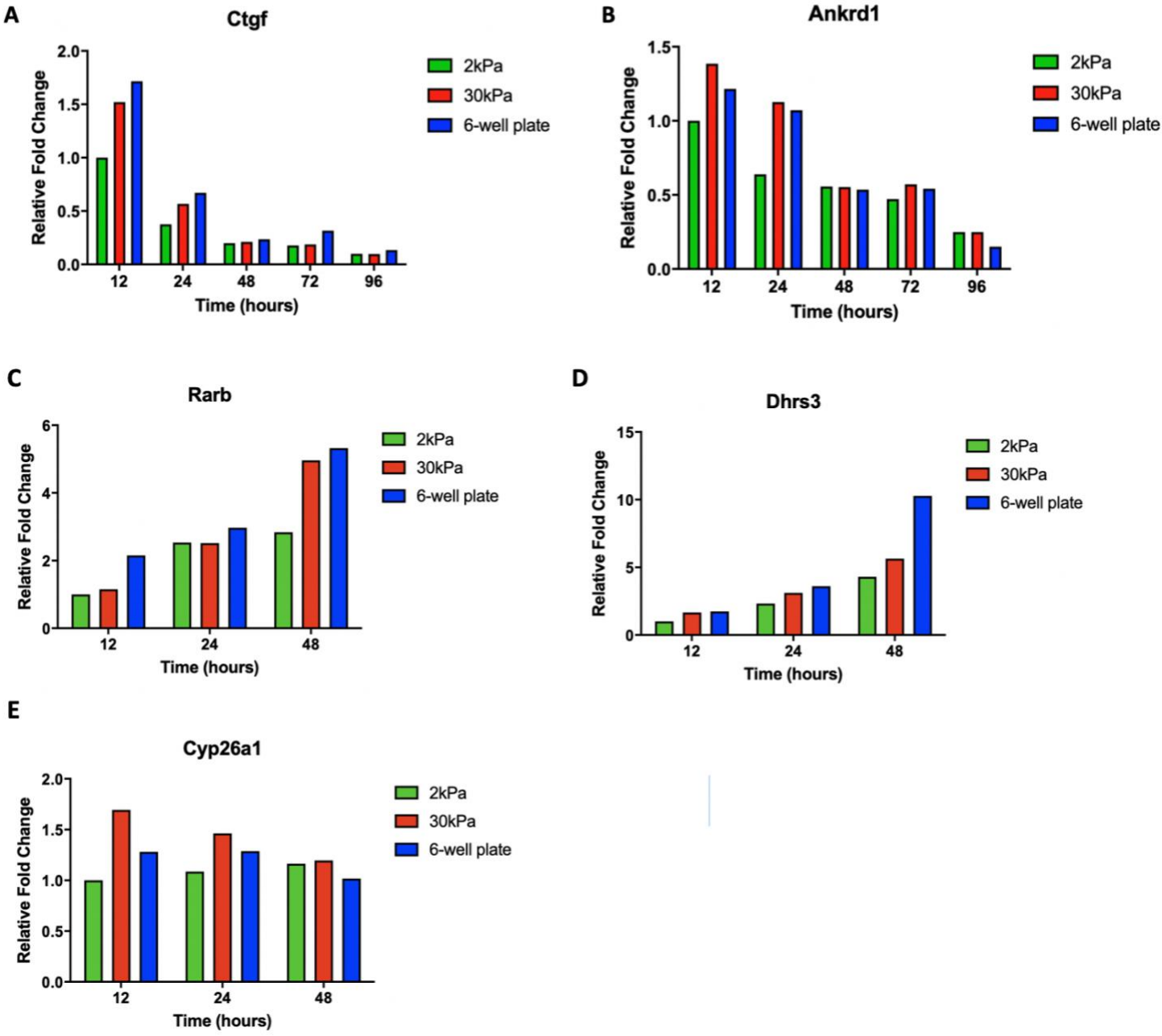

Supplementary Figure 5: Mechanical tension may influence the expression of enzymes and receptors involved in RA-signaling. MEC1 cells were plated on a 2kPa, 30kPa and a 6-well plate. mRNA was extracted at 12, 24, 48, 72, and 96 hours and RT-qPCR was performed on all samples. The experiment was conducted once in technical duplicates (N=1) and the $2^{-\Delta\Delta CT}$ method was used to calculate the fold change by normalizing the gene of interest to the housekeeping genes: *Hprt1* and *Gapdh*. Next all samples were normalized to the 12hour 2kPa control sample. The data is presented in relative fold change by averaging the two technical duplicates.

8.2 Attempting to construct a stable two-hybrid Gal4-RAR;UAS-tk-Gaussia luciferase reporter system in MEC1 and NIH3T3 cells

The first step of creating this stable two-hybrid Gal4-RAR;UAS-tk-Gaussia luciferase reporter system was to determine the concentration of G418 needed to select stables by creating a G418 kill curve (Supplementary Figure 6). It was observationally noted that the 4000 μg/ml G418 concentration killed all of the MEC1 cells in two days. As well, the 2000 μg/ml and 1000 μg/ml G418 concentrations killed all the MEC1 cells in four and eight days respectively. Therefore, it was decided that the MEC1 cells transfected with pGluc-mini-tk-2-UAS plasmid would be cultured in media supplemented with 1000 μg/ml of G418 for to select and isolate stable clones. To select NIH3T3 stables with G418, a concentration of 1000 μg/ml was already predetermined.

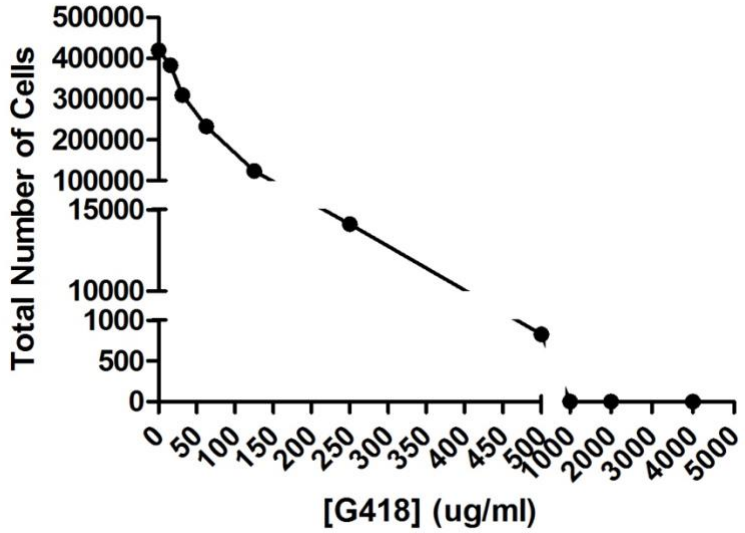

Supplementary Figure 6: G418 kill curve for MEC1 cells. To optimize the concentration of G418 to select stable MEC1 cell clones, 10,000 MEC1 cells were plated in a 24-well plate and treated with ten different concentrations of G418: 4000 μg/ml, 2000 μg/ml, 1000 μg/ml, 500 μg/ml, 250 μg/ml, 125 μg/ml, 62.5 μg/ml, 31.3 μg/ml, 15.6 μg/ml, and 0 μg/ml. The media was changed every 2-3 days to allow continued growth, with the same concentrations of G418. The cells were allowed to grow, and observations were taken every 2-days. After 10 days the cells were counted, using a hematocytometer, to create a G418 kill curve.

First, we attempted to create a RA reporter cell line through viral infection. Both MEC1 and NIH3T3 cells and were transduced with a viral vector pMX-IG containing Gal4-RAR and GFP. A fluorescent cell imager was used to determine if the virally infected cells expressed GFP to ensure the viral infection worked. Supplementary Figure 7 depicted that both the virally infected MEC1 and NIH3T3 cells did express GFP. Therefore, virally infected MEC1 and NIH3T3 cells were cloned by serial dilution and clones were tested for the expression of pMX-IG Gal4-RAR by transiently transfecting in pGluc-mini-tk-2-UAS and adding 10nM TTNPB, a stable RA analog. Unfortunately, there were no NIH3T3 clones that expressed GFP and the twelve MEC1 Gal4-RAR/UAS-Gluc stable cloned cell lines that expressed GFP were deemed unsuitable for use as a RA reporter, since TTNPB did not induce a robust response in comparison to DMSO (Table 2).

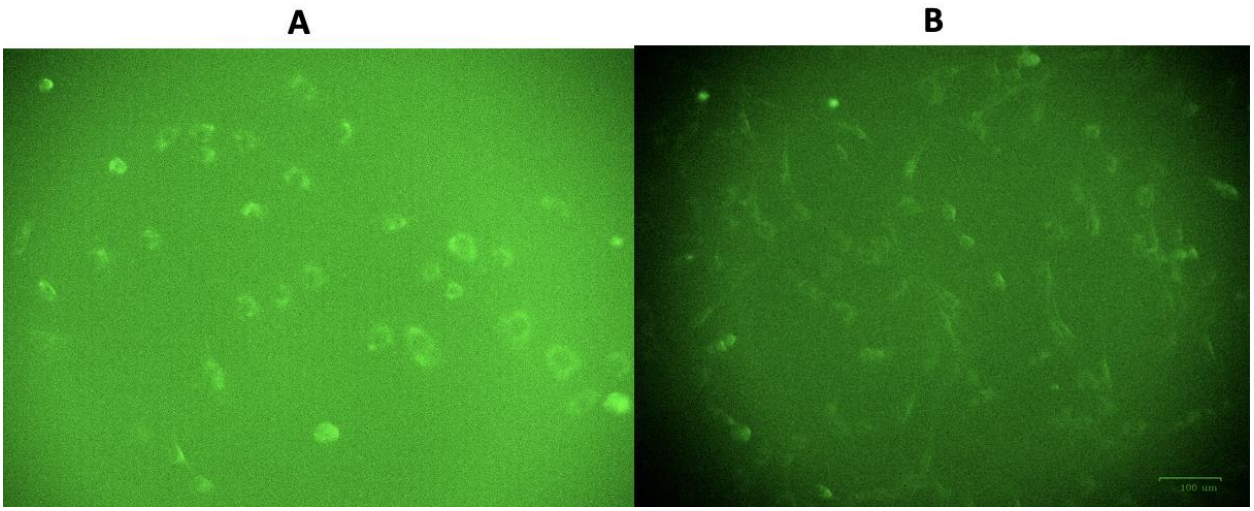

Supplementary Figure 7: MEC1 cells (A) and NIH3T3 cells (B) virally infected with pCS2p+Gal4-RAR expressed GFP.

Supplementary Table 1: MEC1 cloned cell lines following viral infection with retrovirus harbouring pMX-IG Gal4-RAR and transiently transfected with pGluc-mini-tk-2-UAS and then treated with 10nM TTNPB or DMSO. The fold change was calculated by normalizing the TTNPB sample to the DMSO sample of each clone.

Clone	DMSO (RFU)	10 nM TTNPB (RFU)	Fold Change
1	15,903	11,504	1
2	6,973	5,028	1
3	20,713	19,108	1
4	4,300	4,127	1
5	5,260	4,686	1
6	2,766	2,651	1
7	6,151	6,242	1
9	4,402	2,697	1
10	3,807	2,733	1
11	7,410	6,964	1
12	32,070	29,022	1

The second method used to create a RA reporter cell line was by transfection with lipofectamine. To begin, both MEC1 and NIH3T3 cells were transfected with pGluc-mini-tk-2-UAS plasmid. Stable clones were then isolated by single cell per well dilution and selected with G418 media to create a cell line. Clones were tested for the expression of pGluc-mini-tk-2-UAS by transiently transfecting in pCS2p+Gal4-RAR, adding 10nM TTNPB or DMSO, and then measuring the Gaussia luciferase signal with a luminometer. Four clones of pGluc-mini-tk-2-UAS-MEC1 (Table 3) and 12 clones of pGluc-mini-tk-2-UAS- NIH3T3 (Table 4) were isolated.

Table 3 illustrates that only pGluc-mini-tk-2-UAS- MEC1 clone four slightly expressed pGluc-mini-tk-2-UAS by 3-fold when the 10 nM of TTNPB sample was normalized to the DMSO control sample. Therefore we did not succeed in establishing a stable Gal4-RAR;UAS-tk-Gaussia luciferase reporter system in MEC1 cells and it was decided to perform the evaluation of RA formation by transiently transfecting two-hybrid Gal4-RAR;UAS-tk-Gaussia luciferase reporter system experiments in MEC1 cells transiently.

Table 4 showed that pGluc-mini-tk-2-UAS- NIH3T3 clone 5 had a fold change of 33 when the TTNPB treated sample was compared to the DMSO control. Therefore, it was determined that pGluc-mini-tk-2-UAS- NIH3T3 clone 5 expressed the pGluc-mini-tk-2-UAS plasmid. Next pGluc-mini-tk-2-UAS- NIH3T3 clone 5 was attempted to be transfected with the pCS2p+Gal4-RAR plasmid to isolate, select and create clones that expressed both pGluc-mini-tk-2-UAS and pCS2p+Gal4-RAR plasmids; however, clones were unable to be created.

Supplementary Table 2: pGluc-mini-tk-2-UAS- MEC1 stable clone 4 slightly expressed the pGluc-mini-tk-2-UAS plasmid. All samples were transiently transfected with pCS2p+Gal4-RAR and then treated with 10nM TTNPB or DMSO. The fold change was calculated by normalizing the TTNPB sample to the DMSO sample of each clone.

Clone	**DMSO (RFU)**	**10 nM TTNPB (RFU)**	**Fold Change**
1	2,015	2,588	1
2	4,072	8,048	2
3	1,676	1,872	1
4	4,448	14,352	3

Supplementary Table 3: pGluc-mini-tk-2-UAS- NIH3T3 stable clone 5 transfected transiently with pCS2p+Gal4-RAR responds to exogenous RAR agonist. Activation of Gal4-RAR was assessed by treatment with 10nM TTNPB or DMSO. The fold change was calculated by normalizing the TTNPB sample to the DMSO sample of each clone.

Clone	**DMSO (RFU)**	**10 nM TTNPB (RFU)**	**Fold Change**
1	127,081	145,294	1
2	440,214	1,630,389	4
3	36,342	216,482	4
4	18,470,666	20,000877	1
5	14,695	485,422	33
6	3,078	2,650	1
7	104,508	723,522	7
8	1,759	1,936	1
9	2,103	2,325	1
10	13,252,609	20,000,880	1.5
11	272,193	544,927	2
12	3,226	54,297	16

Since a complete stable two-hybrid Gal4-RAR;UAS-tk-Gaussia luciferase reporter system could not be created in the NIH3T3 cell line, it was decided that the pGluc-mini-tk-2-UAS- NIH3T3 clone 5, would be used in the reporter by transfecting in the pCS2p+Gal4-RAR plasmid transiently. To test if this new approach would work, a mini experiment was conducted where pCS2p+Gal4-RAR was transiently transfected into the pGluc-mini-tk-2-UAS- NIH3T3 cell line and treated with either 6 μM of retinol or DMSO as a vehicle control. Another control used, was transfecting the pGluc-mini-tk-2-UAS- NIH3T3 cell line with both the pGluc-mini-tk-2-UAS and pCS2p+Gal4-RAR plasmids to evaluate the expression of the pGluc-mini-tk-2-UAS plasmid in clone 5. As illustrated in Table 5, when pCS2p+Gal4-RAR was transiently transfected into the pGluc-mini-tk-2-UAS- NIH3T3 clone 5 cell line, a two-hybrid Gal4-RAR;UAS-tk-Gaussia luciferase reporter system was created because there was a fold change of 61 when the retinol sample was compared to the DMSO sample. Interestingly, when both the pGluc-mini-tk-2-UAS and pCS2p+Gal4-RAR plasmids were transfected into the pGluc-mini-tk-2-UAS- NIH3T3 clone 5 cell line, there was a 3,546 fold-change compared to the pCS2p+Gal4-RAR+DMSO sample and a 58 fold change compared to the Gal4-RAR + 6 μM retinol sample. Therefore, the pGluc-mini-tk-2-UAS- NIH3T3 clone 5 cell line yielded a two-hybrid Gal4-RAR;UAS-tk-Gaussia luciferase reporter system with greater sensitivity when both the pGluc-mini-tk-2-UAS and pCS2p+Gal4-RAR plasmids were transiently transfected into the pGluc-mini-tk-2-UAS- NIH3T3 clone 5 cell line.

Supplementary Table 4: Optimizing the two-hybrid Gal4-RAR;UAS-tk-Gaussia luciferase reporter system in NIH3T3 clone 5 cells that already express pGluc-mini-tk-2-UAS. The fold change was calculated by normalizing to the Gal4-RAR +DMSO sample. * Indicates that the fold change was calculated by normalizing to the Gal4-RAR + 6 μM retinol sample.

Treatment	RFU	Fold Change
Gal4-RAR +DMSO	4,479	1
Gal4-RAR + 6 μM ROL	273,093	61
Gal4-RAR + pGluc-mini-tk-2-UAS+ 6 μM retinol	15,964,371	3,564 58*